MEMBRANE BIOREACTOR PRODUCTION OF LIGNIN AND MANGANESE PEROXIDASE

By

M.S. Solomon

A dissertation submitted in fulfilment of the requirements for the degree in Master of Technology in Chemical Engineering at the Cape Technikon.

Supervisor: Prof. F.W. Petersen

The Cape Technikon

October 2001

DECLARATION

I hereby certify that this dissertation is my own original work, except where specifically acknowledged in the text. Neither the present dissertation nor any part thereof has previously been submitted at any other University or Technikon.

M.S.Solomon

September 2001

ACKNOWLEDGEMENTS

ABSTRACT

The white-rot fungus (WRF), *Phanerochaete chrysosporium,* is a well known micro-organism which produces liginolytic enzymes. These enzymes can play a major role in the bioremediation of a diverse range of environmental aromatic pollutants present in industrial effluents. Bioremediation of aromatic pollutants using ligninolytic enzymes has been extensively researched by academic, industrial and government institutions, and has been shown to have considerable potential for industrial applications.

Previously the production of these enzymes was done using batch cultures. However, this resulted in low yields of enzyme production and therefore an alternative method had to be developed. Little success on scale-up and industrialisation of conventional bioreactor systems has been attained due to problems associated with the continuous production of the pollutant degrading enzymes. It was proposed to construct an effective capillary membrane bioreactor, which would provide an ideal growing environment to continuously culture an immobilised biofilm of *P. chrysosporium* (Strain BKMF-1767) for the continuous production of the ligninolytic enzymes, *Lignin(LiP) and Manganese(MnP) Peroxidase.* A novel membrane gradostat reactor (MGR) was shown to be superior to more conventional systems of laboratory scale enzyme production (Leukes *et.al.,* 1996 and Leukes, 1999). This concept was based on simulating the native state of the WRF, which has evolved on a wood-air interface and involved immobilisng the fungus onto an externally skinless ultrafiltration membrane. The MGR however, was not subjected to optimisation on a laboratory scale.

The gradostat reactor and concept was used in this work and was operated in the dead-end filtration mode. The viability of the polysulphone membrane for cultivation of the fungus was investigated. The suitability of the membrane bioreactor for enzyme production was evaluated. The effect of microbial growth on membrane pressure and permeability was monitored. A possible procedure for scaling up from a single fibre membrane bioreactor to a multi-capillary system was evaluated.

Results indicated that the polysulphone membrane was ideal for the cultivation of *P chrysosporium*, as the micro-organism was successfully immobilised in the macrovoids of the membrane resulting in uniform biofilm growth along the outside of the membrane. The production of *Lignin* and *Manganese Peroxidase* was demonstrated. The enzyme was secreted and then transported into the permeate without a rapid decline in activity. Growth within the relatively confined macrovoids of the membrane contributed to the loss of membrane permeability. A modified Bruining Model was successfully applied in the prediction of pressure and permeability along the membrane

The study also evaluated the effect of potentially important parameters on the production of the enzymes within the membrane bioreactor. These parameters include air flow (O_2 concentration), temperature, nutrient flow, relative redox potential and nutrient concentrations

A sensitivity analyses was performed on temperature and O_2 concentration. The bioreactor was exposed to normal room temperature and a controlled temperature at 37°C. The reactors were then exposed to different O_2 concentration between 21% and 99%. It was found that the optimum temperature for enzymes production is 37^0C. When oxygen was used instead of air, there was an increase in enzyme activity. From the reults obtained, it was clear that unique culture conditions are required for the production of *LiP* and *MnP* from *Phanerochaete chrysosporium*. These culture conditions are essential for the optimisation and stability of the bioreactor.

TABLE OF CONTENTS

Chapter 3: Theory

Chapter 4: Materials and Methods

Chapter 5: Suitability of a single fibre capillary membrane bioreactor (SFMBR) for biofilm development and continuous enzyme production

Chapter 6: Optimisation of operating parameters

Chapter 7: Monitoring the effect of microbial growth on membrane pressure and permeability

Chapter 8: Evaluating a possible scale-up procedure to a multi-capillary system

Chapter 9:   Conclusions and recommendations

LIST OF FIGURES

LIST OF TABLES

CHAPTER 1

BACKGROUND

1.1. Introduction

Internationally, research and development are paving the way for cost-effective use of membranes in an ever-widening sphere of separation applications. The increasing demand on our restricted water resources and the increasing pollution of these water resources strongly merit research into new and economically viable treatment processes.

The white rot fungus *Phanerachaete chrysosporium* and its extracellular enzymes *Lignin* and *Manganese Peroxidase* are both known to catalyse the transformation and degradation of several recalcitrant aromatic pollutants. In terms of their ecological *niche*, white rot fungi (WRF) are those organisms that are able to degrade lignin, the structural polymer found in woody plants. Lignin is a three dimensional polymer consisting of non-repeating phenyl propanoid units linked by various carbon-carbon and ether bonds. This stereo irregularity of lignin makes it very resistant to be attacked by enzymes. In addition, it is also impossible for lignin to be absorbed and degraded by intracellular enzymes. (Govender, 2000).

These fungi generally do not use lignin as a carbon source for growth; instead they degrade the lignin to release the cellulose that is contained toward the interior of the wood fibre. The same unique, non-specific mechanisms that give these fungi the ability to degrade lignin also allow them to degrade a wide range of pollutants to yield carbon dioxide. Along with their ability to degrade these chemicals, WRF possess a number of advantages not associated with other bioremediation systems. Because the key components of the white rot fungal lignin degrading system are extracellular, the fungi can degrade insoluble chemicals such as many of the hazardous environmental pollutants without assimilating the toxic chemicals intracellularly, thus reducing toxigenic effects on the white rot fungi.

These enzymes are produced by the fungi's response to low levels of key sources of carbon, nitrogen or sulphur nutrients. Existing methods of producing secondary metabolites for extended periods of time are normally batch processes. These processes are often slow and the yields low. Difficulties have been experienced in attempting to up-scale these processes for large-scale commercial use. The ligninolytic enzyme systems however is still dependent on the presence of certain growth and environmental conditions (Kirk et. al, 1978; Kirk et al, 1986; Leisola and Feichter, 1985). This becomes a problem when the bioreactor configuration and nutrient composition is being selected for large-scale applications using WRF because the design of the reactor is complicated by the number of associated variable parameters.

Several problems have been encountered in attempting to achieve efficient production of the ligninolytic enzymes from this WRF and in employing the fungus for waste water treatment making use of conventional bioreactor technology. Ultrafiltration (UF) is a well-known pressure driven membrane operation that offers a potential one-step clarification and disinfection of surface waters, to produce good quality water. Compared to conventional clarification procedures for the production of potable water, membrane ultrafiltration offers a number of distinct advantages including ease of maintenance and process control, superior water quality and less chemical addition (Edwards et.al, 1999).

The application of this promising fungus in large scale waste water treatment and or commercial production of ligninases has been hampered by the lack of bioreactor systems yielding consistent level production under long term steady state conditions and controlled growth of the fungus (Venkatadri and Irvine, 1993).

The research hypothesis was therefore to construct an effective capillary membrane bioreactor which provides a suitable growing environment to continuously culture an immobilised biofilm of *Phanerachaete chrysosporium* (Strain BKMF 1767) for the continuous production of *Lignin* and *Manganese Peroxidase* (*LiP* and *MnP*).

1.2 Research Objectives

An Eskom project was launched in collaboration with Rhodes and Stellenbosch Universities and ML Sultan and Peninsula Technikons with engineering and microbiology skills in an attempt to use membrane technology as a solution to providing a continuous bioreactor system for large-scale applications of the WRF *Phanerochaete chrysosporium*. This effort was aimed at merging local expertise in membrane science, chemical engineering and microbiology in a multi-disciplinary approach towards coupling WRF technology with membrane bioreactor systems for industrial applications.

The objectives for this study were :

- To construct and commission an experimental rig (bioreactor) for the continuous production of enzymes.

- To investigate the use of this novel membrane bioreactor system for studies on the continuous production of lignin peroxidase.

- To identify the operating parameters that affect the enzyme production.

- To perform a sensitivity analysis on the parameters identified.

- To evaluate a possible scale-up procedure.

CHAPTER 2

LITERATURE REVIEW

2.1   Bioremediation

Bioremediation, the use of biological treatment systems to destroy or reduce the concentrations of hazardous waste from contaminated sites, has found widespread appeal in recent years. Applications include clean-up of ground water, soils, lagoons, process streams and even large stretches of oil-contaminated shorelines (Leukes, 1999). Currently, microbial systems are most widely employed in bioremediation programmes, generally in the treatment of soils and water contaminated with organic pollutants.

Bioremediation has yet to be accepted as a routine treatment technology and the environmental industry is wary of applying bioremediation as a routine treatment technology (Head, 1998). Industrial companies seek to operate within the requirements of the law, but to enable them to do so, the necessary technology for pollutant elimination must be made available (Hamer, 1993). The challenge to biotechnology is to generate efficient, cost-effective and environmentally safe bioremediation technologies to replace existing standard technologies.

2.2   Bioremediation of Aromatic Pollutants

The success of bioremediation in the treatment of hazardous, recalcitrant organics has received much attention since the 1980's. Promising and innovative research has been undertaken to address contamination by aromatic compounds using biotechnology solutions. The potential advantages of biotechnology, rather than physio-chemical treatments are operation under milder, less corrosive conditions; operation in a catalytic manner; operation on trace level organic compounds and on organics not removed by existing physio-chemical processes; reduced consumption of

oxidants; reduced amounts of adsorbent materials, greater efficiency of biocatalysts and biosorbents and hence greater yield and process efficiency; less expensive process equipment and consequently lower capital investment (Belfort, 1989; Leukes, 1999; Nicell *et al.*, 1992).

2.3   Lignin Biodegradation

Lignin is a group of high-molecular-weight amorphous materials, comprising of polymers of phenylpropanoid compounds, giving strength to certain tissues. It is the second most abundant natural polymer, making up 15 to 30% of the woody cell walls of the soft and hard woods. This abundant polymer is a valuable potential resource and is the second most renewable carbon source on earth (Tien, 1987).

Biodegradation is the breakdown of living organisms of a compound to its chemical constituents. Biodegradation is also a general term referring to the undesired microbial-mediated destruction of paper, paint, metals, textiles, concrete and other materials.

A few types of microbes, predominantly the filamentous fungi, are capable of degrading and oxidising lignin to CO_2. White rot basidiomycete fungi are the only known organisms that are capable of degrading lignin extensively to CO_2 and H_2O_2 in pure cultures. Researchers have screened a large number of white rot fungi (WRF) for their ability to degrade lignin. One fungus, *P. chrysosporium*, was found to exhibit high rates of lignin degradation, rapid growth in liquid cultures and rapid sporulation.

Lignin is degraded only during secondary metabolism, which is triggered by depletion of nutrients such as nitrogen, carbon and sulphur. In addition to lignin degradation, several other features of secondary metabolism in *P. chrysosporium*, triggered by N limitation, have been studied. An understanding of the basic mechanism of lignin degradation by *P. chrysosporium* led to the proposal that fungi might be useful for the biodegradation of environmental pollutants.

2.4   The White Rot Fungus (WRF) : *Phanerochaete chrysosporium*

2.4.1   Biochemistry of *P. chrysosporium*

Most of the filamentous fungi that are important in biotechnology are members of the Deuteromycetes. *P. chrysosporium* is a member of the Basidiomysetes, but it is in the filamentous stage, rather than the sporophore, that is used in the biotechnology (Walsh, 1998). The basidiomycete, *P. chrysosporium,* means "visible hair, golden spore:

Phaneros	-	a combining form meaning visible or apparent
chaete	-	hair
crys	-	crystal
sporium	-	spores

It is a fungus with unusual degradative capabilities. This organism is termed a white rot fungus, WRF, because of its ability to degrade lignin, a randomly linked phenylpropane-based polymeric component of wood. *P. chrysosporium* belongs to a family of wood rotting fungi, that excrete highly effective extracellular oxidative enzymes (ligninases) capable of degrading not only lignin, but also a wide variety of compounds. Lignin decomposing fungi, particularly the WRF, are being increasingly evaluated for their potential in a variety of biotechnology uses (Tien and Kirk, 1988).

Basidiomycete white-rot fungi such as *P. chrysosporium* are becoming increasingly important in environmental biotechnology because they are able to metabolise a variety of organic chemicals, many of which are pollutants. They have the ability to produce non-specific ligninases which can be used to degrade pollutants both in liquid effluents and in soils. When oxygen is available and nitrogen limiting in a glucose based feed, the organism produces *Lignin Peroxidase (LiP)* and *Manganese Peroxidase (MnP)* as secondary metabolites (Tien and Kirk 1988; Glen and Gold, 1988).

The basic growth cycle of an organism (fungus) is shown in Figure 2.1 and the application of this will be explained in more detail in section 2.9.4.
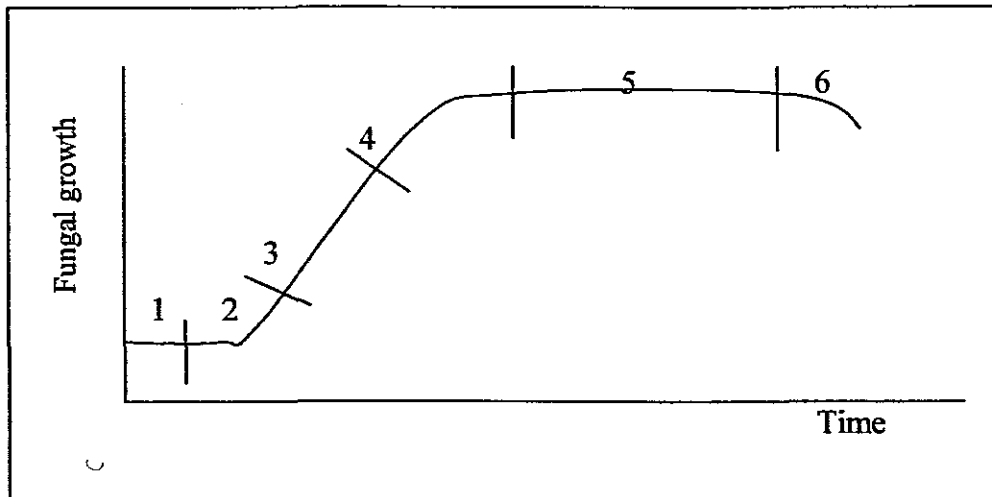
Figure 2.1:   The basic growth cycle of an organism

Where:

1   =   lag phase / period (new culture is getting used to environment)

2   =   accelerated growth (makes use of environment)

3   =   exponential growth (maturation of culture)

4   =   decelerated growth (environmental limitation sets in)

5   =   stationary phase (tries to keep stable)

6   =   decline, death of culture (environment exhausted)

This graph fits batch reactors perfectly where there is a finite amount (limiting factor) of space and food. With a continuous reactor it is easier to keep the culture in the secondary metabolic stage (end of phase 4 to beginning of stage 5). It is in this stage that the required enzymes are produced. In theory the continuous system enables the culture to be kept in phase 5. Individual fungi may die, but the culture continues. The problems with continuous systems are that the chances of contamination are high and strain degradation tends to happen after a time.

2.4.2 Differentiation within the biofilm

Biofilms consists of micro-organisms immobilised at a substratum surface and typically embedded in an organic polymer matrix of microbial origin. They develop on virtually all surfaces immersed in natural aqueous environments, including both biological (plants and animals) and abiological (concrete, cement, plastics, etc.). Biofilms form particularly rapidly in flowing aqueous systems where a regular nutrient supply is provided to the micro-organisms.

A phenomenon commonly seen in a maturing biofilm of a fungus, is the stratification of the biofilm in which the primary layering differentiates an exposed aerobic (oxygen present) and protected inner anaerobic (oxygen absent) layer. This is normally referred to as biofilm differentiation. Competition between cells in a maturing biofilm in response to environmental conditions can lead to an effect related to stress. This trauma can be created by a shift in one or more environmental factors, which no longer allows growth (Leukes, 1999).

2.5 Enzymes

The ligninolytic enzymes of the WRF have been extensively studied and investigated (Kirk and Farrell, 1987; Tien, 1987). Two extracellular enzymes, *Lignin Peroxidase* (*LiP*) and *Manganese Peroxidase* (*MnP*) were discovered in *P. chrysosporium* (Tien and Kirk, 1988; Glen and Gold, 1988). Under the appropriate conditions these enzymes are capable of either degradation (Tien and Kirk, 1983), or polymerisation (Haemmerli *et al.*, 1986) of *lignin peroxidase*.

Enzymes consist of proteins that are synthesized in cells. Enzymes have a specific activity (i.e. only react with specific compounds) and structure (i.e. all *LiP* enzymes have the same structure). These enzymes act as a catalyst, but differ from chemical catalyst in the way that they can be denatured (loss of activity). This denaturisation happens due to pH changes, temperature extremes, oxidation, organic solvents and detergents. The organism is forced to produce enzymes to order. This can be done by using additives, temperature variations or in our case starvation.

Enzymes operate on these reaction principles:

$$E + R \rightleftharpoons \{ER\} \rightleftharpoons E + P$$

E	=	Enzyme		ER	=	intermediate
R	=	Reactant		p	=	product

The enzyme is free again to convert other reactant until it gets denatured.

2.5.1 Lignin Peroxidase (*LiP*)

LiP, a family of extracellular glycosylated proteins, is an enzyme used as a catalyst of the oxidative depolymerization of lignin (Reddy and D'Souza, 1994). A number of assays are available to measure its activity. Among the most convenient is the oxidation of 3,4-dimethoxybenzyl alcohol (veratryl alcohol). *LiP* catalyses the oxidation of non-phenolic lignin model compounds such as veratryl alcohol to veratraldehyde (Tien, 1987).

2.5.2 Manganese Peroxidase (*MnP*)

MnP is another extracellular enzyme expressed during secondary metabolism as part of the lignin-degradative system of *P.chrysosporium*. *MnP* is also believed to be important in lignin degradation by this organism. (Reddy and D'Souza, 1994). The oxidation of lignin and other phenols by *MnP* is dependent on free manganous ion. The primary reducing substrate in the *MnP* catalytic cycle is Mn(II). *MnP*(II) peroxidase oxidises Mn(II) to Mn(III), which in turn oxidises a variety of organic compounds.

2.6 Industrial applications

There are an increasing number of areas where bioreactors are serious alternatives to conventional chemical reactors. In the pharmaceutical industry micro-organisms and enzymes can be used to produce specific stereo-isomers selectively. In such applications the limitations of bioreactors are clearly outweighed by the advantage in their use. The fact that the products are formed in rather dilute aqueous solutions and at relatively low rates may be of secondary importance and it may then be economically feasible to employ multiple separation stages in their purification.

2.6.1 Paper and Pulp Industry

LiP from *P. chrysosporium* have been investigated and under the appropriate conditions these enzymes are capable of either degradation or polymerisation of lignin preparations (Tien and Kirk, 1983). Either reaction may be advantageous to pulp and paper industries: the former for removal of lignin by-products from the pulp bleaching process and the latter for converting low molecular weight waste compounds into higher mass polymers which could be more easily filtered out of the process stream for subsequent incineration or landfilling. At present, these bleaching by-products are the major source of water pollution caused by the pulp industry which must employ complicated and expensive treatment systems to eliminate as much of these wastes as possible. In addition, discharge restrictions are becoming more stringent the world over and improvements in existing treatment facilities will be required in order for mills to comply with these new regulations.

Growing interest was focused on fungi, which have potentialities in solving environmental problems. This is the case of *P.chrysosporium* that can degrade aromatics and remove the coloured compounds from effluents of the pulp and paper industry. At present bleaching by-products are the major source of water pollution caused by the pulp industry which must employ complicated and expensive treatment systems to eliminate as much of these wastes as possible.

The WRF that degrade lignin have potential utility as biocatalysts for the removal of toxic organic chemicals from waste waters. *P. chrysosporium*, has been reported to degrade the chlorinated lignins and low-molecular weights chloro-organics that result from kraft wood pulping and are a major source of water pollution.

2.6.2   Waste water treatment

These systems can be used for the treatment of domestic sewage. Both potable-water supply and industrial applications of membranes are increasing concomitantly with the technical improvements and cost reductions of membranes, modules and systems. Membranes are also being increasingly used in hybrid systems and as a solution in integrated industrial water management, such as the production of potable water for developing communities, abatement of environmental pollution and industrial re-use of water.

LiP may find considerable use in the future as a treatment for pollution abatement. However, to employ enzymes in such treatments will require an economical and efficient system of application. Immobilisation of *LiP* onto inert carriers may be the most effective means for carrying out this goal. Immobilised enzymes may be incorporated into continuous process streams and can be continuously recycled when used with batch systems. In addition immobilised forms are often more stable than free enzymes.

2.6.3   Gold industry

The enzymes produced have commercial applications as they could be used by the gold mining industry to assist the process of extraction of gold from wooden supports used underground by the mining industry (Martin, 2000).

The large quantities of wood chips produced at mines from damaged underground timber contain gold that cannot be completely recovered by cyanidation. A fungus or enzyme that can degrade a portion of the wood matrix will allow the gold that was

previously locked up, to come into contact with the cyanide solution during beneficiation, thereby improving recoveries. *P. chrysosporium* and its extracellular enzymes are able to selectively breakdown lignin, which is one of the major components of wood (Martin, 2000).

2.6.4 Wine industry

Many waste materials are recognised to contain potentially useful components, should further processing be cost effective. One such example is the solid residue from the wine industry (a compost-like material comprised of stalks, skins, pips and other solid material from the grape). This material is recognised to be rich in polyphenolics. It has been recognised that valuable starting materials for the formation of antioxidants such as resveratrole, eugenol and vanilin by biotransformation are present. Preliminary research has indicated that enzyme-catalysed biotransformations can be used to upgrade the extracted components.

2.7. Membrane Bioreactors

Membrane Bioreactors represent the concrescence of the two highly exciting and rapidly evolving fields of biotechnolgy and materials science. (Leukes, 2000).

2.7.1 Bioreactor Technology

According to Ishizaki *et al.* (1998), a bioreactor is a device for conducting chemical reactions by using micro-organisms or enzymes immolilised on a porous media. Four major membrane bioreactor formats have evolved, which are currently researched or applied. These four formats are: biomass retention bioreactors; bubbleless oxygenation bioreactors; fixed film reactors and extractive membrane bioreactors. The bioreactor used in this study is classified under fixed film bioreactors (Leukes, 2000).

Fixed film membrane bioreactors are operated in a mode in which the membrane acts as a support matrix for the biological catalyst. The biocatalyst can be a biofilm of living cells (bacteria, fungi or algae), resting or permeabilised cells, or enzymes. The membrane acts as a filtration barrier to provide the biofilm with sterile, low-molecular mass nutrient source. This type of reactor is well suited for high efficiency conversion of waste water materials to valuable products. The high efficiency results from the better mass transfer provided through mass perfusion bioreactors as compared to conventional submerged culture tank reactors (bubble column and continuous stirred tank reactors) and other micro-encapsulation, immobilisation or fixed film systems. Cost reductions in medium preparation are provided through the filtration characteristics of the membrane. Further process efficiency is conferred through continuous operation over extended periods, active biomass retention at high dilution rates and continuous product removal from the biofilm, thereby minimising product inhibition (Leukes, 2000).

The membranes can be flat sheet membranes in plate-and frame configuration, capillaries, tubular membranes or hollow fibres constructed of organic polymers or ceramic materials and are usually micro filtration (MF) membranes. Excellent results have been achieve using ultrafiltration (UF) membranes (Leukes,. 1999; Govender, 2000). The membrane structure is specially developed to provide maximum surface area for attachment or entrapment of the bio-catalyst, while the materials are chosen for maximal compatibility with the bio-catalyst and the effluent components. The bio-catalyst can be situated on either the internal or external surface of the membrane, with the nutrient feed perfusing from the shell or lumenal compartment (Richardson and Peacock, 1994).

2.7.2 Membrane Technology

The use of membranes has become established practice for a wide range of large scale industrial separation processes. One major issue that plagues many of these processes, reducing their efficiency and the service life of membranes, is surface fouling. Membrane fouling is receiving increased attention at a fundamental research level. Models are appearing or being developed which predict the expected fouling or

establishes the limiting operating conditions under which fouling would still be tolerable and non-permanent.

Ultrafiltration is a pressure-driven membrane filtration operation that allows the removal of species of sub-micron-size from water. Low-molecular-mass cut-off ultrafiltration membranes provide not only the means to reduce microbial counts in water, but readily remove components that contribute colour and turbidity to such water. It is a filtration technology that can be applied to the production of potable water from contaminated surface and subsurface water resources and can also be applied to wastewater remediation and the pre-treatment of sea water and other water, for desalination by reverse osmosis.

2.7.3 Membranes

Membranes are thin films of porous material, which can be used for a number of chemical separations. The small pores of the membranes can serve as a physical barrier, preventing passage of certain materials such as salt, bacteria and viruses while allowing the free passage of water and air.

A number of techniques are available to prepare synthetic membranes and the choice of the material limits the preparation technique employed (Howell, *et. al.*, 1993)
Membrane preparation techniques include:

- Precipitation by controlled evaporation
- Precipitation from the vapour phase
- Thermal precipitation
- Interfacial precipitation

According to Howell *et.al.* (1993) the performance of membrane systems is determined by transport processes. These influence the three interdependent stages, which involve:

- Convective and diffusive flows on the feed side of the membrane
- Permeation of material through the membrane
- Transfer of material into the permeate stream

Microfiltration (MF) membranes are typically used to reject suspended solids. Ultrafiltration (UF) membranes, containing much smaller pores, are able to reject macromolecular solutes in the molecular weight range of about 10^{-3} to 10^{-6}. In the case of nanofiltration (NF) the pores are so small that they are able to reject microsolutes in the range of 200 to 1000 Dalton (Da).
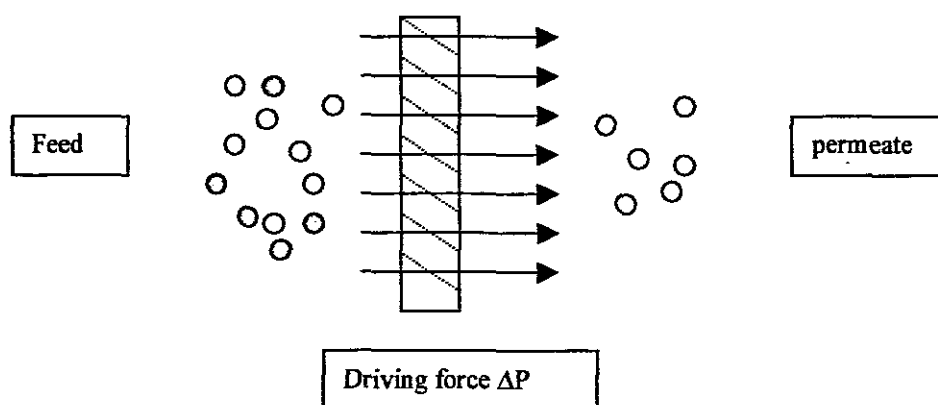
Figure 2.2: The application of pressure driven membrane processes (ΔP) in relation to particle or solute size.

The membrane morphology as depicted in Figure 2.2 (Govender, 2000) is a simplification, which serves to illustrate the basic principles in structure, transport and application more readily (Howell et.al., 1993). The morphology can be further classified into symmetric and asymmetric structure. The thickness of symmetric membranes (porous or non-porous) ranges roughly between 10 to 200 µm. Asymmetric membranes consist of a dense top layer (skin) with a thickness of 0.1 to 0.5 µm. These membranes combine the high selectivity of a dense membrane with the high permeation rate of a very thin membrane (Howell et.al., 1993).

2.7.4 Capillary Membranes

According to a report to the WRC (No. 632/1/97), by Jacobs and Sanderson (1997), capillary membranes by definition, are narrow-bore tubular-type membranes, typically with outside diameter that ranges between 0.7 mm to 3 mm, and inside diameters that range from 0.4 to 2.4 mm. Unlike the large-bore tubular membrane types, capillary membranes, because of their small diameters, are self-supporting.

The capillary membrane described in this report fall in the category of integrally skinned asymmetric membranes. Integrally skinned refers to the skin layer of the membrane being an integrated part of the membrane's substructure. Asymmetric refers to the graded porosity of the membrane's substructure which is most dense just below the skin layer, but increasingly porous with distance away from the skin layer. The substructure may be entirely sponge-like, or it may contain finger-like macrovoids (Jacobs and Sanderson, 1997).

Although many membranes are made from polymer films, membranes can be formed from ceramics, carbon fibre and porous metal substrates. The pores can range from atomic dimensions (<10 angstroms) to 100+ microns. Pores of 15 – 70 nm in diameter are required for immobilising enzymes and pores over 5 – 30 µm in diameter are required for immobilising micro-organisms.

Numerous other carriers have been tried for the immobilisation of *P. chrysosporium*, such as nylon web, polyurethane foam, silicone tubing, sintered glass, porous ceramics, polypropylene stainless steel, agarose and agar gel beads. *P. chrysosporium* has been immobilised successfully on nylon mesh and polyurethane foam, but these supports are not rigid enough for use in large bioreactors, and removal of the spent mycelium is infeasible. The externally unskinned polysulphone membranes used for this project provide a unique substructure matrix within which a fungus of a filamentous nature can be immobilised for biocatalysis.

2.8.   Polysulphone Capillary Membrane

Many UF capillary membranes are available on the commercial market. It was therefore important that the development of a new membrane should improve and not duplicate existing membranes. The research was conducted by Leukes, W. and Jacobs, E.; in association with other WRC-funded projects so that it would complement the development of membrane-process technology. The programme areas concerned were in the fields of biotechnology (membrane bioreactors and new membranes for use in membrane bioreactors) and in the production of potable water from the highly coloured water in the Southern Cape (Jacobs and Leukes, 1996; Jacobs and Sanderson, 1997).

2.8.1   Production development (manufacture of a novel membrane)

According to Jacobs and Leukes (1996) and Jacobs and Sanderson (1997), there were two directives for the development of the skinless membrane. One was to design a membrane-fabrication protocol that would result in the production of a low–pressure medium-molecular-mass cut-off (MMCO) UF membrane producing potable water. The other requirement was to generate a membrane that would allow the life cycle of a fungus to be manipulated in a membrane bioreactor to stimulate the continuous production of secondary metabolites (enzymes) useful in the bioremediation of objectionable non-biodegradable organic species in water.

In the latter case it was argued that a suitable membrane for this application should be one that was internally skinned, with a substructure containing closely-packed narrow-bore macrovoids that extend all the way from just below the skin layer to the membrane periphery. The fungus is to be grown within the confines of these macrovoids. Further to inoculate the macrovoids with spores, the macrovoids had to be accessible from the outside. This would be possible only if the membrane had no skin layer on the outside.

The pressure across an UF membrane depends on the resistance of the membrane skin layer, its supporting sub-layer(s) and the membrane substructure. If any of these resistances could be reduced, the overall resistance to transport would be reduced and it would be possible to operate the membrane at lower transmembrane pressures.

2.8.2 Observation of pore structure

Pore size can be evaluated approximately by microscopic observation. The optical microscope can be used for macro-porous materials with pore diameters down to 50 μm. Scanning electron microscopy (SEM) is more convenient and more useful than optical microscopy. Pore size can be measured precisely using SEM and image analysis techniques are useful because SEM images of pore structure can be analysed numerically by a computer.
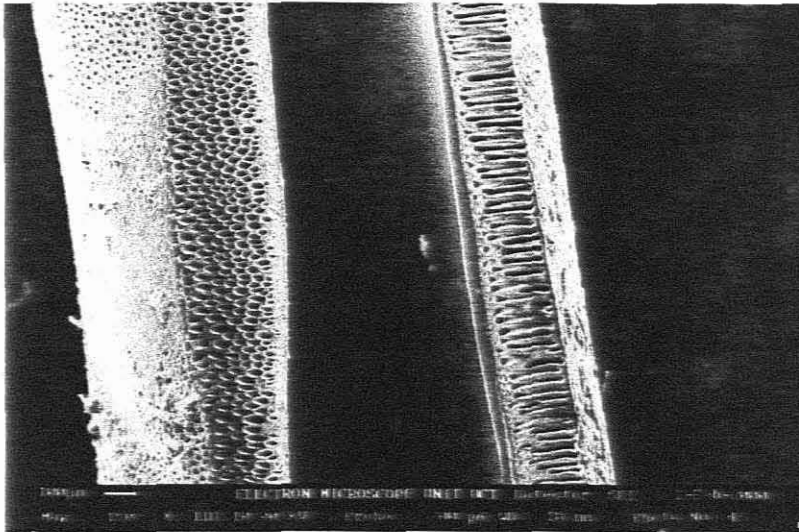
Figure 2.3: SEM photograph of a longitudinally sectioned sample of the polysulphone internally skinned and externally unskinned membrane

The left side of the membrane was folded over to observe the outside surface of the membrane. A striking feature of the membrane was the regularity of the macrovoids present in the sub-structure and the complete absence of an external layer which allowed the macrovoids to be inoculated with fungal spores by reverse filtration.

It was estimated that there are 9.6 x 10^6 of these narrow bore macrovoids in a meter-length of the membrane. The membrane has an instantaneous burst-pressure of >1800 kPa. It was difficult to reproduce the unskinned membranes and slight variations occurred. The membranes proved useful for the immobilisation of fungi and enzymes and are extensively being tested in novel biotechnological approaches in wastewater remediation (Jacobs and Sanderson, 1997).

2.8.3 Flow Through the Externally Skinless Membrane

The Hagen-Poiseuille model is often used to describe liquid flow through the pores of a membrane:

$$J = \frac{\varepsilon \, d_p^2 \, \Delta P}{32 \, \Delta \chi \, \mu}$$

ε -   number of pores

d_p -   pore diameter [m]

ΔP -   applied hydrodynamic pressure [Pa]

$\Delta \chi$ -   membrane thickness [m]

μ -   solvent viscosity [Pa.s]

This relationship shows clearly that membrane flux is directly proportional to the number of pores in the membrane skin-layer, the pore dimensions and the applied pressure. It also shows that the flux is inversely proportional to the membrane thickness. It is evident from the equation that the flux of a membrane with certain fixed pore size can be increased by reducing the thickness of the membrane skin (i.e. by reducing the membrane resistance), or by increasing the number of pores in the membrane. If the membrane resistance were to be reduced, the driving force required to produce a unit volume of product would likewise be lower (Jacobs and Sanderson, 1997).

It is primarily the morphological properties of the skin layer on the inside of the membrane that effect separation. Any skin on the outside of the membrane will

contribute to the pressure drop across the membrane and not to the separation efficiency of the membrane. The overall membrane resistance can therefore be lowered if:

* The thickness of the internal skin layer is reduced
* The porosity of the spongy sub-layer is increased and
* The definition of the external skin layer reduced.

If the walls of the macrovoids in the wall of the membrane were also skinned, they could contribute substantially to the pressure-drop across the membrane wall. It was therefore important for the walls of the macrovoids to be open-porous, particularly if the membrane has no external skin-layer; and if the macropores extend all the way from the membrane periphery to the internal skin layer. Membrane resistance would then essentially be a function of the properties of the skin layer (Jacobs and Sanderson, 1997).

2.9   Biotechnology of WRF enzyme production

Factors limiting microbial growth must also be understood and controlled. In modern biotechnology micro-organisms with specific genetic characteristics can be constructed to meet the desired objectives. The media and growth conditions used in industrial processes often are created to provide specific limitations on microbial growth and functioning. Different types of products are produced during and after the completion of microbial growth. Stopping growth at a specific point often is a necessary part of an industrial process. In many situations it is important to inhibit microbial degradation of material, or biodegradation. In other situations it is desirable to facilitate these degradation processes through bioenhancement or bioremediation. Microbial cells and their products can be used in immobilised forms and have many uses, including the removal of metals from process streams.

2.9.1 Method of producing secondary metabolites

Continuous production of ligninolytic enzymes has not been widely reported for WRF. It has been difficult to achieve since these enzymes are produced as secondary metabolites (Govender, 2000). Continuous processes reported for ligninolytic enzyme production in *P. chrysosporium* have involved regeneration of mycelium in successive growth production cycles (Feijoo *et.al.*, 1994). This type of system gave peaks of LiP activity during production phase before a regeneration of biomass phase of approximately 6 days was required. Activity was shown to decline after each successive cycle (Venkatadri and Irvine, 1993).

2.9.2 Nutrient gradients

It has been shown that nutrient gradients are established in biofilms of immobilised organisms. Substrate gradients results in heterogeneous distributions of viable cells owing to growth and death of cells. The profile of substrate concentration versus the distance from the surface of the biofilm is determined by the following:

- Microbial substrate uptake rate, which is a function of micro-organism concentration and their affinities for the substrate;
- Substrate transport rate through the film, which depends on substrate diffusivity through the biofilm;
- Substrate transport rate to the biofilm, which is a function of microbial substrate uptake rate, substrate diffusivity through the water and hydrodynamics near the biofilm surface (Siebel, 1992).

Nutrient and physical gradients not only occur in immobilised cells but also in natural biofilms and other environments. Spatial heterogeneity and the general lack of nutrients in natural environments means that molecular diffusion is the dominant transport process for nutrients. For these reasons dynamic models have been developed describing simultaneous substrate diffusion, consumption and growth. Similar research has been undertaken to characterise the structural homogeneity of biofilms resulting from spatial gradients (Walsh and Malone, 1995).

In view of the above-mentioned phenomena, it was conceived that spatial concentration gradients could be exploited to continuously produce secondary metabolites as it is triggered by nutrient starvation. Thus, reactors were considered that operate on the basis of the maintenance of steady-state nutrient gradients. Such reactors were termed "gradostats" (Wimpenny, 1990).

2.9.3   Gradostat systems

The term gradostat was first used by Lovit and Wimpenny (1981) to describe a chamber where steady state nutrients and oxygen gradients can be established and maintained at steady state in order to study various ecological implications of similar environments in nature. Various other format of gradostats are described (Leukes, 1999) and attached growth perfusion systems were evaluated for continuous ligninase production of *P. chrysosporium*. One of the most effective of these is membrane bioreactors.

2.9.4   Membrane Gradostat Reactor

From a study of the requirements for bioreactor design for *P. chrysosporium*, consideration of the native state of this organism and the characteristics of membrane bioreactors, a novel membrane gradostat reactor was conceptualised as a solution to continuous production of enzymes and bioremediation using *P. chrysosporium*. It was based on the establishment of nutrient gradients in a perfusion biofilm reactor configuration. Thus, a problem of nutrient gradients in membrane bioreactors and biofilms was formulated into a solution to the problem of continuous secondary metabolite production in filamentous fungi (Leukes, 1999).

The term "membrane gradostat " is used to describe a biofilm reactor with a good potential for industrial application, which uses a synthetic capillary ultrafiltration membrane as a support matrix for the biofilm. The term gradostat applies since although gas and liquid nutrient gradients flow is uni-directional, bi-directional contact occurs between the primary an secondary growth phases of the biomass

(Leukes, 1999). The essence of this system is described below and is depicted schematically in Figure 2.4.
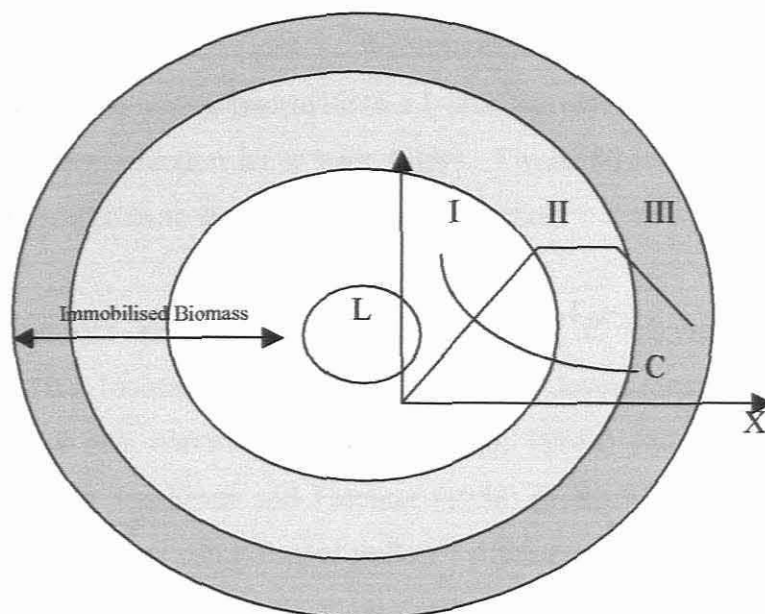
Figure 2.4 : Schematic representation of the membrane gradostat concept with superimposed batch culture growth curve. (I) Primary growth phase, (II) Stationary growth phase, (III) Decline phase. (Modified from Leukes, 1999).

L – lumen of the capillary membrane from which the nutrient is supplied.

X – radial distance from the lumen in the direction of the nutrient flow

C – concentration of growth limiting substrate

In practice the concept would involve immobilising fungal biomass onto the spongy layer of a capillary membrane and developing a biofilm of sufficient thickness, density and activity to establish a radial nutrient gradient across the biofilm. New biomass would then be produced continuously near the surface of the membrane where nutrient rich conditions prevail. This biomass would be pushed outward by newly formed biomass to an area of low nutrient concentration. Here the biomass passes into secondary metabolism activating its enzyme production system at he hyphial tips. Inactive biomass and spores produced are sloughed off the outermost reaches of the biofilm by the turbulent air supply passing through the extra-cellular (shell side) space. There would therefore be no need to regenerate biomass and force it into secondary metabolism by alternating growth and production medium cycles. (Leukes, 1999).

2.10   Other bioreactor systems

Initial attempts at the productions of *lignin peroxidase* in conventional stirred tank reactors were unsuccessful. Kirk *et al* (1986) produced 130 U/l of *LiP* activity using a 2.5-L rotating biological contactor (RBC). Willerhausen *et.al.* (1987) demonstrated mycelial growth on silicone tubing inserted into a 1-litre bioreactor, produced 232 U/l and maintained enzyme production for at least 4 days. Tween 80 and veratryl alcohol were used as culture additives to enhance enzyme production.

Cultivation of nylon-web and polyurethane immobilized *P. chrysosporium* was attempted in 8- and 10-L bioreactors (Linko, 1988a,b). *LiP* levels seemed to fluctuate from ~100 to 750 U/l in a continuous system (Linko, 1988a) without resulting in steady state production. Janshekar and Fiechter (1988) produced 62 U/l in a 30-L pilot scale stirred tank reactor using fungal pellets. Attempts to up-scale to a 200-L reactor resulted in the growth of mycelial flocks and no lignin peroxidase production. Other systems recently used include an air-lift reactor yielding 780 U/l, reactors with nylon sheet immobilization yielding 1035 U/l and a reactor with sintered glass immobilization yielding 2200 U/l. Also, high activities were reported in some small cultures of up to 100 ml using various mutant strains and modified culture conditions (Capdevila *et.al*, 1989 and 1990)

Innovative biofilm systems such as silicone membrane bioreactors (Venkatadri and Irvine, 1993) gave higher yields of LiP than conventional systems. This was attributed to reactor configurations that provided excellent O_2 mass transfer, because of solution-diffusion type transport of O_2 through the silicone rubber. Critical analysis of the requirements for bioreactor design for *P. chrysosporium* and consideration of the native state of the WRF and the characteristics of membrane bioreactors led to the development of a novel membrne gradostat (MGR) for continuous ligninase production (Leukes *et. al.*, 1996).

The various reported *LiP* activities must be compared with caution because of the wide differences in both the culture conditions used and conditions used to assay enzyme activity. Such information would be desirable to assess the application potential of this system in a continuous hazardous waste treatment process.

2.11 Significance of literature study

This literature review highlights the background information required for this project. It explains the fungus, *P. chrysosporium* and the method of producing secondary metabolites.

Few studies have reported the use of *P. chrysosporium* based reactor systems for waste treatment. Much of the research work conducted so far on the degradation of hazardous compounds by *P. chrysosporium* has been carried out at the flask-scale and has not been optimised. From the literature study it is clear that consistent high level enzyme production has been hampered by the lack of continuous bioreactor systems. Low levels of *LiP* produced by *P. chrysosporium*, slow growth of the organism resulting in low degradation rates, the lack of reliable bioreactor systems and the lack of criteria for convenient scale-up are some of the constraints in the application of this fungal system.

Thus far, the lack of systems yielding (1) consistent production of high levels of lignin peroxidase , (2) steady state continuous enzyme production and fungal activity over extended periods of time, (3) controlled growth of the fungus and (4) criteria for convenient scale-up has impeded the progress in the use of *P.chrysosporium* in large-scale waste treatment and enzyme production applications.

In dryer areas of the world membranes are fast becoming an accepted method for the reclamation of domestic wastewater. A wide range of hazardous compounds are transformed by the white rot fungus *P. chrysosporium* and its extracellular enzyme *LiP*. Low levels of *LiP* produced by P. chrysosporium, slow growth of the organism resulting in low degradation rates, and the lack of reliable bioreactor systems and the lack of criteria for convenient scale-up are some of the constraints in the application of this fungal system in hazardous waste treatment. This research therefore focused on the use of a biofilm membrane reactor system for the improved production of *LiP*.

CHAPTER 3
THEORY

3.1   General Description of pressure and permeability correlations in hollow fibre membrane modules

A coherent description of flow phenomena in hollow fibre membrane devices was given by Bruining (1989), that predicts the pressures and flows occurring under various operating modes. The analysis had relevance to the more general case of laminar and turbulent flow in porous ducts.

Flow phenomena in porous ducts have been studied. A general model was derived that predicts the pressure drop and the magnitude and direction of flows in hollow fibre modules for different modes of operation. Only two dimensionless parameters were needed to predict all pressures and flows. One parameter is equal to the ratio of viscous flow resistance in the fibres and the fibre wall permeation resistance whereas the other is related to the entrance flow and its physical properties. The analysis was carried out for an incompressible pure fluid with laminar or turbulent flow inside the fibres. A constant pressure on the module shell side was assumed.

Figure 3.1 (Bruining, 1989) shows some of the flow configurations that can be realised with hollow fibre modules. Each mode of operation can be characterised by the quantity F_2, which denotes the fraction retentate, defined as the fibre side exit flow divided by the fibre side entrance flow. Though all configurations are guided by the same physical principles, the pressure drop that will occur as well as the magnitude and direction of the flows will be different in each case.

A number of flow configurations have been discussed in the literature. Chatterjee and Belfort (1986) gave an extensive review of the work which has been carried out on flow in porous ducts. Whereas most of the previous work has been for slits, tubes and annuli, they studied flow in a spiral wound membrane module.
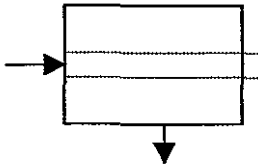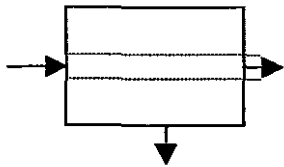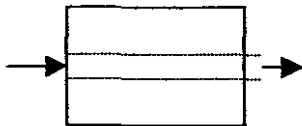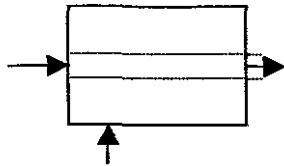
Permeation Process	Situation	Retentate (F_2)
Dead-end filtration		$F_2 = 0$
Continuous open shell mode		$0 < F_2 < 1$
Closed-shell Mode		$F_2 = 1$
Suction of permeate		$F_2 > 1$

Figure 3.1: Some modes of operation of hollow fibre devices (cited in Bruining, 1989)

Quaile and Levy (1975) studied a laminar flow dead-end filtration. Recently Tharakan and Chau (1986) presented data on pressure drops and flows for different modes of operation of hollow fibre modules among which the closed-shell mode. Unfortunately, no mathematical analysis was presented in their paper.

3.2. Theory on flow, pressure and permeability

An analysis was given by Bruining (1986) of flows and pressures in hollow fibre modules, how they are interrelated for different modes of operation of a device and how they depend on the entrance flow rate and medium physical properties, as well as fibre dimensions and fibre wall permeability.
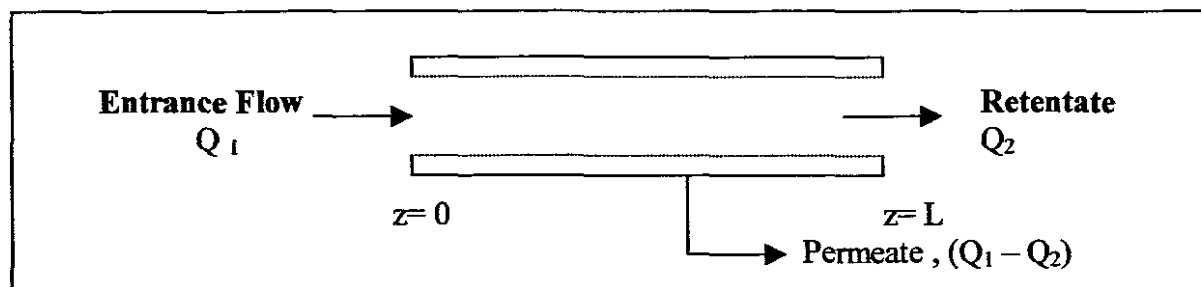
Figure 3.2: **Laminar flow inside a hollow fibre module with a constant shell side pressure (Modified from Bruining, 1989)**

Consider a single fibre capillary membrane as shown in Figure 3.2. Let Q_1 be the volumetric flow rate entering at $z = 0$, where z is the distance from the entrance of the membrane. Define the pressure at the entrance of the module as P_1, the pressure at the exit of the fibre as P_2 and let the pressure on the shell side be P_3. At any distance z from the entrance the flow rate inside the fibre is Q and the pressure P.

A mass balance over a slice dz of the fibre gives

$$\frac{dQ}{dz} = -\Pi d_i J \quad \text{where} \quad J = \frac{K (P - P_3)}{\mu d_w} \quad \text{.................3.1}$$

$$\text{and} \quad d_w = \frac{1}{2} d_i \ln \frac{d_o}{d_i}$$

where :

J	=	local permeation flux (m/s)
d_w	=	average wall thickness (m)
d_i	=	inner fibre diameter (m)
d_o	=	outer fibre diameter (m)
μ	=	fluid viscosity (Pa.s)

K tends to change with biofilm growth on the membrane and is referred to as the fibre wall permeability coefficient (m^2), rather than permeability constant.

For this set of equations the boundary conditions are

At $\quad z = 0 : Q = Q_1$ $\qquad\qquad$ then $\quad P = P_1$....................................3.2

Now the following dimensionless groups can be introduced:

$x = z/L$, where L = fibre length (m)...3.3

$P_r \quad = \quad \dfrac{P - P_3}{P_1 - P_3}$ $\qquad\qquad$ [a dimensionless pressure]............3.4

$\Psi \quad = \quad \dfrac{128\,\mu\,L\,Q}{\Pi\,d_i^{\,4}\,(P_1 - P_3)}$ $\qquad$ [a dimensionless flow rate inside the fibre].....................................3.5

$T_L \quad = \quad \dfrac{128\,K\,L^{\,2}}{d_i^{\,3}\,d_w}$ $\qquad\qquad$ [a dimensionless transport modulus]..3.6

T_L is a dimensionless (laminar flow) transport modulus representing the ratio of viscous flow resistance inside the fibre and the fibre wall permeation resistance.

After mathematical manipulation and by differentiation with respect to x and substitution the following homogeneous second-order differential equation was obtained:

$\dfrac{d^2 P_r}{dx^2} = T_L P_r$..3.7

The solution of this equation is

$$P_r = \cosh(x\sqrt{T_L}) - \frac{\Psi_1}{\sqrt{T_L}} \sinh(x\sqrt{T_L}) \dots\dots\dots\dots\dots 3.8$$

By substitution of $\Psi = \Psi_2$ and $P_r = P_{r2}$ at $x = 1$ the following expressions are obtained:

$$P_{r2} = \cosh(\sqrt{T_L}) - \frac{\Psi_1}{\sqrt{T_L}} \sinh(\sqrt{T_L}) \dots\dots\dots\dots\dots 3.9$$

By defining the fraction of retentate at $x = 1$ as $F_2 = \dfrac{\Psi}{\Psi_2} = \dfrac{Q_2}{Q_1})\dots 3.10$

the following unique relation between F_2, T_L and Ψ_1 is found:

$$\Psi_1 = \frac{\sqrt{T_L}}{\cosh\sqrt{T_L} - \dfrac{\sinh\sqrt{T_L}}{F_2}} \dots\dots\dots\dots\dots\dots\dots 3.11$$

For each mode of operation of a hollow fibre module a value of F_2 can be substituted into Equation 3.11. In the case of a dead-end filtration experiment, without a shell side pressure drop, it is known that $F_2 = 0$.

After mathematical manipulation the following equation was obtained:

$$\sqrt{T_L} = \ln\left[\frac{1 + (1-P_{r2}^2)^{1/2}}{P_{r2}}\right] \dots\dots\dots\dots\dots 3.12$$

By measuring P_1, P_2 and P_3, the value of P_{r2} can be found and the value of T_L can be calculated. One can carry out experiments with different geometries (L, d_i, d_w) and find values for the membrane permeability K.

3.3. Fluid permeability, filtration and flux

The permeability of a membrane is defined as the ability of the membrane to be permeated, in other words to allow a fluid to pass through its porous structure or the ability of the membrane to be penetrated throughout.

When using porous materials in applications with fluid permeation, high fluid permeability is usually required for a high filtration rate. Fluid permeability provides information about the pore structure, such as the tortuosity of pore connections. A fluid permeation test is sometimes used to measure the pore size of porous materials. By measuring the flux of a non-wetting fluid as a function of the pressure drop across the membrane it is possible to determine the pore size distribution.

The fluid permeability of porous materials depends on the degree of open porosity, pore size, pore shape and the tortuosity of pore network. Fluid flows in porous materials can be classified into several types. In general, fluid permeation of micro-porous materials follows Darcy flow. When a liquid such as water passes through a porous material, the flow velocity, v, is proportional to the pressure drop across the porous material, ΔP, in the linear flow case and can be expressed as follows:

$$v = \frac{Q}{A} = \frac{K_p}{\mu} \frac{\Delta P}{\Delta \chi} \quad \text{...........................3.13}$$

Where:

v	=	fluid velocity through membrane (m/s)
Q	=	volumetric flow rate (m³/s)
A	=	cross-sectional area of a porous material (m²)
K_p	=	proportional constant known as permeability coefficient
ΔP	=	pressure drop across the porous material (Pa)
μ	=	viscosity of the liquid (Pa.s)
Δχ	=	thickness of porous material (m)

Assuming that all penetrating pores are cylindrical in shape and that all open pores are penetrating ones, the liquid flow can be represented by the Hagen–Poiseuille flow equation as shown in section 2.8.3.

In filtration, two modes of operation exists; that is dead-end filtration and cross flow filtration. In dead-end filtration the feed flow is perpendicular to the membrane surface, so that the retained particles accumulate and form a cake layer the membrane surface. The thickness of the cake layer increases with filtration time and consequently the permeation rate decrease with increasing cake layer thickness. The pressure drop across the layer similarly increases with time. In cross-flow this does not happen to the same extent, as the scouring action of the fluid in cross-flow motion has a limiting effect on the thickness to which the gel-layer can build up. Initially, the flux will decrease rapidly, but steady state gel-layer thickness is soon attained. The pressure drop follows the same trend if resistance due to adsorption does not prove to be predominant. The thickness of this initial layer is a function of the membrane permeability, cross-flow velocity and process fluid. The flux decline is caused by biofilm growth. This is caused by cord development inside the macroviods of the membrane.

Membrane Flux / Time

Pressure Drop / Time

Time
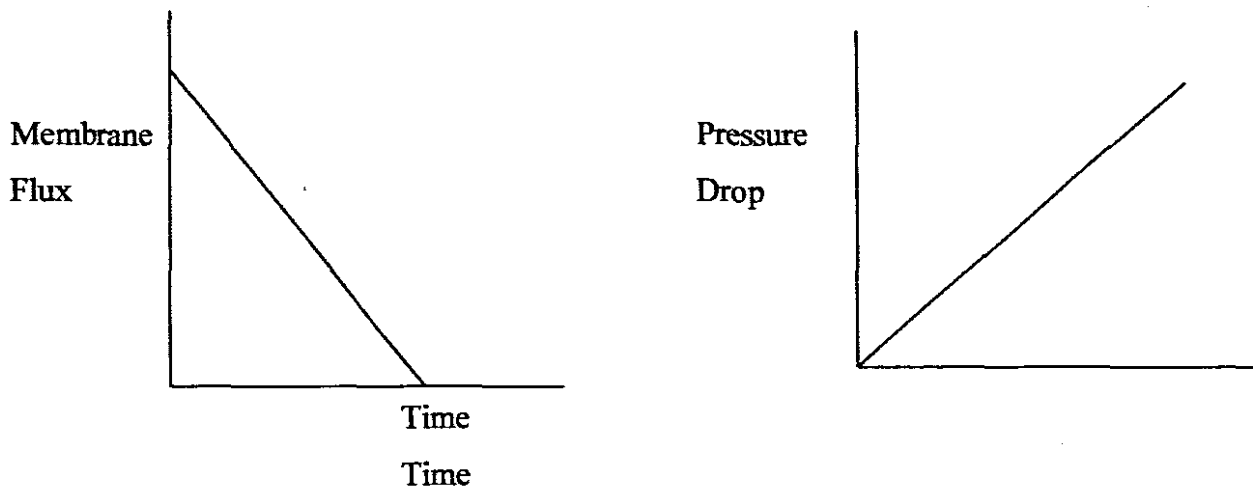
Figure 3.3: **Dead-end filtration**

Many factors affect the rate of permeate flow though a membrane; operating pressure and temperature are two of them. An increase in temperature reduces the viscosity of the feed liquid and thereby increases the flux. Membrane flux is conditionally proportional to the operating pressure. For a pressure drop below Δp_{min}, the membrane is impermeable, and as the pressure difference across the membrane reaches Δp_{min}, the fluid flow through the largest pores. As the Δp is increased, smaller pores are flooded. At a pressure drop Δp_{max}, all the pores become permeable and the flux becomes proportional to the pressure difference according to the Hagen-Poiseuille equation, see Figure 3.4 (Mc Guire, *et.al.*, 1995; martinez-Diez, *et.al.*, 2000).

When operating with an inoculated membrane, a further increase in pressure will result in a much-reduced increase in flux because the resistance of the biofilm increases so that a limiting flux value J will be attained.
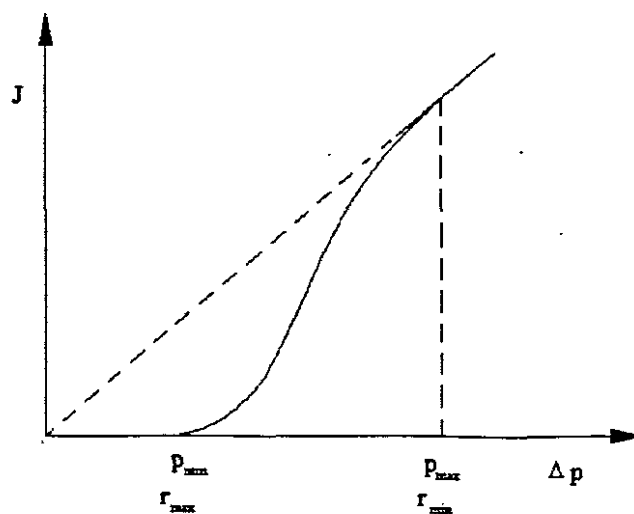
Figure 3.4 : Relationship between flux and applied pressure across membrane

J – membrane flux (m/s)

J_L – limiting permeate flux (m/s)

ΔP – Applied Pressure drop across membrane (Pa.)

3.4. Membrane Flux for Tubular or Capillary membranes

Membrane flux refers to the volume of media transported through the membrane per unit area per unit time.

$$\text{Membrane flux} = \frac{V}{(A \times t)} = \frac{V}{L (\Pi \times d_i) \times N \times t} \quad \dots\dots 3.14$$

where:

V = volume (m^3)

A = membrane area (m^2)

t = time (s)

L = tubular length (m)

d = inside diameter of the membrane (m)

N = total number of membranes in the module

3.5 Summary

The modified Bruining model was used to determine the effect of biofilm growth on membrane pressure and permeability and these results can be found in Chapter 7. The fluid permeation tests were performed as this is a fundamental aspect of the entire subject of the pressure drop study presented in this thesis, but will not be submitted as part of this thesis.

CHAPTER 4

MATERIALS AND METHODS

4.1   Method of producing secondary metabolites

A membrane gradostat bioreactor has been shown to compare favorable with more conventional systems of large-scale enzyme production. This includes a method of producing secondary metabolites, in particular for the bioremediation of wastewater containing certain pollutants. Immobilisation of the fungal cells on a support and particularly the control of the distribution of the biomass in the bioreactor, offers the possibilities for better control of the process, easier product separation and continuous operation.

The method used in this study provides a porous substratum that has a biofilm of microorganism attached thereto. A nutrient solution flows through the substratum, at a rate that is sufficiently low for a nutrient gradient to be established across the biofilm. The nutrient concentration at a high level along the gradient is sufficiently high to support primary growth of the micro-organism and the nutrient concentration at low level along the gradient being sufficiently low to induce secondary metabolite production. The substrate is in the form of a hollow fibre membrane having a relatively thin, porous skin on the inside and a relatively thick, finger-like externally unskinned void structure radiating outward from the skin (Leukes, 1999).

LiP and *MnP* production is seen during secondary metabolism and is completely suppressed under conditions of excess nitrogen and carbon. Excess Mn(II) in the medium on the other hand, suppresses *LiP* production but enhances MnP production. LiP activity is affected by idiophasic extracellular proteases (Reddy and D'Souza, 1994). The optimum production of these enzymes is also dependent on culture conditions and the nutrient composition of the feed (Capdevilla *et. al.*, 1990). The geometry and hydrodynamic aspect of the reactor are also variables that impact on the growth and productivity of *P. chrysosporium.*

4.2   Microbial culture medium development and growth conditions

The medium used to grow a micro-organism is critical because it can influence the economic competitiveness of a particular process.   Not only must the medium be sterilised but aeration, pH adjustment, sampling and process monitoring must be carried out under rigorously controlled conditions.   Many barriers exist, that limit oxygen transfer from air to an enzyme within the micro-organism.   In spite of having a high oxygen concentration with the air, the barriers to transfer into the liquid medium and finally across the cell membrane result in a low level of oxygen at the enzyme.   Only by maintaining a high aeration rate is it possible to assure that oxygen will not limit microbial activity.

4.2.1   Strain growth and maintenance of the fungus

P. chrysosporium strain BKMF 1767 was used in this study.   It was maintained on supplemented malt agar slants as described in Appendix A (A1 – A3).

4.2.2   Spore solution preparation and concentration

The spore solution for the inoculation of the reactor was prepared as described in Appendix A (A4). The separation of spores from mycelial is described in Appendix A (A5) and the determination of spore purity and concentration is described in A6.

4.2.3   Nutrient medium composition

The medium used was the standard medium of Tien and Kirk (1988) and was prepared as described in Appendix B (B1 – B8).

4.3.   Experimental Set-up

4.3.1   Module Assembly

Care was taken not to handle the membranes too much.   Only the ends of the membrane were held with the fingers.   It was important that the membranes were handled gently and with the minimum amount of movement and distortion. Cracking the membranes could have caused various complications such as:

- spore contamination in the lumen of the membrane during inoculation
- disruptive nutrient flow through the lumen of the membrane
- disruptive permeation

All autoclavable components were washed and autoclaved.   The membrane was placed through the glass tubes, into the centre of the manifold.   The glass tubes were fixed into the manifold using seals and end caps as shown in Figure 4.2.   The membrane was sealed into the glass tubes, one side at a time.   A suitable resin or glue was chosen for this and should was applied using a syringe.   A syringe seemed to work better because a certain amount of pressure could be applied.   The manifold was left over night before the other end was sealed.   Care was taken to ensure that no air bubbles were made in the glue as this could have led to problems such as:

- disruptive flow rates
- nutrient flow into the manifold
- contamination of the membrane or the escape of spores into the surrounding tubing
- a build up in pressure causing the seals to burst, which could have jeopardized the experiment at a later stage.

Before the second end of the membrane was sealed, the membrane was tensioned slightly.   Once the membrane was sealed into the manifold, the glue was trimmed down using a scalpel or razor blade.   This ensured that the membrane openings were exposed and open.   Once all of the above was achieved, the membrane was hydrated. It was important to ensure that the glass rods were properly sealed at the ends to avoid any leaks during the experiment.

4.3.2 Hydrating the Membrane

Hydrating the membrane essentially served two purposes:

- getting rid of the preservatives on the membrane
- checking that the manifold was sealed before its assembly into the rig

Tap water was pumped through the lumen of the membrane at a very slow rate, until it passed through the length of the membrane. The ends were then sealed, forcing the water to permeate through the membrane. This was done very carefully and with a fair amount if patience because if the flow rate was too high the following could have happened:

- the seals could burst because of the increase in pressure inside the manifold
- the membrane could burst because of the sudden increase in pressure inside the membrane

Once it was ensured that there were no leaks within the manifold and that the membrane was permeating sufficiently the entire manifold was submerged in tap water. The purpose of this was two fold:

- once the membrane was wet, it had to stay wet.
- the chlorine in tap water helped to get rid of the preservatives on the membrane

4.3.3 Setting up the Reactor Rig

Before setting up the reactor rig, careful consideration was given to the type of set-up that was required e.g. single membranes, membranes are parallel, dead-end or open-ended, etc. Figures 4.1 and 4.2 illustrate a single membrane in a dead-end filtration mode. The tubing used in the set up was kept to a minimum with the least amount of joints in it. All joints in the tubing were tied with cable ties. Water was passed through the system to check for any leaks as any leak could jeopardize the system by:

- causing contamination sites
- disrupting flow rates
- disrupting the pressure of the system

Once the entire system was leak proof, sterilization was started.

Air Pump Humidifier
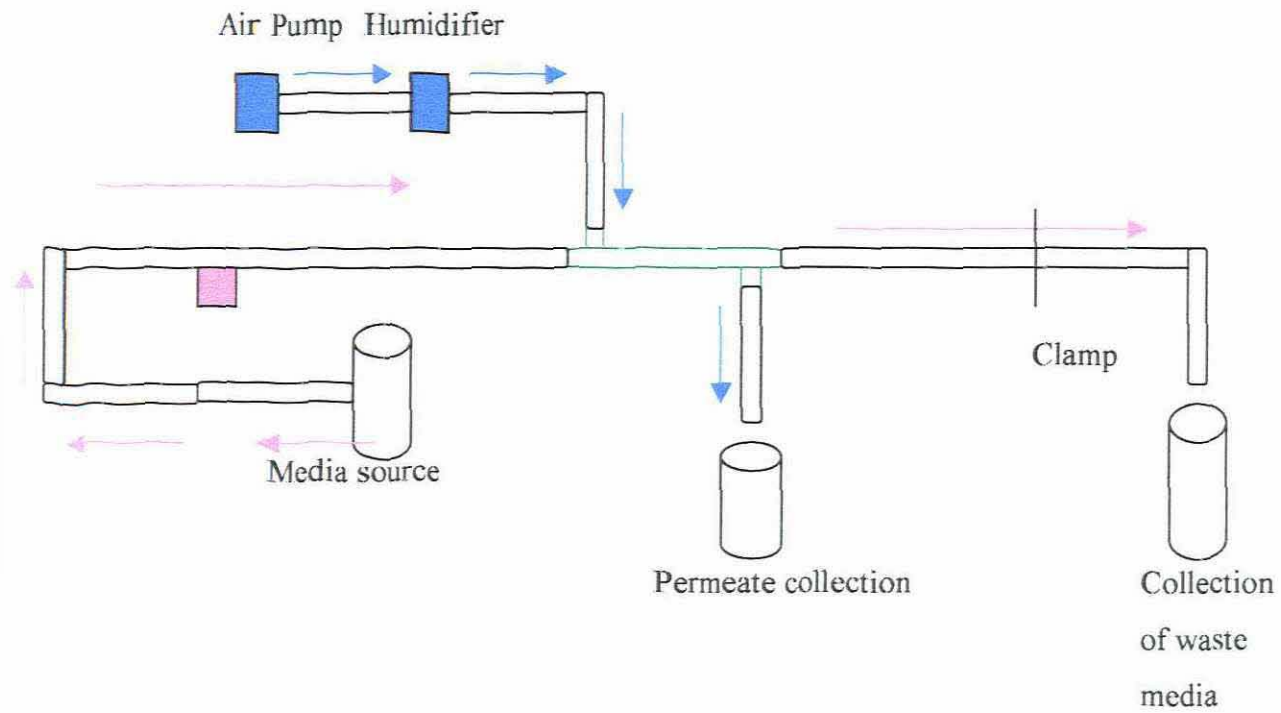
Figure 4.1:   **Diagram of semi-continuous reactor rig**

Air

Media

Single Fibre Membrane Manifold
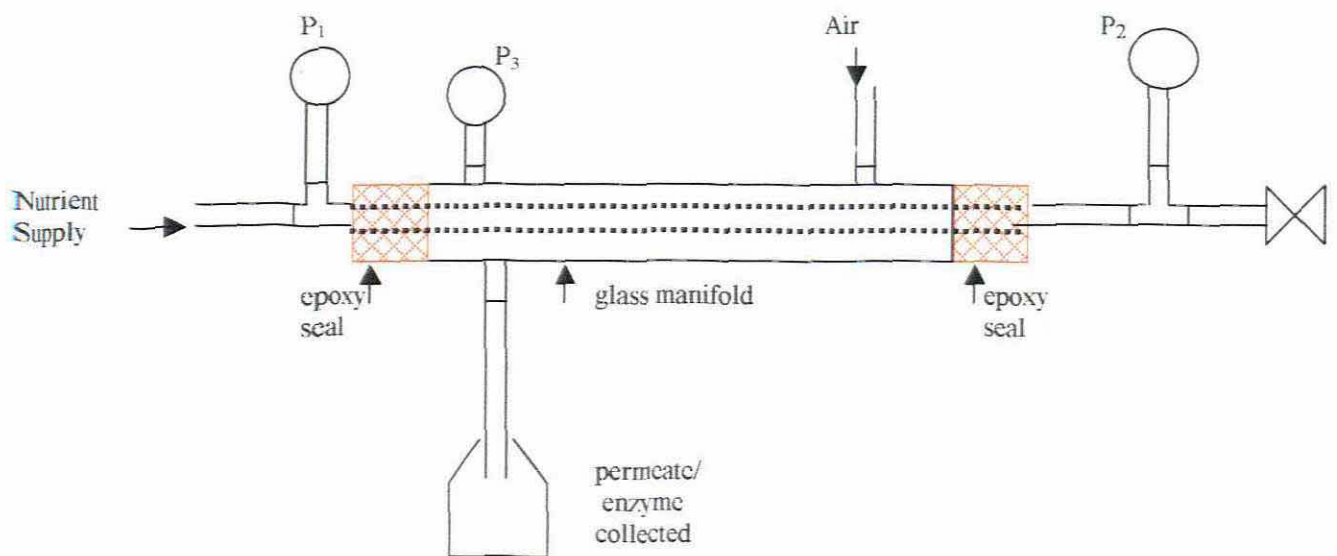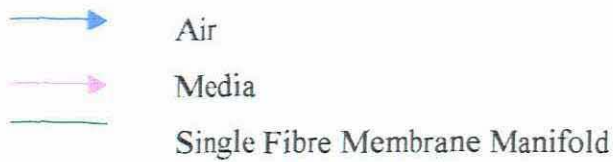
Figure 4.2:   **Single fibre membrane bioreactor (SFMBR) connections and set-up**

4.3.4 Sterilising the Reactor and the Reactor Components

Micro-organisms occur ubiquitously in nature, so the design of any bioreactor system must prevent the entry of contaminating microbes at inlets, exits and analyses ports for gases and liquids. Sterility design is also critical for regularity and containment purposes. With regards to *P. chrysosporium* in South Africa, the Plant Protection Research Institute stipulates complete containment (Leukes, 1999) especially in the case of the more potent lignin degrading strain BKMF-1767. An efficient and effective sterilisation procedure is therefore imperative. The development of a sterilization procedure is a combination of robust design of the reactor system coupled with an appropriate choice of sterilising agent.

Various procedures (autoclaving and steam sterilizing) and or commercially available chemicals can be used to sterilize. In traditional UF systems using UF capillary membranes the emphasis is on cleaning rather than sterilization. Hypochlorite treatment of membranes leads to unwanted salt residue build up on the membranes which is undesirable in bioreactors, while ethanol and hydrogen peroxide only disinfect the liquid phase. A 4% formaldehyde was used by Leukes (1999) as a sterilizing agent due to its volatility; such that it could sterilize the gas phase equally well.

Formaldehyde was run through the system for a minimum of 6 hours. The reactor was then rinsed with autoclaved sterile distilled water, at least twice the volume of formaldehyde. Water was usually run through the system overnight to ensure that the reactor is thoroughly rinsed. Failure to rinse the rig properly will:

- contaminate the media source
- change the pH of the system
- could lead to the deterioration of the membranes

4.3.5 Reactor membrane inoculation

The separation of spores and mycelia was crucial for continuous studies because it was necessary to ensure that mycelia fragments did not block the pores of the externally unskinned membrane surface, thus preventing spores from being immobilised by entrapment into the macrovoid cavities rather than by adsorption onto the surface. Each reactor was inoculated with a million spores.

After sterilization the reactor was set up for inoculation via the permeate line. The inoculation procedure was carried out by pumping the spore suspension through the permeate line, up against gravity. Once the manifold was filled with the spore suspension the nutrient inlet and outlet and air inlet were closed of to force the spores to adhere onto the membrane (referred to as **reverse filtration**). The water was forced to the lumen, the outlet line was opened to allow the water to flow out and decrease the pressure on the membrane, thus preventing it from bursting.

The duration for inoculation was between 6 - 9 hours, depending on the amount of reactors inoculated. If the procedure is done too quickly, the following may occur:

- the membrane will burst as a result of an increase in pressure
- the seals of the manifolds will burst because of an increase in pressure
- the entire system is compromised and the manifold will have to be reconstructed.

4.3.6   Reactor Acclimatisation

The reactor is set up with nutrient medium and air and left to run overnight before the experiment is allowed to run. This allows for the spores on the membrane to become acclimatised to the sets of conditions set out by the reactor. Additionally any stray spores that have not adhered to the membrane are blown off the membrane by the airflow that goes over the membrane. Once completed the rig is ready and the experiment can run.

4.3.7   Reactor design and experimental parameters:

The basic design of the bioreactor used in these studies consisted of a 1 mm diameter capillary membrane inserted into the middle of a 17cm x 1 cm glass manifold onto which the fungus was immobilised. The epoxy was allowed to cure for at least 24 hours, the membrane and epoxy that extended from each end of the reactor were cut off, leaving the reactor ends sealed except for the membrane lumen.

The membrane consisted of a single fibre polysulphone externally unskinned and internally skinned capillary membrane of 0.2 μm pore size. Nutrient medium was similar to that employed by Tien and Kirk (1988). Glucose was used as the carbon source and the nitrogen source was ammonium chloride. A peristaltic pump provided the nutrient feed to the inside of the membrane at a flow of 3 ml/hr.

Air was filter sterilised and humidified before passing through the reactor shell and nutrient medium was pumped through the membrane lumen. Liquid samples of permeate were collected into a glass beaker and analysed on a daily basis for temperature, pH, redox, volume, *LiP* and *MnP* activities, glucose and ammonium concentration measurements, to monitor the progress of the cultivation. Pressures for the lumen inlet and outlet, and shell side space were measured.

Some experiments were performed at room temperature and some was placed inside an incubator maintained at of 37 °C. The reactor was operated continuously until the

membrane clogged up and no permeate was collected or no enzyme activity was picked up. Once this occurred the reactor was dismantled and segments of the membrane (1mm in length) were placed in gluteraldehyde as storage and initial preparation for microscopic examination.

Electron microscopy was used to measure cell densities and to assess the fungal morphology. It also indicated the growth and immobilisation characteristics of the fungus in the macrovoids on the exterior surface of the membrane.

Figure 4.3: Photograph of a SFMBR set-up

The SFMBR, as shown in Figures 4.2 and 4.3, was developed with the following dimensions:

Reactor length:	=	0.17 m
Reactor Outside Diameter	=	0.011 m
Reactor Inside Diameter	=	0.007 m
Reactor XSA	=	9.4×10^{-5} m^2
Reactor inside surface area	=	6.1×10^{-4} m^2
Reactor Volume	=	5.14×10^{-4} m^3
Total Membrane Length	=	0.215 m
Active membrane length	=	0.15 m
Membrane inside diameter	=	0.0009 m
Membrane outside diameter	=	0.001 m
Membrane XSA	=	6.362×10^{-7} m^2
Membrane Volume	=	9.54×10^{-8} m^3
Extra-capillary reactor volume	=	5.14×10^{-4} m^3

4.4   Assays

Liquid samples of permeate were collected into a glass beaker and analysed on a daily basis for temperature, pH, redox, volume, *LiP* and *MnP* activities, glucose and ammonium concentration measurements, to monitor the progress of the cultivation.

4.4.1   *Lignin Peroxidase (LiP) activity*

LiP catalyses the H_2O_2-dependent oxidation of a wide rage of lignin-related aromatic compounds.   A number of assays are available to measure its activity.   Among the most convenient is the oxidation of 3,4-dimethoxybenzyl (veratryl alcohol) to yield veratraldehyde.   Veratraldehyde absorbs intensively at 310 nm and the alcohol does not.   Although the activity shows a pH optimum to be ±2, assays were typically

performed at pH 2.5 – 3.5, due to the instability of the *LiP* at pH values lower than 2.5 (Tien, 1987). Care was taken not to incubate the enzyme in H_2O_2 in the absence of veratryl alcohol or in pH 2.5 buffer since these treatments result in the inactivation of the enzymes. Assays were done using quartz cuvettes. The method used for *LiP* activity, which is the oxidation of veratryl alcohol to veratraldehyde, is described in Appendix C1 (Tien and Kirk, 1988).

.

4.4.2 *Manganese Peroxidase (MnP)* activity

MnP is totally and only dependent on Mn(II). MnP(II) peroxidase oxidises Mn(II) to Mn(III). Mn(III) is a non-specific oxidant, which in turn oxidises a variety of organic compounds (Glen and Gold, 1988) such as ABTS. ABTS oxidation by the peroxidase is dependent on the α-hydroxy acids such as lactate, malate, tartrate and citrate.

The method used for *MnP* activity, which is the oxidation of ABTS, is described in Appendix C2.

4.4.3 pH determination

pH was monitored on a daily basis using a Hanna HI 8314 membrane pH meter and pH probe set on the pH mode. The meter was calibrated periodically to make use that the measurements were accurate.

4.4.4 Relative Redox potential

The formation of enzyme activity was monitored by analysing the redox potential of the permeate. The relative redox potential was monitored on a daily basis using the same pH meter and pH probe as described before but set on the mV mode.

4.4.5 Glucose concentration

Glucose concentration determinations were carried out using a protocol as stated by Clark and Switzer (1976). The methods together with the preparation of the glucose standards curve is described in Appendix D1. All assays were normalised against this curve and extracellular concentrations were calculated.

4.4.6 Ammonium concentration

A spectroquant Ammonium Test Kit (Merk ®) was used to measure the amount of ammonium present in the permeate. Because the suite of ligninolytic enzymes from *P. chrysosporium* are only produced under conditions of nutrient limitation, in this case nitrogen limitation, it was necessary to monitor whether or not nitrogen limitation did indeed occur. The assay employed was related to the subsequent decrease of ammonium present in the nutrient media. The rationale behind this was to monitor the decrease of an initial concentration of 39 mg/L of ammonium tartrate in the media. The assay was carried out using the manufacturer's specifications (Walsh, 1998).

CHAPTER 5

SUITABILITY OF A SINGLE FIBRE CAPILLARY MEMBRANE BIOREACTOR FOR BIOFILM DEVELOPMENT AND CONTINUOUS ENZYME PRODUCTION

5.1 Introduction

Cell immobilization is a useful technique but problems have been experienced with the variety of entrapment matrixes in use. These problems include diffusion restrictions, reduced biocatalyst activity, lack of open spaces for growth of cells, rupture due to insufficient mechanical strength and possible toxicity caused by synthetic polymers (Govender, 2000). The potential main advantages claimed for the use of immobilized cells include easy operation and reuse of the cells, high cell concentrations and flexibility in reactor design and operation (Freeman, 1998).

The use of a membrane as an immobilization matrix presents advantages, but fungal immobilization using membranes as support matrixes is an engineering technology with limited laboratory scale success. UF membranes as support matrixes are virtually undocumented.

The method of producing secondary metabolites in this study comprised of providing a porous substratum (polysulfone externally unskinned capillary membrane) which has an immobilised biofilm of micro-organism, *P. chrysosporium* BKMF 1767, attached thereto (Leukes *et al*, 1996).

5.2   Experiment Conditions

The SCFMBR, as shown in Figures 4.2 and 4.3, was inoculated with one million spores and was run under the following conditions / parameters.

Nutrient Feed flow rate   =   3 ml/hr

Nutrient Feed temperature   =   as shown in Table 5.1 and 5.2

Air flow rate   =   as shown in Table 5.1 and 5.2

Air temperature: =   as shown in Table 5.1 and 5.2

Reactor temperature: =   as shown in Table 5.1 and 5.2

Permeate Temperature: =   as shown in Table 5.1 and 5.2

The bioreactors were then evaluated for their suitability for biofilm development and enzyme production in the various conditions. In order to characterize the membrane-immobilised fungal biofilm for the continuous production of enzymes, it was necessary to dismantle the reactor, remove the membrane and prepare sections of it for Scanning Electron Microscopy (SEM) photographs. Structural development of *P. chrysosporium* within these macrovoids was observed and correlated to immobilization effectiveness.

5.3   Fungal Immobilisation and Spore attachment

5.3.1   Spore Attachment

The membranes were designed to provide a unique substructure matrix within which a fungus of filamentous nature could be immobilized for biocatalysis. It was reasoned that the ideal membrane should be internally skinned with an annular wall consisting entirely of narrow bore, closely packed, finger-like cavities (macrovoids), radiating outwards from just below the skin layer (Jacobs and Leukes, 1996).
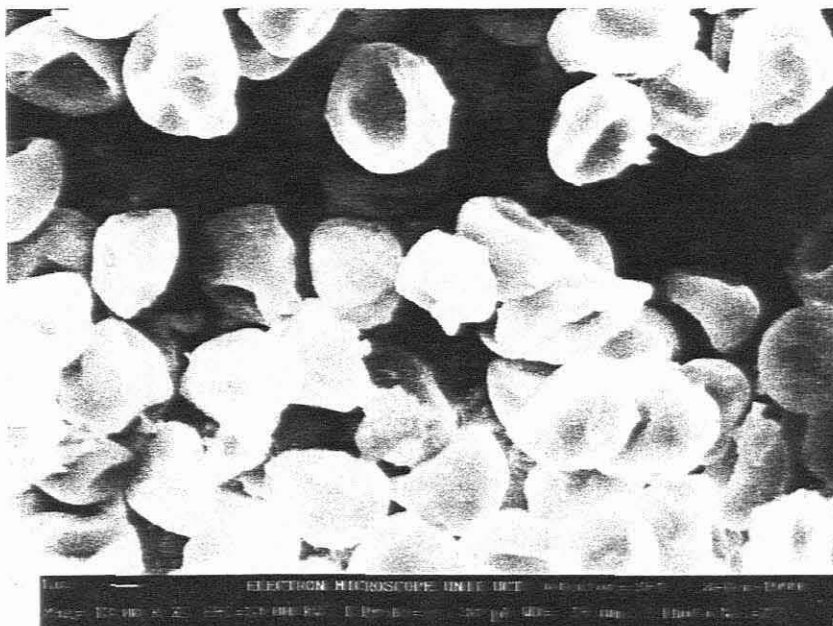
Figure 5.1: Fungal mass consisting of spores

The structure, size and shape of the fungal mass were examined and it has been determined that the fungal mass consists of spores, as shown in Figure 5.1. They are spherical in shape and approximately 2 μm in size. The photograph also shows that some of the spores have collapsed. This phenomenon could have occurred because the membrane samples were dried on silica for 2 days before analysed. Consequently, it was decided that the membranes would be preserved in gluteraldehyde instead and not dried on silica. It is believed that because the fungus is forced into a secondary metabolism stage the fungus would start sporulating again. This may account for the appearance of spores in this and subsequent photographs.

5.3.2 Cord Development

Figure 5.2 shows that spores are clearly visible in the macrovoids. This implies that the inoculation procedure was successful as the spores were in fact forced into the macrovoids using reverse filtration. Reasons as to why these spores did not germinate are numerous. One of the reasons could be that *P,chrysosporium* was cultivated on

malt extract agar slants on a continuous basis and that the older spores may have become non-viable.
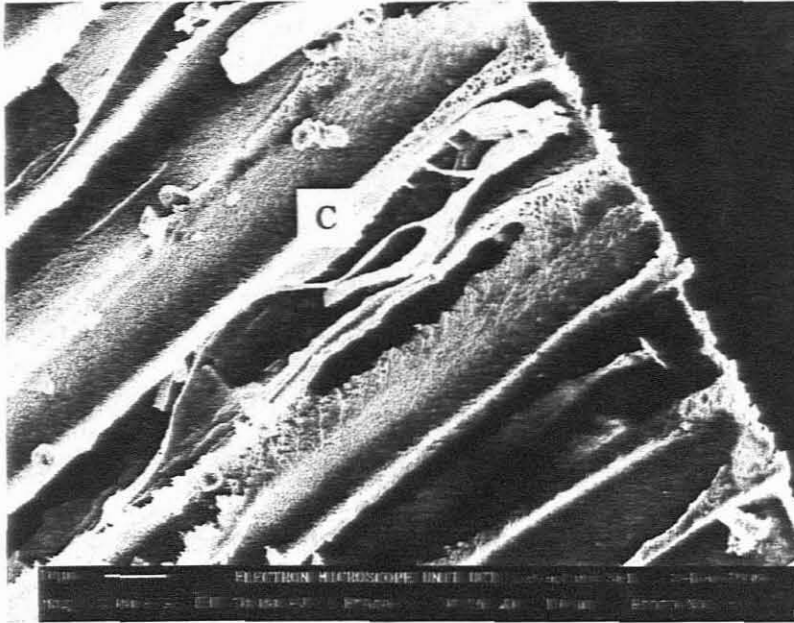
Figure 5.2:   **Cord formation in the macrovoids**

Furthermore, a cord (C) is clearly visible in one of the macrovoids. The density of the cords varied between species and under different conditions. Literature indicated that these cords have been observed in other strains of *P. chrysosporium* when these strains were subjected to the same growth conditions (Walsh, 1998). It is believed that the function of the cords is to anchor the fungus in the membrane. In this way the fungus is adequately immobilized on the membrane. Furthermore, it has been suggested that this membrane system may in fact mimic the way in which the fungus grows in nature, as the macrovoids may in fact resemble the xylem and phloem tubes of woody plants.

Because the spores are forced towards the lumen of the membrane it was assumed that the cords grow from the lumen-side of the membrane to the shell side of the membrane.
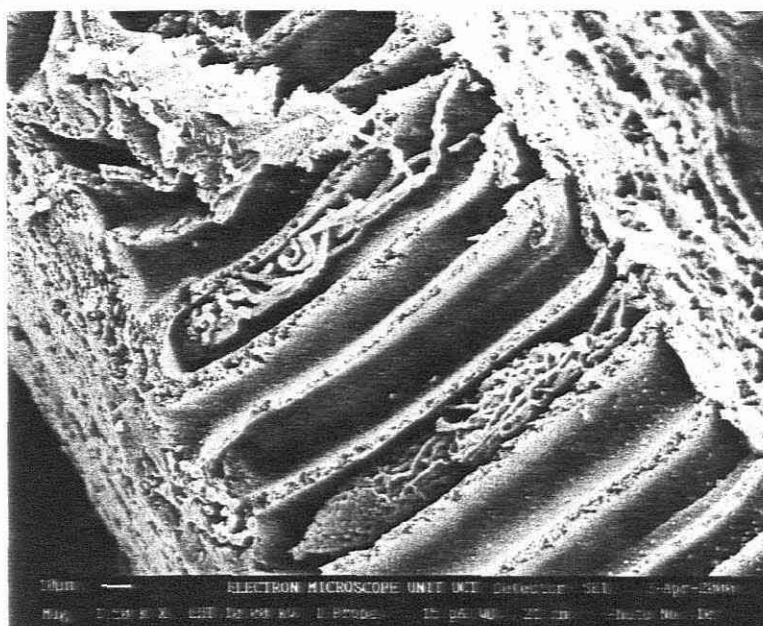
Figure 5.3:   Spore attachment and cord development within the macrovoids of the membrane

Figure 5.3 further illustrates cord development. Spores forced into the macrovoids during inoculation by means of reverse filtration germinate hyphae becoming dense structures (cords), which grow up out of the macrovoids and across the surface of the membrane. The cords became covered in polysaccharide as they matured.

Figure 5.4 illustrates the progression of the biomass across the membrane surface. The cords emerged from the macrovoid and spread across the surface of the membrane after about three days, depending on the operating conditions.
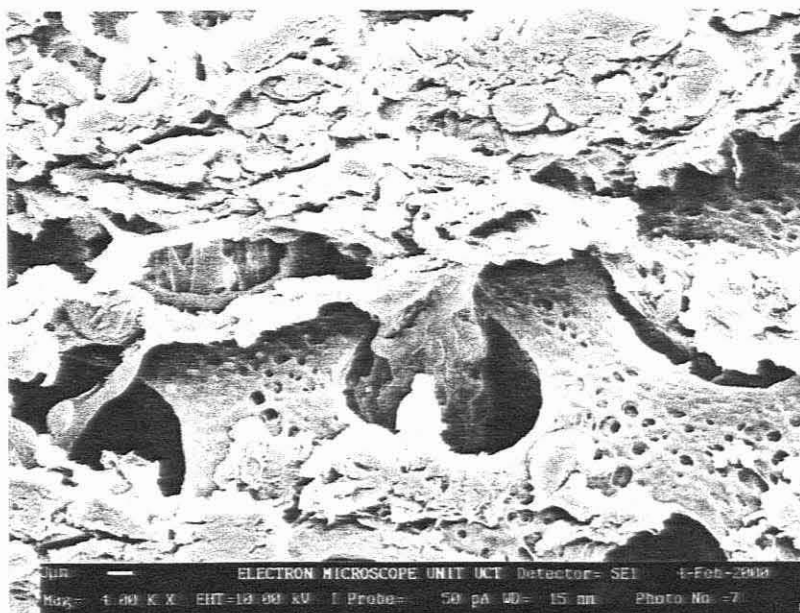
Figure 5.4: Progression of the biomass across the membrane surface

Channeling
structure
of fungus
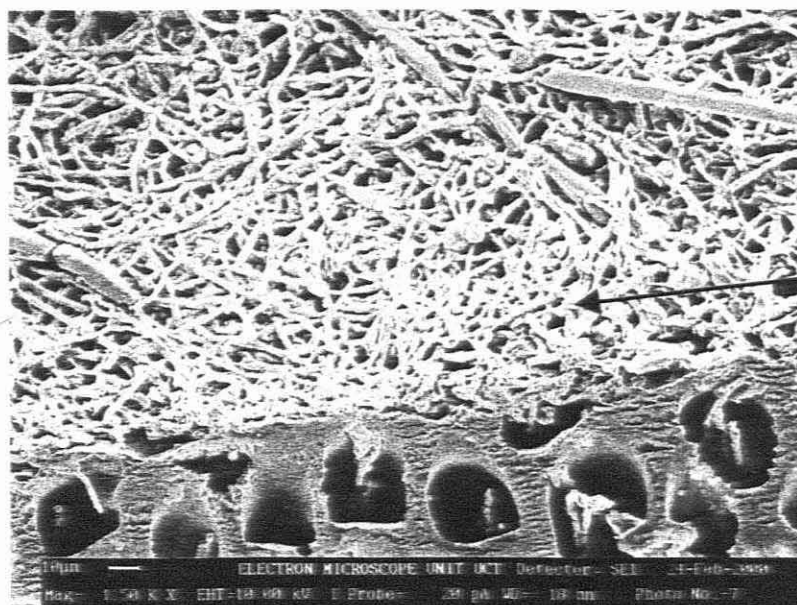
Figure 5.5: Channeling structure of *P. chrysosporium*

Figure 5.5 shows that *P. chrysosporium BKMF 1767* has a unique channeling system across the surface of the membrane, which enables the fungus to obtain its nutrient supply.

5.4   Biofilm development and the demonstration of morphological differentiation.

5.4.1   Biofilm Development

The biomass development on the membrane as shown in Figures 5.4 and 5.5 increased in thickness over the length of the experiment to approximately 450 - 500µm as shown in Figure 5.6. There were two definite zones within the biofilm as depicted by Z_1 and Z_2, indicating that the differentiation within the biomass was clearly visible.
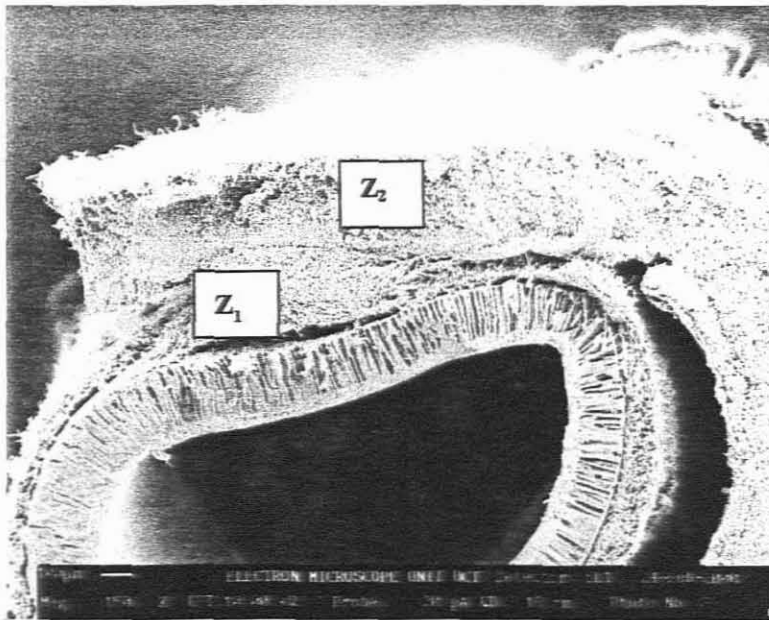
Figure 5.6: Cross section of the membrane inlet side after 14 days

In this photograph, the layer associated with the membrane (Z_1) was approximately 100µm thick, where as the layer associated with the air (Z_2) was approximately 350µm thick [450 – 500 µm in total]. The polysulphone membrane, appoximately 200µm, and the membrane macrovoids, approximately 150µm long and 15µm in diameter, are also clearly visible in this figure.

5.4.2 Morphological Differentiation within the biofilm
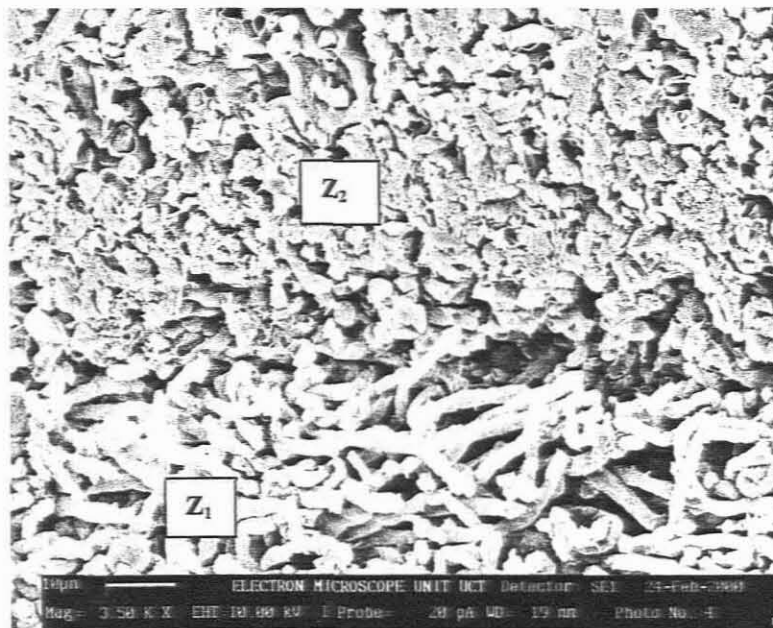
Figure 5.7: Morphological Differentiation within the biofilm

Figure 5.7 is an enhancement of the biofilm shown in Figure 5.6. The layer associated with the membrane (Z_1) appeared to be less compact than the layer associated with the air interface (Z_2). The layer associated with the membrane also appeared to consist of hollow hyphae, whereas the layer associated with the air interface consisted of intrahyphae. Clearly, differentiation within the biofilm has been observed.

5.5. Illustration of Gradostat concept

Figure 5.6, a photograph of the membrane inlet after 14 days, shows a biofilm of sufficient thickness for a nutrient gradient to be established across the biofilm. Figure 5.7 clearly illustrates biofilm differention, new biomass produced near the surface of the membrane where nutrient rich conditions prevailed, which was later pushed outward by the newly formed biomass to an area of low nutrient concentrations.
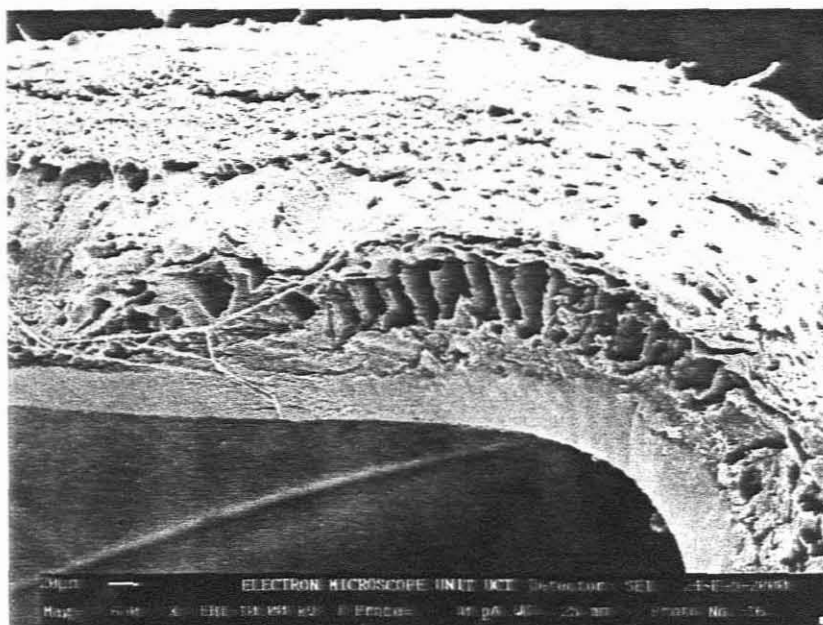
Figure 5.8:   Cross section of the membrane outlet side after 14 days

Figure 5.8 is a SEM photograph of the end of the membrane after 14 days. Biofilm development was practically non-existent and measured approximately 200 μm, indicating that thicker biofilms were obtained at the membrane inlet where higher nutrient conditions prevailed and thinner biofilms at the end where low nutrient conditions prevailed. This proved that the gradostat concept (nutrient gradients across the biofilm and along the membrane) was used successfully in this reactor.

5.6   Biofilm thicknesses obtained

Table 5.1 is a summary of the biofilm thicknesses obtained at the beginning, middle and ends of the membranes, under various conditions of temperature, air and nutrient feed flow rates as shown in Table 5.2.

Table 5.1 : Biofilm thicknesses obtained at the inlet, middle and outlet of the membrane after 14 days, under different conditions.

Run	Mode of operation	Begin (μm)	Middle (μm)	End (μm)	Temp (°C)	Differen-tiation	Enzymes detected	Contami-nation
1	Open-ended	456 - 500			37	Not very clear	No	Bacteria
2	Open-ended	100 - 200	66 - 133		37	Yes	No	Yeast
3	Dead-end	450		100	Room (26.4)	Yes	Yes	Bacteria
4	Dead-end	300		180	Room (25.3)	Yes	Yes	Trichoderma
5	Dead-end	32	20	50	Room (25.8)	Yes	Yes	Growth at the membrane inlet
6	Dead-end	100	140	300	Room (23.8)	Yes	Yes	Trichoderma
7	Dead-end	450	462	460	Room (19.3)	Yes	Yes	Yeast
8	Dead-end	475	485	447	25	Yes	Yes	Yeast
9	Dead-end	555	420	253	37	Yes	Yes	

In most experiments, thicker biofilms were developed at the inlet of the membrane where there was a higher concentration of nutrients and lower concentration of O_2 and thinner biofilms at the end, where there was a lower concentration of nutrients and higher concentration of O_2. Thicker biofilms were developed at higher temperatures of about 37°C than at lower room temperatures, with the thickest of ± 500 μm.

5.7   Contamination

Table 5.1 also indicates that contamination was omni-present. Different types of contamination were picked up and were one of the biggest obstacles to overcome.

5.7.1   Bacteria

Figure 5.9 revealed the appearance of bacteria (B). It was difficult to classify the bacteria further as magnifying the photograph proved difficult. The source of contamination was also difficult to determine. It was assumed that the bacteria could only have entered the membrane through an external source like the media. The presence of these bacteria may have accounted for the absence of enzyme in this experiment because the bacteria may have used the enzymes as a protein source.
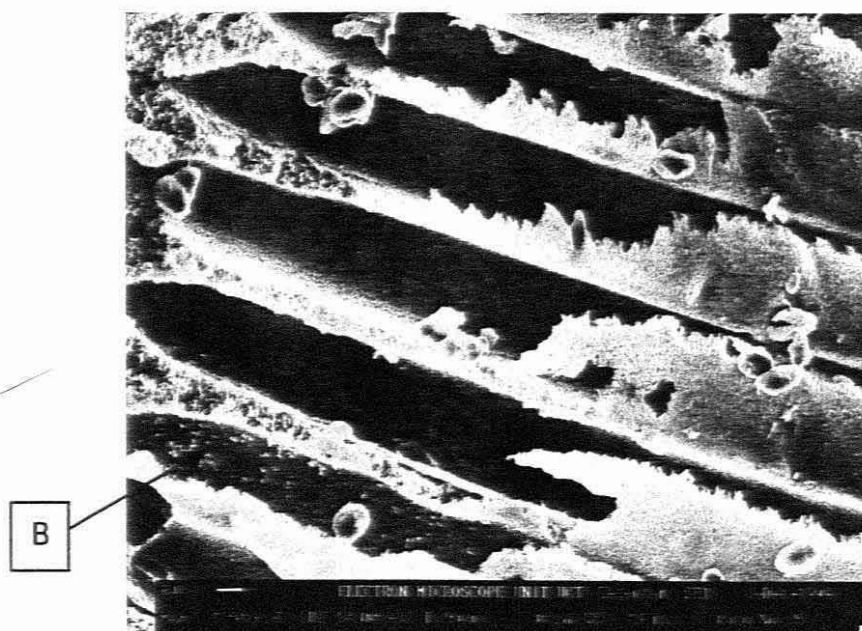
Figure 5.9: Bacterial contamination in the macrovoids.

5.7.2 Crystal formation

Figures 5.10 a, b and c, show a series of crystal formation on the biomass. The only way these crystals could have formed was by a phenomenon known as "salting out". Salting out usually occurs from buffered solutions. The reason as to why it occurred in this experiment is still unknown. A chemical analysis of these crystals confirmed that the crystals comprised of potassuim and phophorous – no doubt the products of buffers. Crystals were observed in previous work and were believed to be indicators of *MnP* activity.
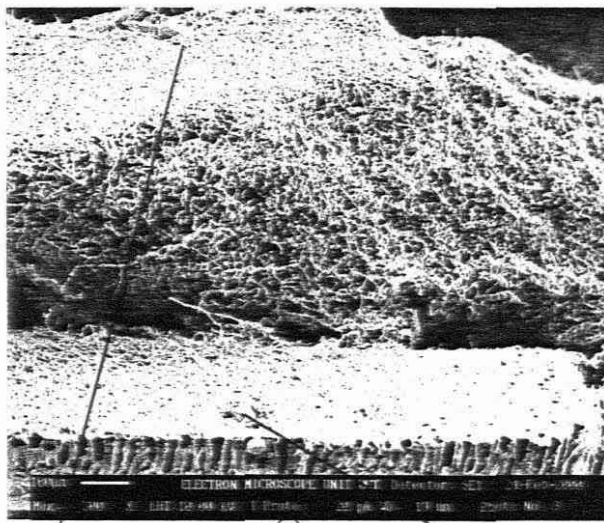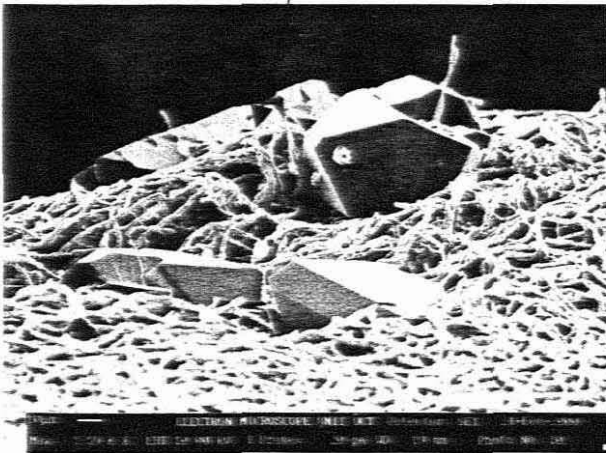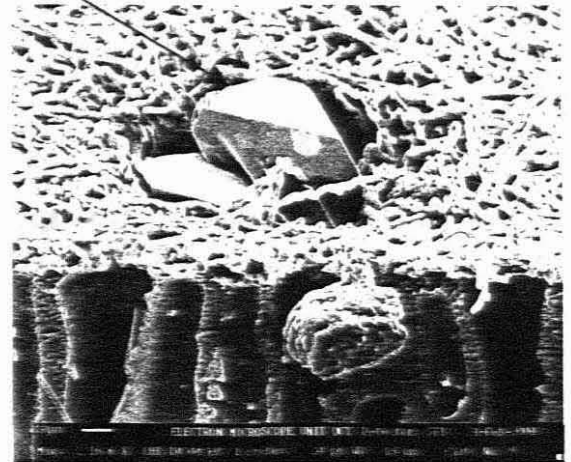
Figures 10 a, b and c : Crystal formation on the biomass

5.7.3 *Trichoderma viridae* (Green Contaminant)

For one of the experiments at room temperature a green contaminant was visible on the outside of the membrane, as shown in Figure 5.11. It continued to grow throughout the duration of the experiment, but *P.chrysosporium* still predominated on the membrane and it did seem that the *BKMF 1767* strain had the advantage. Using SEM analysis it was temporarily classified as a *Trichoderma viridae*.
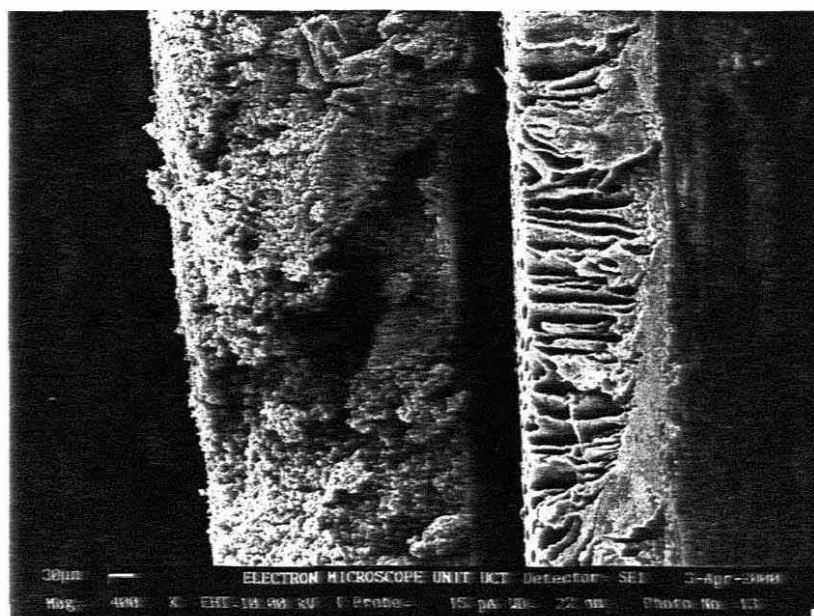
Figure 5.11: *Trichoderma viridae* contaminant

From Figure 5.11 the thickness of the *T. viridae* contaminant was determined and measured approximately 300µm. It was evident from this that the contaminant had the ability to grow as prolifically as *P. chrysosporium* under the same set of conditions. More stringent sterilising measures, such as longer sterilisation times when setting up and running the reactors at higher temperatures, had to be taken to eliminate this contaminant all together in subsequent experiments.
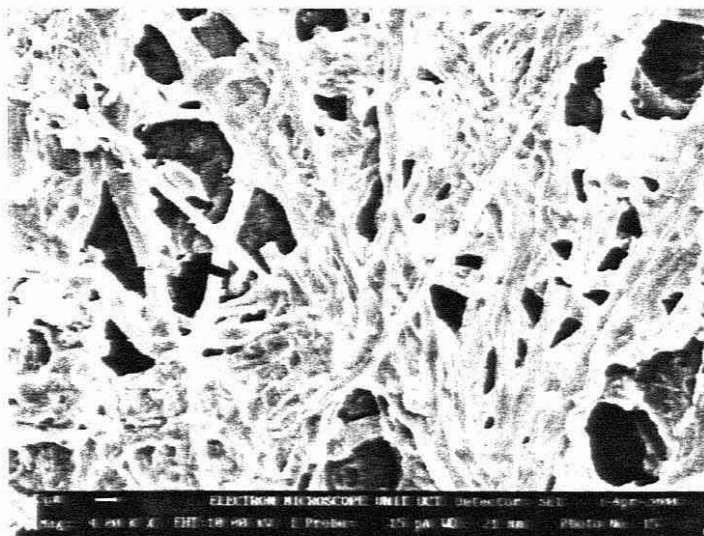
Figure 5.12:   *Trichoderma viridae* **morphology.**

The *Trichoderma viridae* contaminant seemed to be amorphous with a substantial amount of polysaccharide, as seen in Figure 5.12. Figure 5.13 illustrated a type of fruiting body, a feature that seemed to be unique to the *Trichoderma viridae* contaminant, that has not been detected in *P. chrysosporium* before.
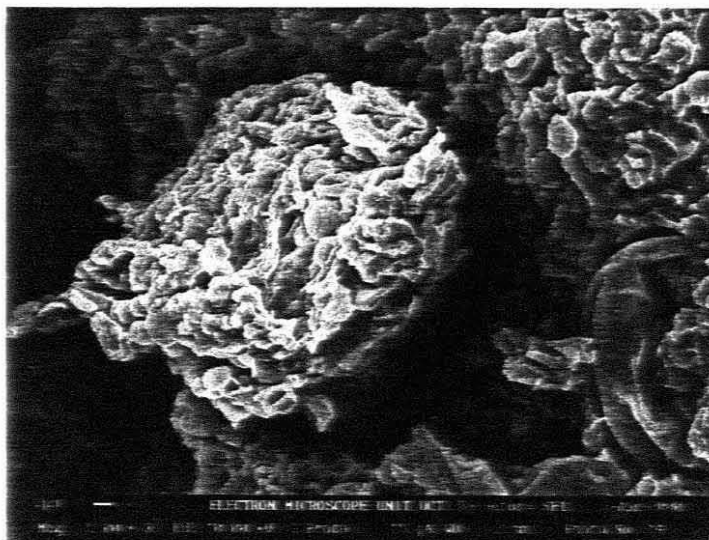
Figure 5.13:   **Fruiting body of the *Trichoderma viridae***

5.8   Enzyme Production

The small scale single fibre capillary membrane bioreactor (SFCMBR) was used for initial studies for continuous ligninase production. These reactors were easy to set-up, convenient to work with, inexpensive and have a simple reactor geometry that is well characterised (Edwards, 1999 and Leukes, 1999), as shown in Chapter 4. The previous section clearly illustrated that fungal immobilisation and differentiation were successful. Differentiation within the biofilm was an indication that nutrient gradients were established across the biofilm.. This is important because enzymes are produced when the fungus is starved of certain nutrients.

Experiments and literature indicated that these enzymes are produced once the fungus is starved and goes into secondary metabolism. Two commercial enzymes were tested for - *Manganese and Lignin Peroxidase.*
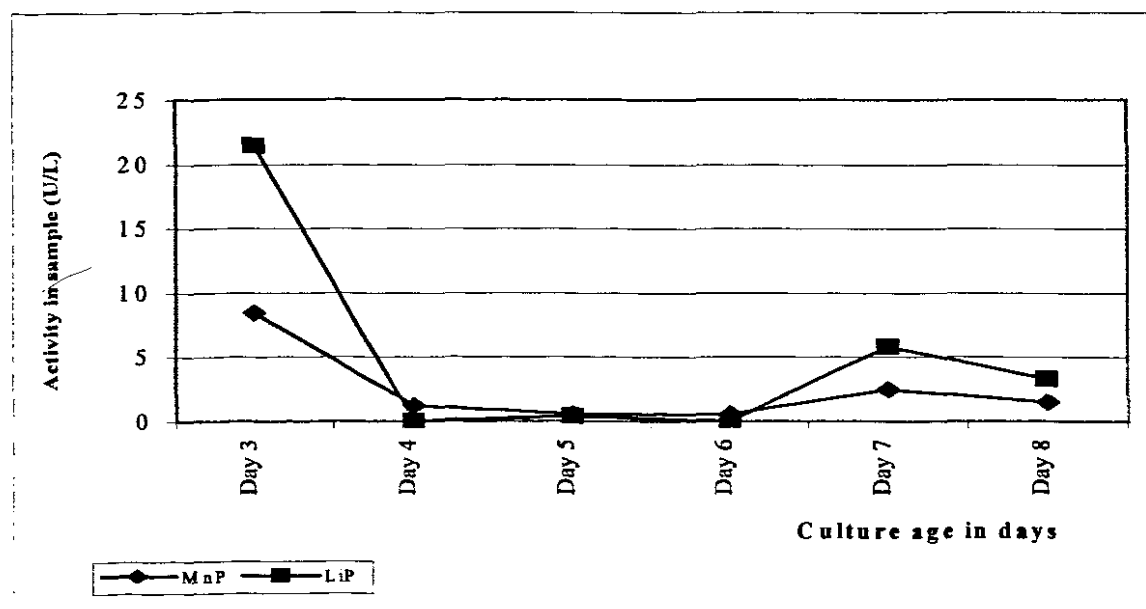
Figure 5.14 (a): Enzyme activity for run 3
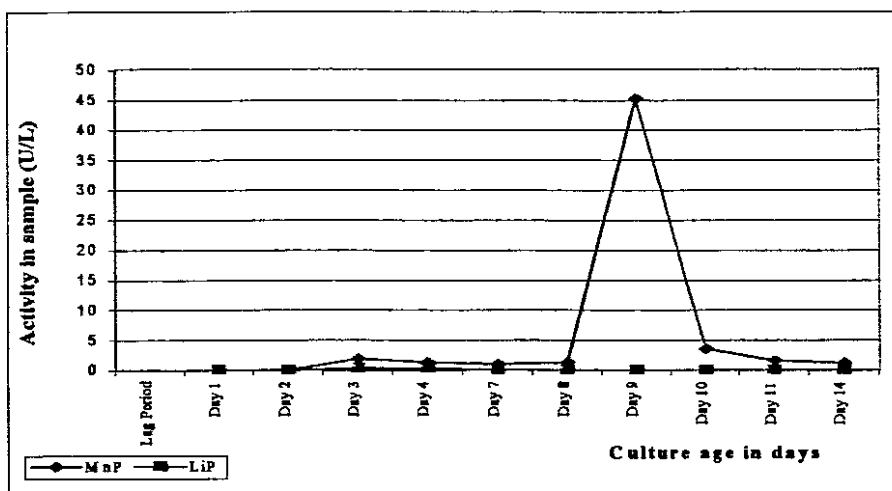
Figure 5.14 (b): Enzyme activity for run 4
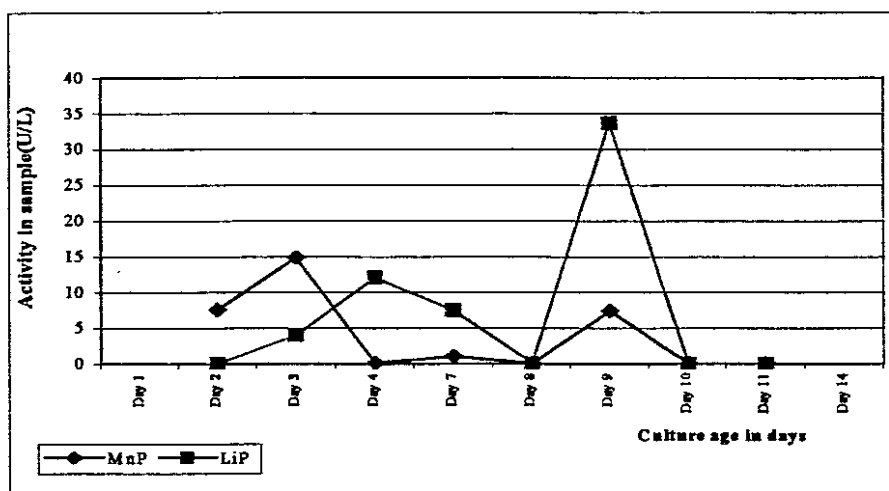
Figure 5.14 (c): Enzyme activity for run 5
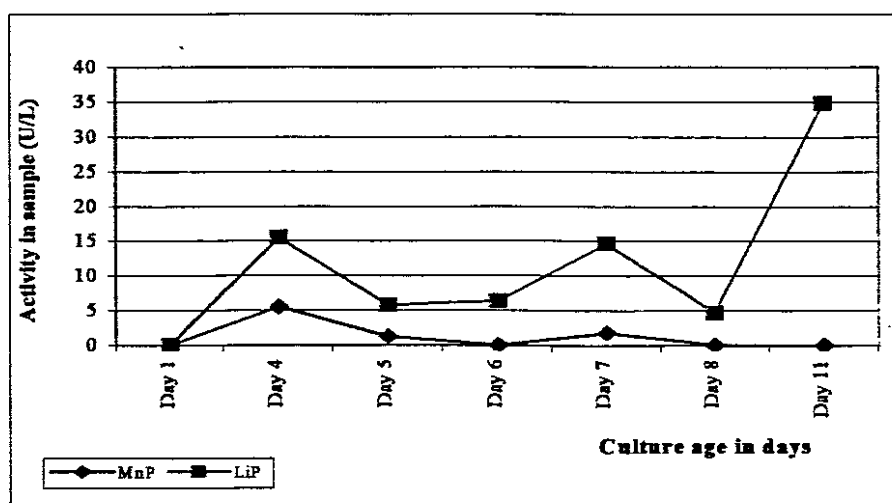
Figure 5.14 (d): Enzyme activity for run 6

As shown in Figures 5.14 a - d, continuous production with peaks of *LiP* and *MnP* activity was observed. This was detected during the production stage before a regeneration of biomass phase of 4 to 6 days. Activity seemed to decline after each successive cycle. Both enzymes were produced but peaked on certain days depending on the conditions (refer to Table 5.2).

Table 5.2: Peak enzyme activity results under different conditions

	Experiment	Day	Activity (U/L)	pH	Temp (^{0}C)	Relative Redox Potential	Glucose conc. (g/L)	NH_4^+ Conc. (g/L)	Nutrient supplied . (ml/hr)	Air Flow (L/min)	Pipe Dia (mm)
MnP	3	3	8.4	3.32	25.6	212	0.81	1.997	2.69	2.6	0.005
	4	9	45.22	2.92	25.2	202	0.93	0.377	0.83	2.6	0.005
	5	3	14.78	3.86	25.7	203	0.86	1.871	1.96	1.08	0.008
	6	4	5.48	2.77	23.7	228	0.85	2.068	0.96	1.08	0.008
	7	7	16.16	3.94	19.1	159	0.89	0.0299	2.54	2.6	0.008
	8	5	10.82	2.91	17.2	222	0.9	0.4192	2.22	2.6	0.008
LiP	3	9	5.81	3.25	26.6	206	0.83	5.189	1.67	2.6	0.005
	4	-								2.6	0.005
	5	9	33.89	6.69	25.0	223	1.0	14.096	0.23	1.08	0.008
	6	11	34.89	2.89	24.1	225	0.86	2.343	0.83	1.08	0.008
	7	7	4.71	3.94	19.1	159	0.89	0.0299	2.54	2.6	0.008
	8	5	60.6	2.91	17.2	222	0.9	0.4192	2.22	2.6	0.008

Table 5.2 summarises the peak enzyme activity results under the different conditions. It is clear from the table that, peak activity for *MnP* was observed on days 3 and 4 and *LiP* from day 9 and 10, depending on the conditions. Higher activities were observed at higher temperatures, lower nutrient flow rates, lower glucose and ammonium concentrations, indicating that these parameters all affect enzyme production and will be discussed in more detail in Chapter 6.

5.9 Problems experienced

Many problems were experienced with perfecting the environmental conditions within the reactor for optimum fungal growth. Contamination was observed when the nutrient feed was continuously circulated. Contamination in the nutrient feed pipe lines obstructed the flow of feed to the reactor, affecting growth and permeation. It

was difficult to sterilise the system by steam sterilisation due to the heat lability of the membranes. Chemical sterilisation methods resulted in the problem of residual toxicity in the bioreactor, as it was difficult to adequately flush all corners of the bioreactor with the sterilising agent and then with enough water to remove all traces of the chemical.

5.10 Summary

P. chrysosporium was successfully cultivated in the single-fibre membrane bioreactor (SFMBR). Inoculation of the membrane reactor resulted in the growth of the fungus in the form of mycelia immobilized on the outside of the walls of the membrane within the manifold. The mycelia grew as a uniform thin film over the membrane owing to the large surface area available for attached growth.

The microporous structure and hydrophilic surface of the membrane allowed free exchange of nutrients and metabolic products between the cells, which were immobilized on the outside of the membrane and the circulation media flowing on the lumen side of the membrane. *Lignin* and *Manganese Peroxidase* were successfully secreted and transported into the permeate without any rapid decline in activity.

The membrane bioreactor used here has some of the problems common to other membrane devices. However, with further development in membrane technology, these problems may be overcome and these membrane bioreactors should be applicable to many areas of biotechnology.

CHAPTER 6

OPTIMISATION OF OPERATING PARAMETERS

6.1. Introduction

Full exploitation of the potential advantages of immobilised cell reactors strongly depends on the selection of a set of processing parameters allowing for high enzyme productivity combined with operational stability. Optimisation of the process involved improving the existing system and an understanding of the interrelationship between these parameters will allow for rational, systematic design and evaluation of the process.

Before any optimization result can be understood, one must consider the flexibility of the process and the related sensitivity of the results. A process must be able to operate with different feedstocks, under varying environmental conditions, over a range of activities, at different production rates and so on.

6.2 Effect of processing parameters on the feasibility and operational stability of the bioreactor.

From literature and experiments it was clear that the parameters affecting this process include air flow rate, O_2 concentration, nutrient feed flow rate, temperature, pH and nutrient (ammonium and glucose) concentration.

6.2.1. Air flow

Since the organism is an aerobe, its growth is influenced by the dissolved oxygen concentration. Most of our work involved using air as the source of oxygen. Using the conditions of experiments 3 and 5, as shown in Table 5.2, that was performed at an air flow rate of 2.6 and 1.08 L/min respectively, the following information was obtained:

At an air flow rate of 2.6 L/min at room temperature, biofilm development was visible on membrane after 3 days. The biofilm thickness at the membrane inlet measured approximately 450 – 500 µm (as was shown in Figure 5.6). When the air flow rate was decreased to 1.08 L/min at room temperature, biofilm development was only visible after 6 days. The biofilm thickness at the inlet side of the membrane measured approximately 300µm (as shown in Figure 6.1.).
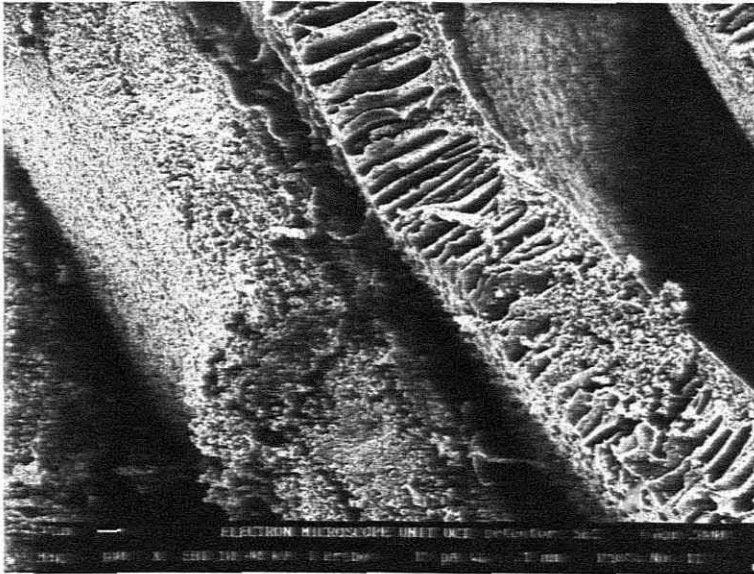
Figure 6.1: Cross section of the membrane inlet side after 14 days

Similarly, Figure 6.2 illustrates the biofilm thickness at the outlet of the membrane to be approximately 190µm at a flow rate of 1.08 L/min, as opposed to 200µm at a flow rate of 2.6 L/min (as was shown in Figure 5.8). The gradostat concept was still illustrated in this experiment even though a decrease in airflow rate decreased overall biofilm thickness.
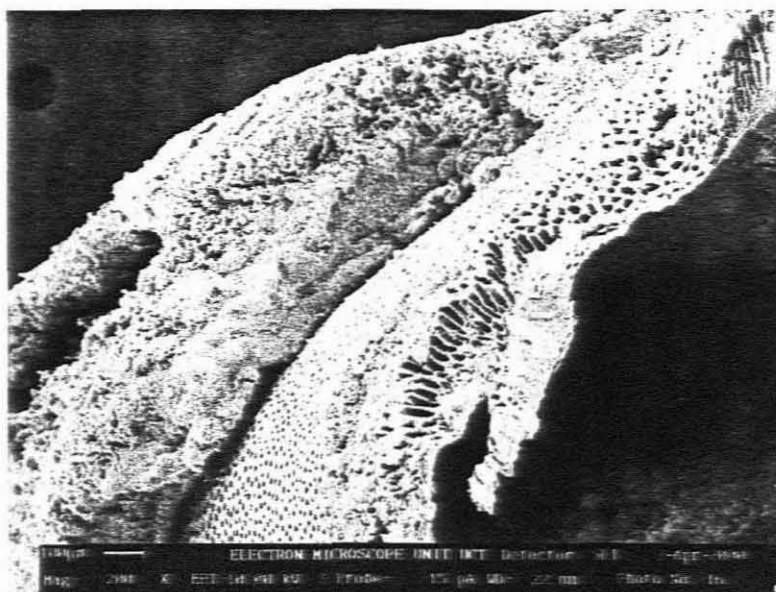
Figure 6.2: Cross section of the outlet side membrane after 14 days

6.2.2. Temperature

As shown in Tables 5.1 and 5.2, the room temperature gradually decreased from an average of 26.5°C to an average of 23 °C for experiments 3 to 6, with the lowest during the winter at 17°C for experiments 7 and 8.

Literature has shown that enzyme activity is more stable at lower temperature. However, a decrease in temperature did affect biofilm growth on the membrane. Biofilm was only visible after 4 to 6 days, at lower temperatures and air flow rates as apposed to 3 to 4 days at higher temperatures. As was shown in Table 5.1, the biofilm thicknesses obtained were also thinner at room temperature (300 – 450 μm) than when the reactor was incubated at a temperature of 37°C (450 - 555μm).

6.2.3. Nutrient feed flow rate

A laboratory size peristaltic pump was set to supply the nutrient medium at a rate of 2.8 ml/hr. The permeate collected was measured daily to determine the effect, if any, the biomass growth had on the permeability of the membrane.

Results indicated that the permeate collected decreased with time, as seen in Figure 6.3, indicating that biomass growth had a decreasing effect on the permeability of the membrane.
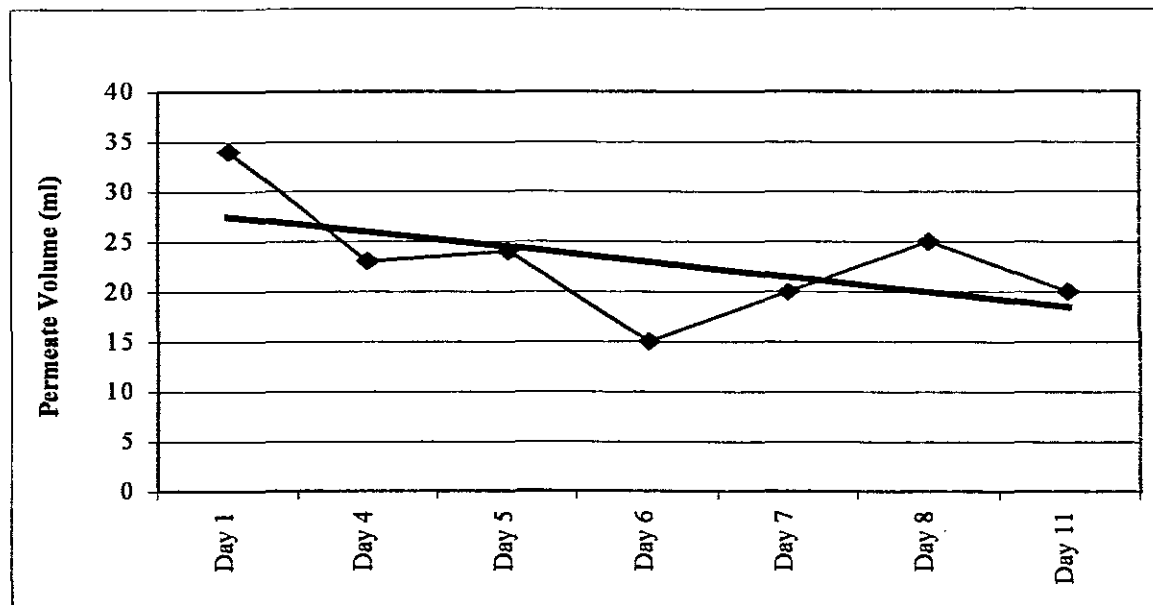
Figure 6.3: Permeate volumes collected during an experimental run

From Table 5.2, higher enzyme activity (45 U/L) was picked up at a low nutrient feed flow rate of 0.83 ml/hr than at a higher flow rate of 2.69 ml/hr,, at the same temperature of 25°C and air flow rate of 2.6 L/min for experiments 3 and 4. The reason for this could be that lower flow rate, i.e. longer residence time, allowed for higher nutrient uptake in the biofilm closer to the membrane, starving the biofilm further away (nutrient gradients across the biofilm), therefore forcing the micro-organism into secondary metabolism stage.

6.2.4 pH

pH measurements as shown in Figure 6.4, indicate that the permeate pH consistently decreased during the experimental period. Although the exact causes for pH changes are not known yet, higher rates of *LiP* production related to larger pH changes. Peak enzyme activities were observed between a pH of 2.8 – 4.5. According to

Lewandowski *et.al.* (1990) the optimum pH for *P. chrysosporium* has been established at 4.0 – 4.5.
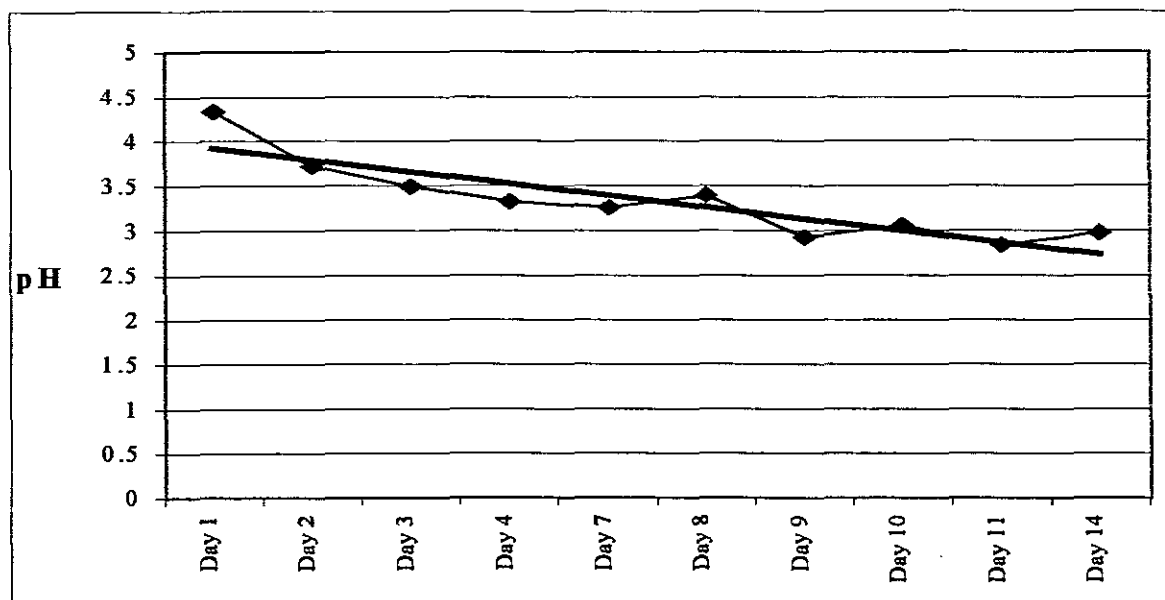
Figure 6.4: Typical pH readings during an experimental run

6.2.5. Relative Redox Potential

From literature it was clear that *LiP* is a heme peroxidase with an unusually high redox potential and low optimum pH. The relative redox potential of the permeate was measured daily to determine whether a correlation could be drawn between the relative redox potential and enzyme activity. Results indicated that no enzyme activity was picked up below a relative redox potential of 200. Enzyme production started after three days and from Figures 6.5 a and b, it is clear that relative redox potential was above 200 at this stage.
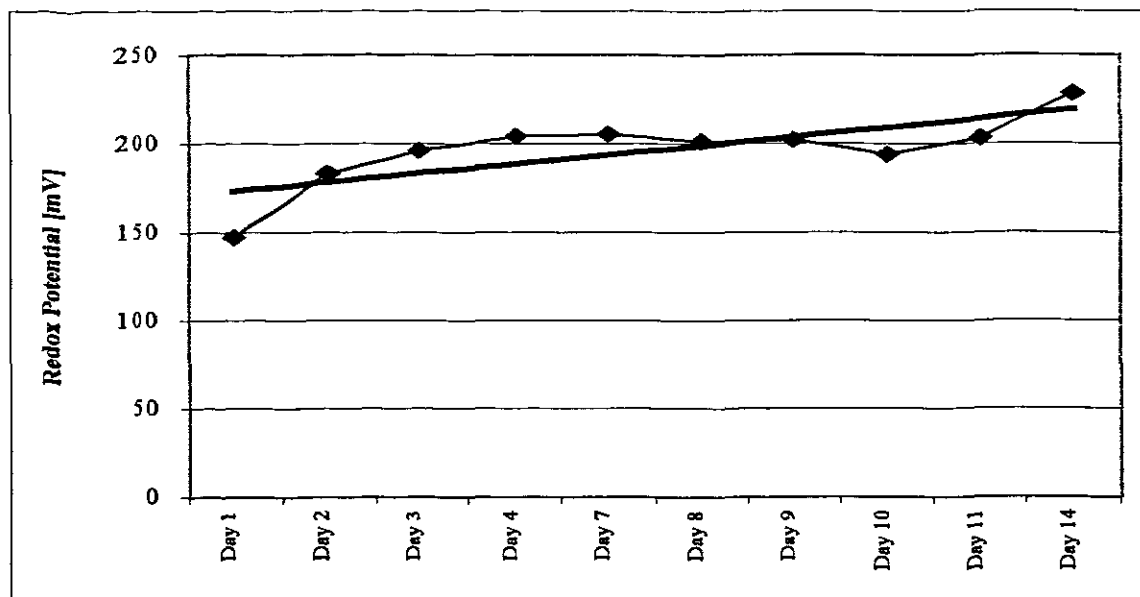
Figure 6.5. (a): Typical Relative redox potential curve
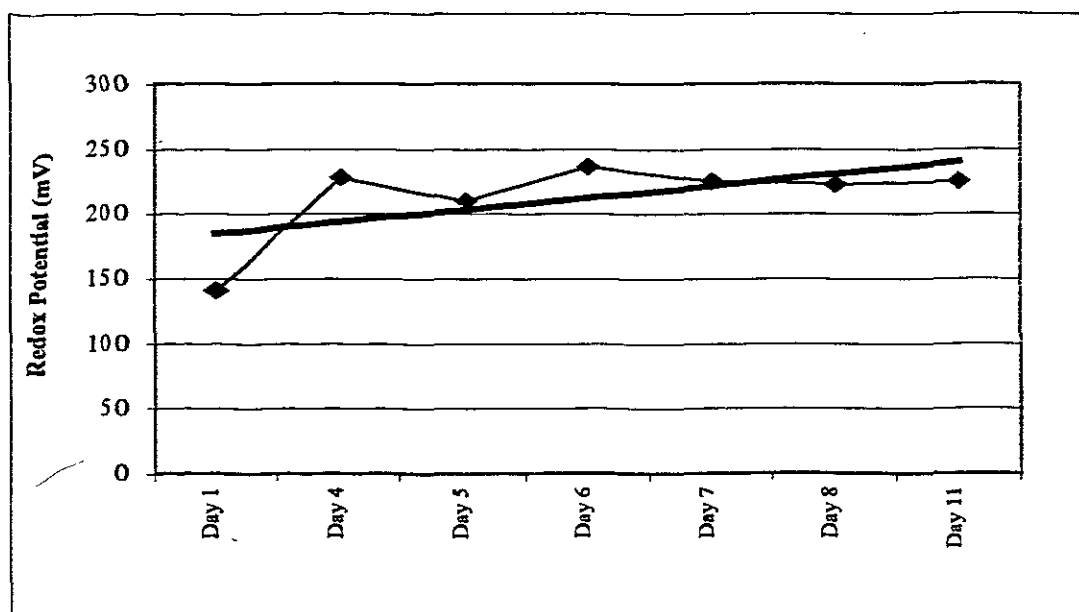
Figure 6.5 (b): Typical Relative redox potential curve

6.2.6. Glucose and Ammonium Consumption

Glucose and ammonium assays were done to determine how much of the glucose (1%) and ammonium (39 g/L) in the supplied nutrient were used by the fungus for primary growth.

As shown in Figures 6.6 and 6.7, a drastic increase in both glucose and ammonium consumption is visible immediately after the lag period. This indicates that although the fungus was not visible on the outside of the membrane on day 1 yet, the immobilized cells were using the nutrient sources for primary growth. Glucose depletion was not reached completely and stabilised when the fungus reached stationary phase. However, ammonium was depleted after 24 hours, emphasising nitrogen starvation.
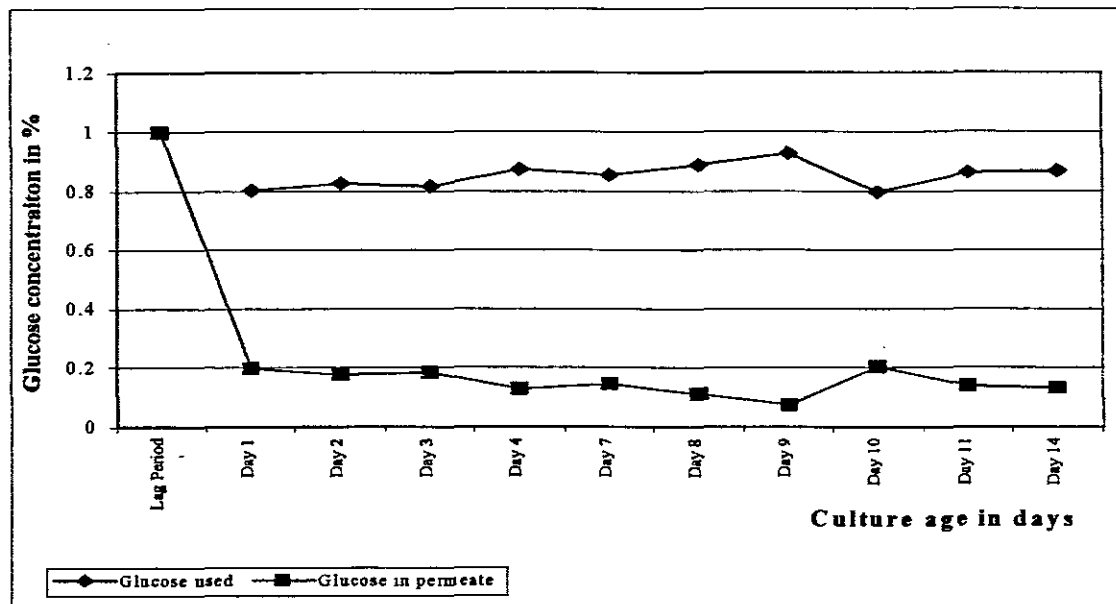
Figure 6.6: Typical Glucose consumption curve
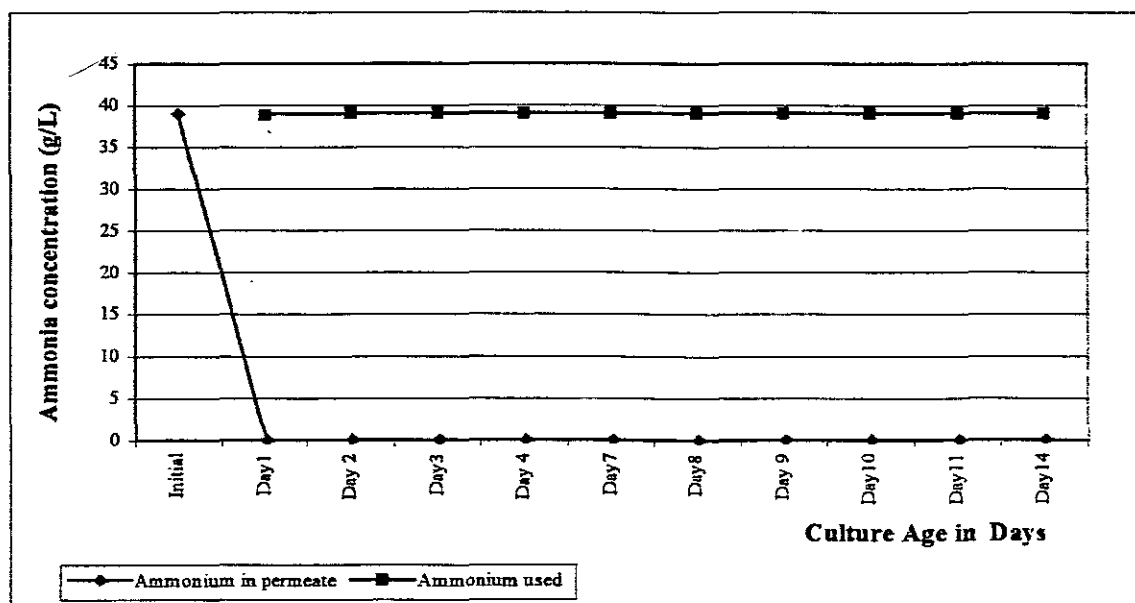
Figure 6.7: Typical Ammonium consumption curve

These results indicate that the air flow rate, O_2 concentration, temperature, pH, relative redox potential and nutrient feed flow rate did in fact affect biofilm growth and enzyme production.

6.3. Selecting key parameters

The previous section highlighted all the processing parameters that have an impact on the operational stability and enzyme production. It was found that the most important external factors affecting enzyme activity are temperature, O_2 concentration, pH, nitrogen and glucose concentrations. An integrated approach is required involving optimization of the complete set of processing parameters in order to maximize operational stability of the bioreactor. Experience and literature indicates that such an optimization process should be primarily focused on:

i)   oxygen supply;

ii)   balanced nutrient supply affecting simultaneously maximal production and stability with minimal cell regeneration / growth;

iii)   operating temperature which will influence the reaction rate and the stability of the cells;

From Freeman and Lilly (1998) quantitative data on potential gradients of cells, oxygen, nutrients, product, pH and temperature throughout different parts of the reactor are insufficient or unavailable. It is for these reasons that a sensitivity analysis on O_2 concentration (air vs oxygen) and operating temperature was attempted, with the aim of optimizing these two parameters. These decision variables were chosen, as these were independent variables over which most control could be exercised and also the ones that most affect biofilm growth.

6.4   Sensitivity Analysis

A sensitivity analysis is defined as a study that should pinpoint the areas most susceptible to change. The purpose is to determine to which factors the enzyme production is most sensitive and to observe the effect of departures from expected values. A sensitivity analysis is a way of examining the effects of uncertainties in the forecasts of the viability of this project.

6.4.1   Temperature

From literature it was established that *P. chrysosporium* has an optimum growth temperature of about 37 to 40°C. The chances of getting any contamination of productive cultures are almost non-existent and enzyme production is maximal under these operating conditions. However, it is also clear from literature that enzymes are more stable at lower temperatures. For this reason the affect of temperature on enzyme production was analysed using a sensitivity analysis.

Two different temperature regimes were studied:
i)   Exposing the immobilised fungus to normal room temperature.
ii)   Exposing the immobilised fungus to a controlled temperature at 37°C.

Both reactors were inoculated with one million spores. The nutrient supply was kept constant at 3ml/hr and air supply of 2.6 L/min. The affects of these treatments on the rate of biofilm development and enzyme production were examined.

6.4.1.1 Effect of temperature on biofilm development

Table 6.1: Biofilm development at different temperatures

Biofilm development			
	15 – 20 °C	**25°C**	**37°C**
Biofilm development	visible on the outside of the membrane after 6 days.	visible on the outside of the membrane after 4 days.	visible on the outside of the membrane after 2 days.
Max Biofilm thickness obtained (μm)	450	500	555

Table 6.1 shows the results that were obtained when the reactors were exposed to different temperature regimes. It is clear from Table 6.1 that biofilm development started much later at temperatures below 25°C, as opposed to when it was operated at higher temperatures of 37°C. Biofilm growth was also much more prolific at temperatures between 25 and 37°C.

6.4.1.2 Effect of temperature on enzyme production

Table 6.2: Peak enzyme activity results at 37°C

	Experiment	Day	Activity (U/L)	Temp (^{0}C)	Glucose conc. (g/L)	NH_4^+ Conc. (g/L)	Air Flow (L/min)	Pipe Dia (mm)
MnP	9	3	25.55	37	0.95	0.3047	2.6	0.008
	10	8	3.39	37	0.95	0.1462	2.6	0.008
	11	3	96.90	37	0.99		2.6	0.008
LiP	9	12	32	37	0.96	0.6147	2.6	0.008
	10	14	7.58	37	0.95	0.0740	2.6	0.008
	11	13	33.74	37	0.99		2.6	0.008

Table 6.2 shows the peak enzyme activities that were observed when the reactors were operated at a controlled temperature of 37°C. The maximum *MnP* activity, of 96.90 U/L, was observed on day 3 and maximum *LiP* activity, of 33.75 U/L, was observed on day 13. These results were compared to the average maximum activities

that were picked up when the experiments were performed at room temperature, as was shown in Table 5.2. These comparisons are summarised in Table 6.3.

Table 6.3: Summary of maximum enzyme activities at different temperatures

Enzyme activity (U/L)			
	15 – 20 °C	25°C	37°C
Enzyme production started	Very late	4 days	3 days
Max *LiP* activity (U/L)	3.3	35	33
Max *MnP* activity (U/L)	16.16	45	96

Minimal *LiP* and *MnP* activities were observed at temperatures below 25°C. Above 25°C *LiP* activity stayed more or less constant at about 35 U/L. Above 25°C *MnP* activity increased two fold to a maximum of about 96 U/L.

6.4.2 O₂ concentration (air vs pure O₂)

P. chrysosporium is an aerobic fungus, its activity is therefore influenced by the dissolved oxygen concentration. The importance of having a pure oxygen environment for good ligninase production is well documented. Aeration using pure oxygen was shown by Faison and Kirk (1985); Dosoretz et. al. (1990 and 1993) and Venkatadri and Irvine (1993) to have a profound effect on the production of ligninases, extracellular proteases and polysaccharides. Faison and Kirk (1985) reported that both ligninolysis and ligninase activities *of P. chrysosporium* were increased in cultures initially supplied with air during their growth phase and then shifted to an oxygen atmosphere. The rate of lignin degradation was reported to be 2 – 3 times greater using pure oxygen rather than air (Kirk *et.al.*, 1986). Because of this, most laboratory-scale studies as well as scale-up attempts have used a pure oxygen environment for high productivities (Dosoretz *et.al.*, 1993; Venkatadri and Irvine, 1993).

Two different oxygenation regimes were evaluated in this study:

i)   Exposing the immobilised fungus to a continuous supply of pure oxygen (98% O_2) at a rate of 2.5L/min.

ii)   Exposing the immobilised fungus to a continuous supply of air (21% O_2) at a rate of 2.5 L/min.

Both reactors were inoculated with one million spores. The nutrient feed flow rate was kept constant at 3 ml/hr. Two reactors were set up, with the two different O_2 regimes. These reactors were then operated first at room temperature and then at a controlled temperature of 37°. The effects of these treatments on the rate of biofilm development and enzyme production were examined.

6.4.2.1   Effect of O_2 concentration on biofilm development

When the two reactors (one with 21% O_2 and one with 98% O_2) were operated at room temperature of about 17°C, no biofilm growth was visible for the first 4 days of the experiment for both O_2 regimes. Permeation through the membranes were similar for both O_2 regimes. This operation was stopped as the temperature proved to be too low for the sensitivity analysis and O_2 concentrations did not have any effect on biofilm growth at this temperature. The permeates from both reactors were collected and compared and is summarised in Table 6.4.

When the reactors were operated at 37°C, no biofilm growth was visible for the first 2 days for both O_2 regimes. However, with the reactor exposed to 98% O_2, no permeation was visible for the first two days either and the pure O_2 was changed to a constant supply of air as well. This reactor started permeating immediately after it was switched over to air, a phenomenon that is still unexplained and needs to be investigated further. Biofilm growth was visible for both reactors on day 3 and the growth rate seemed similar thereafter. The permeates from both reactors were collected and compared and is summarised in Table 6.5.

6.4.2.2 Effect of O₂ concentration on enzyme production

Table 6.4: Air vs pure O₂ at room temperature

Day	Temp		pH		Relative Redox potential	
	air	O₂	air	O	air	O₂
1	17.4	17.3	1.97	1.89	141	145
2	18.2	16.8	4.70	4.56	140	148
3	16.9	17.1	4.54	4.50	143	146

Table 6.4 shows the temperature, pH and relative redox potential of the permeate for the two different regimes (air with 21% O_2 vs 98% O_2) at room temperatures of <20°C. No activity was observed. However, from the information it seemed that the relative redox potential for the 98% O_2 reactor was slightly higher than for the 21% O_2.

Table 6.5: Air vs pure O₂ at 37°C

Day	pH		Relative Redox Potential	
	air	O₂	air	O₂
1	4.23		158	
2	3.63	3.95	191	180
3	3.98	3.55	174	201
4	3.77	3.89	193	190
5	3.48	3.45	201	204
6	3.43	3.44	205	205
7				

Table 6.5 shows pH and relative redox potential of the permeate for the two different regimes (air with 21% O_2 vs 98% O_2) at 37°C. The permeation for the reactor exposed to 98% O_2 was minimal for the first 2 days, a phenomenon that is still unresolved, and therefore no readings could be taken. After it was switched over to air permeation was normal and the permeate results were used as an indication of enzyme activity. It is clear from the information that although the one reactor was only exposed to O_2 for two days the relative redox potential was still higher than the reactor exposed to continuous air supply, which could indicate that the activity in this reactor would be higher as well.

6.5   Summary

The study examined the affect of potentially important parameters on enzyme production in the membrane bioreactor. Factors such as temperature, pH, nutrient and air flow rate, oxygen and substrate concentrations and other interfering compounds have a significant affect on the measured enzyme activity. The data demonstrated that unique culture parameters are critical for *LiP* and *MnP* production from *P. chrysosporium* (strain BKMF 1767). The experiments also demonstrated that enzyme production and the control of certain culture parameters is essential for optimisation and stability of the bioreactor.

The study carried out to investigate the effect of temperature on the feasibility and operational stability of the reactor indicated that temperature did in fact have an influence in the growth rate and enzyme production. The optimum temperature for growth of the fungus was established at 37, as was also reported in literature (Lewandowski, 1990).   No contamination was detected at this temperature. Temperature changes seemed to have a definite effect on *MnP* activity between 25°C and 37°C but not on *LiP*, as *LiP* showed minimal change between 25° and 37°C.

The study carried out to investigate the effect of different O_2 regimes indicated that higher O_2 concentrations did not have any effect on biofilm growth and enzyme activity at temperature below 20°C. Because of limited experimental data, the study carried out to investigate the effect of different O_2 concentrations on biofilm growth and enzyme production at 37°C has to be investigated further before any conclusion can be reached.

The oxygen concentration obtained in the reactor using air seemed adequate as a further increase in enzyme production was not possible when pure oxygen instead of air was used in the experimental set-up.

CHAPTER 7

MONITORING THE EFFECT OF MICROBIAL GROWTH ON MEMBRANE PRESSURE AND PERMEABILITY

7.1   Introduction

According to Linton, *et al.* (1989), a major limitation to the use of hollow-fibre cell cultures is the difficulty of monitoring and controlling their growth and metabolism. Other limitations are the mass transfer rates encountered at high cell densities and the problems associated with excessive cell growth, leading to blinding and rupture of the internal ultrafiltration membrane.   A number of factors are required if the fruits of biotechnology are to be optimally commercialised.   Among these are the design and operation of novel bioreactors and the development of sensors and the necessary models for control algorithms enabling bioprocesses to be efficiently operated.

The objective for this chapter is to investigate the effect of microbial growth on membrane pressure and permeability.   A modification of the Bruining Model (Bruining, 1989) was used to develop a method for the in-situ monitoring and prediction of pressure and permeability along the membrane in the dead-end filtration mode with an incompressible Newtonian fluid in laminar flow inside the membrane. The effect of the microbial growth on the membrane pressure and permeability was monitored.

7.2   Application of theory from Chapter 3

It was assumed that there is no pressure drop on the shell side and that laminar flow is occurring inside the fibre. By measuring P_1, P_2 and P_3, the value of Pr at x = 1, i.e. Pr_2, could be calculated using Equation 3.4 (where $p = p_2$). Pr_2 was then substituted in Equation 3.12 to calculate the value of T_L (at z= L). Knowing the value of T_L and recalling the meaning of T_L from Equation 3.6, the value for the membrane permeability coefficient K, at z = L, could be calculated. In the case of a dead-end filtration experiment, without a shell side pressure drop, it was known that F_2 = 0. T_L was then also used to calculate the value of the dimensionless flow rate, Ψ_1, using Equation 3.11. T_L and Ψ_1 were substituted into Equation 3.8, to calculate P_r at different values of z. Knowing P_r at different values of z, the pressure at this point could be calculated using Equation 3.4 and calculating P. This was repeated for the different days of the experiment.

Using the correlations as described above, measurements were taken and calculations were done for a membrane without biofilm growth (referred to as the control) and a membrane with biofilm growth (referred to as an inoculated membrane).

7.3   Results and Discussion

7.3.1   Pressure Measurements

For the control membrane inlet and outlet pressure readings stayed constant, at approximately 106 325 Pa and 101 675 Pa respectively, throughout the experiment. For an inoculated membrane, as shown in Figure 7.1, inlet pressure readings remained constant for the lag period until biofilm growth was visible on the membrane on day 3 and 4, after which the pressure increased exponentially until it reached a stationary phase again. This could be an indication of the biofilm growth pattern on the membrane as this follows the same pattern as a typical growth curve. Outlet pressure was considerably lower that the inlet pressures, but followed more or less the same pattern.
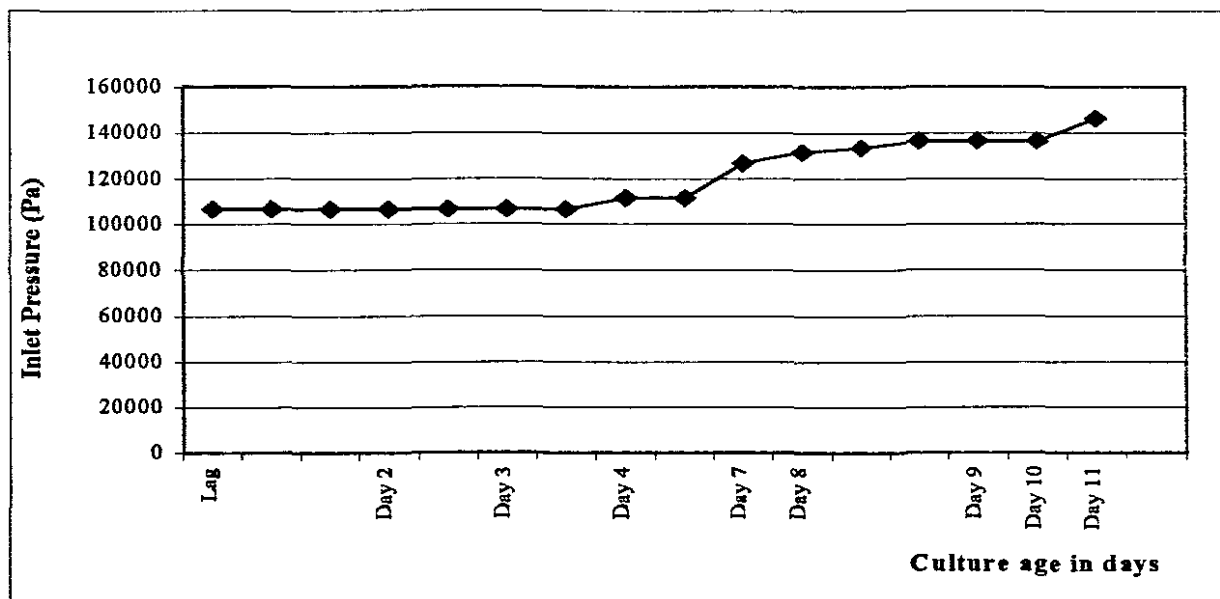
Figure 7.1: Inlet pressure (P_1) for an inoculated membrane.

7.3.2 Pressure Prediction along the membrane

The manometer used to measure the pressure on the reactor side indicated a constant atmospheric pressure. Due to the difficulty of measuring the pressure along the membrane lumen, the model described previously was used to predict the pressure along the membrane. The outlet pressures that were calculated and predicted using the modified Bruining model were compared to the measured outlet pressures. As shown in Figure 7.2, results indicate that the predicted outlet pressure is of the same order of magnitude as the measured outlet pressure, P_2, and therefore proves that this could be a reliable model for predicting the pressure along a hollow fibre membrane.
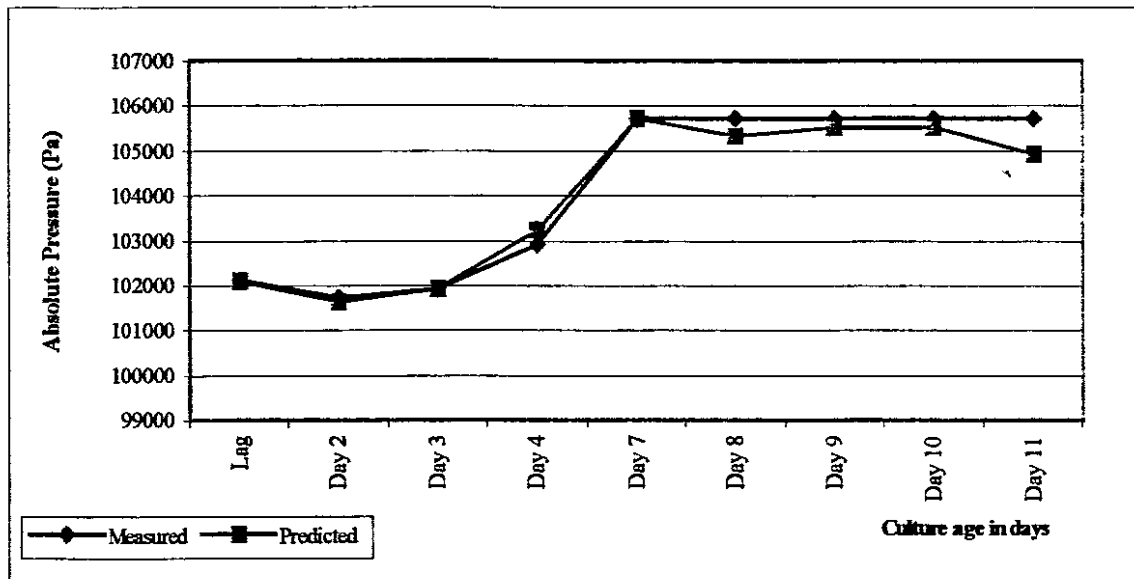
Figure 7.2: Outlet pressure (P$_2$), measured vs predicted, for an inoculated membrane.

The system used was in the dead-end filtration mode and was run at a constant flux.. Figure 7.3 indicates that the pressure decreased from the inlet to the outlet. Inlet pressure increased exponentially after growth was visible on the membrane on day 4. This also indicates that pressure could be used as an indication of the biofilm growth on the membrane. The biofilm on the membrane increased with time, consequently the pressure drop along and across the membrane also increased with time. The axial pressure gradient observed was greater than expected and varied with time. This could be explained by biofilm growth into the lumen. If this is typical behaviour it means that the membrane morphology needs to be adjusted, and action be taken to avoid pinholes which would provide the sites for growth through the membrane.
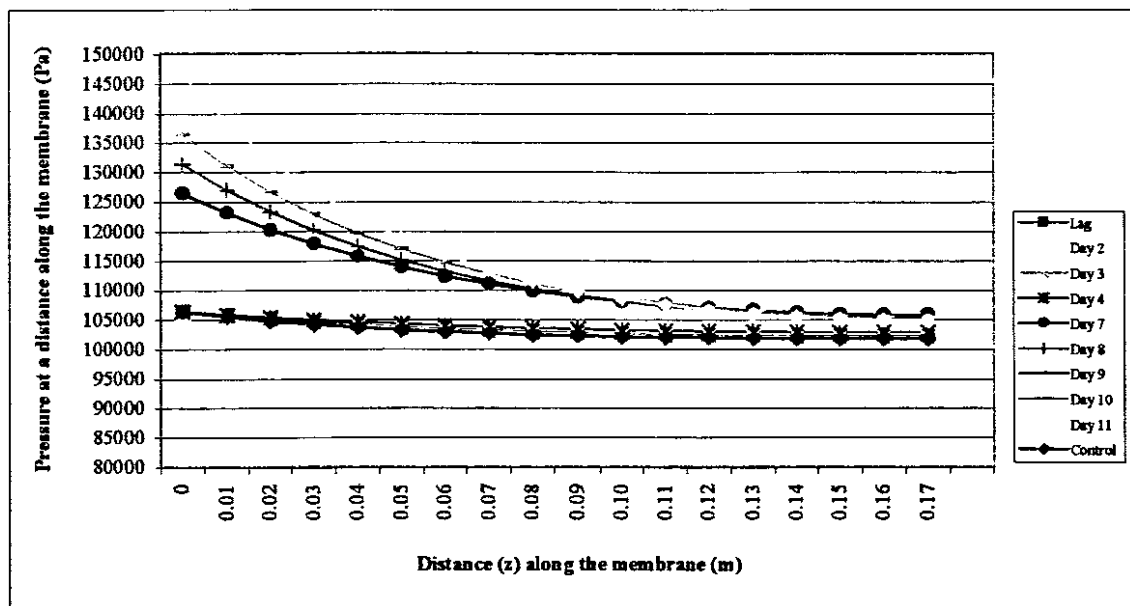
Figure 7.3: Predicted Pressure along a membrane with biofilm growth

7.3.3 Membrane Permeability (K)

As shown in Figure 7.4, the permeability coefficient for the polysulphone hollow-fibre control membrane stayed constant throughout the experiment. Membrane permeability decreased from 2.67 E –11 m^2 at the beginning of the membrane to 1.28 E-12 m^2 at the end of the membrane. This curve remained constant throughout the experiment, indicating that the permeability for a membrane without biofilm growth is consistent.

Comparing this to a membrane with biofilm growth, as shown in the Figure 7.5, the permeability followed the same pattern from the beginning to the end of the membrane but decreased from day 1 to day 11. Permeability at the beginning of the membrane decreased from 2.67 E-11 m^2 on the control to a minimum of 2.00 E-11 m^2 on an inoculated membrane, as shown in Figure 7.5. This was an indication that the biofilm thickness increased from day 1 to day 11 and that the macrovoid space decreased, therefore indicating that membrane permeability decreased as biofilm thickness increased.
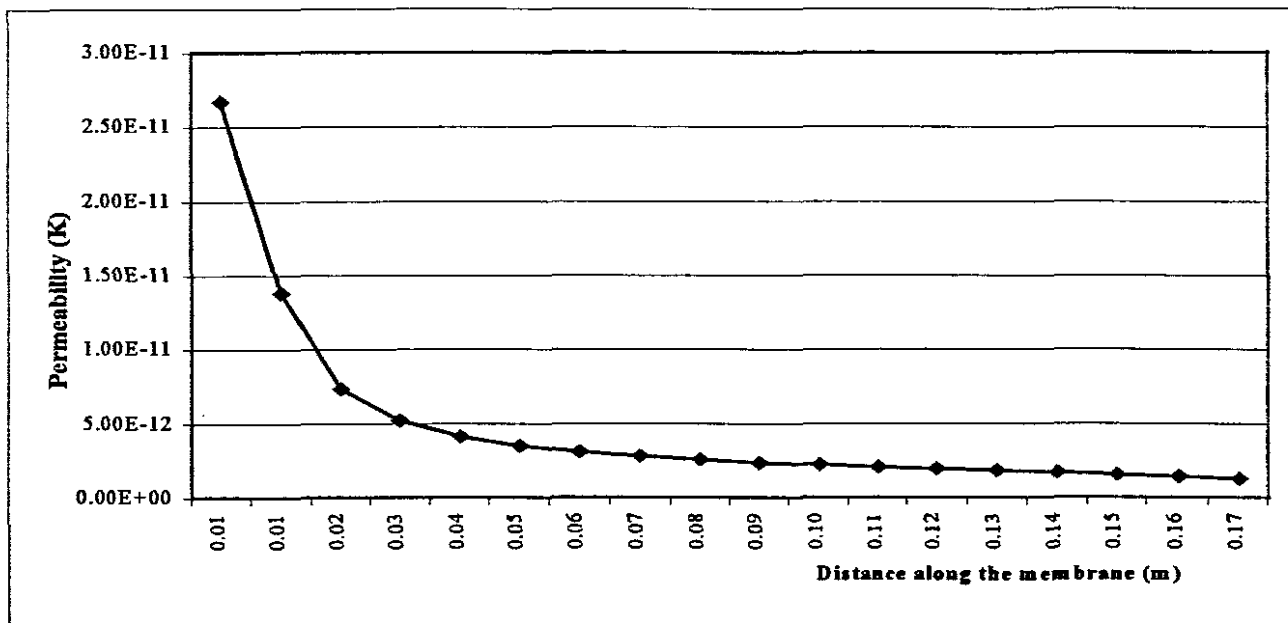
Figure 7.4: Permeability for membrane without growth
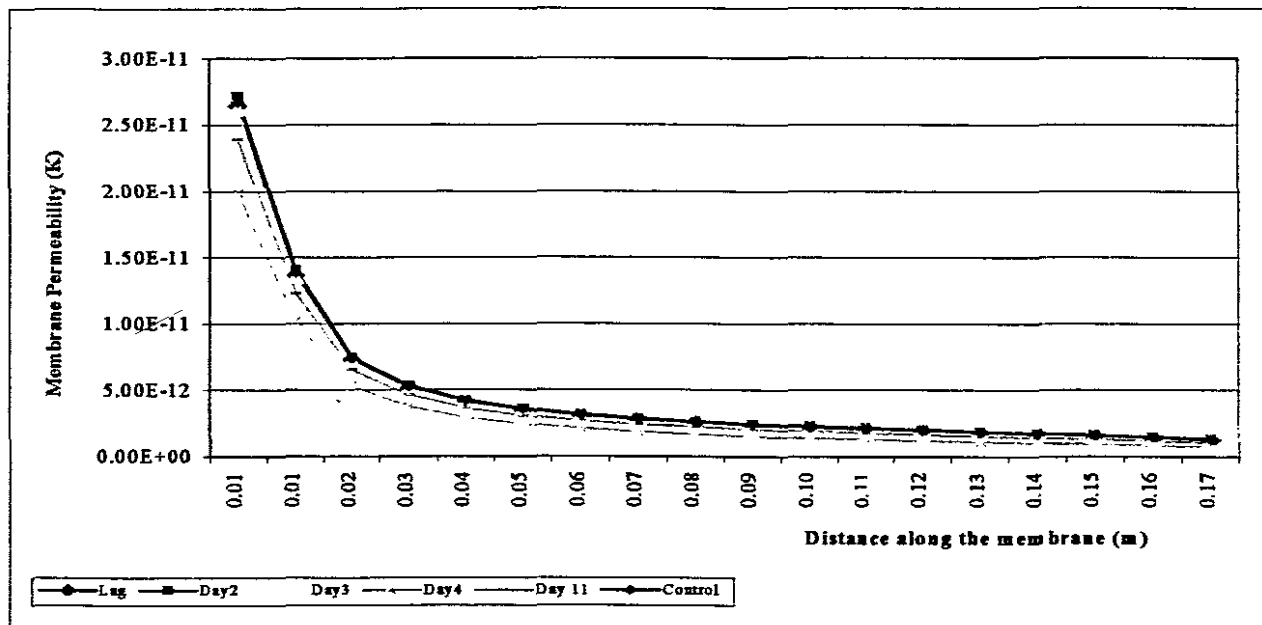
Figure 7.5: Permeability for membrane with growth

7.3.4 Membrane Flux

This reactor was operated in a constant flux mode. The flux of the fluid through the membrane (contact angle > 90° with the membrane material) was measured as a function of the pressure drop across the membrane. The above graphs indicate that the applied pressure across the membrane is indeed the most significant factor affecting the permeability of this specific membrane.

7.4 Summary

For the control (membrane without growth) the pressure decreased from the inlet to the outlet, but remained constant throughout the experiment. Membrane permeability also decreased exponentially from the inlet to the outlet but remained constant throughout the experiment.

For an inoculated membrane (membrane with biofilm) the pressure decreased from the inlet to the outlet, but the axial and radial pressure drops increased as the biofilm thickness increases on the membrane. Growth within the relatively confined macroviods of the membrane contributed to loss of permeability. The pressure and permeability can be used as a measure for biofilm growth on the membrane.

The outlet pressure measured corresponds to the predicted pressure using the modified Bruining model. This model can therefore be used for the prediction of pressure in a hollow fibre internally skinned, externally unskinned polysulphone membrane as was used in this study.

A coherent description of the pressure and permeability phenomena in hollow fibre devices has been given. The analysis also had relevance to the more general case of laminar flow in porous ducts.

CHAPTER 8

EVALUATING A POSSIBLE SCALE-UP PROCEDURE TO A MULTI-CAPILLARY SYSTEM

8.1. Introduction

In chapter 5 the suitability of a single fibre capillary membrane bioreactor for biofilm development and continuous enzyme production was investigated. The primary objectives for investigating the suitability of a membrane bioreactor for continuous production of ligninases were well suited for the single fibre capillary membrane bioreactor (SFCMBR). However, to best study the performance of the membrane bioreactor for comparisons with conventional processes and for application of this type of reactor it is necessary to scale-up from the SFCMBR to a multi capillary membrane bioreactor (MCMBR).

As indicated in Chapter 2, difficulties have been experienced in attempting to scale-up existing bioprocesses for large scale commercial use. These ligninolytic enzyme systems are still dependent on the presence of certain growth and environmental conditions (Kirk *et.al.*, 1986). This becomes a problem when the bioreactor configuration is being selected for large scale application using WRF because the design of the reactor is complicated by the number of associated variable parameters.

The broad objective of this chapter was to evaluate a possible scale-up procedure to a cost effective, easy to assemble and operate, multi-capillary system, by using those process technologies that are already available.

8.2   Scale-up of the reactor

The term scale-up is typically used for the transfer of processes from a laboratory scale (where the scale is typically from 1 to 25L) to production scale, where the scale is 30 to 1000 m^3 (Govender, 2000).

Consensus amongst scale-up criteria is difficult, suggesting it is rather a very intuitive process, which requires careful consideration of the bioprocess requirements from the outset of the design strategy. Ease of exchange, regeneration and flushing of membranes, ease of assembly and of dismantling of the module in actual field applications are vital design features which will become obvious only under prolonged operating conditions (Domröse, et.al.,1998). Failing this the membrane bioreactor will ultimately manifest its limitations as a lack of productivity.

8.3   Types of modules

Various types of capillary membrane modules are known. Module design is generally based around two general types of membranes, flat sheet and tubular. According to Fane (2001), different membrane modules are available and these can be classified into the following:

- *Flat sheet / Flat plate*

    Flat sheet membranes sitting on a plate that provides a porous support for permeate outlet, as shown in Figure 8.1. The flow channels are usually thin, 1 to 3 mm and sometimes fitted with a mesh-like channel spacer. The membranes are stacked in flow channels connected in series or parallel
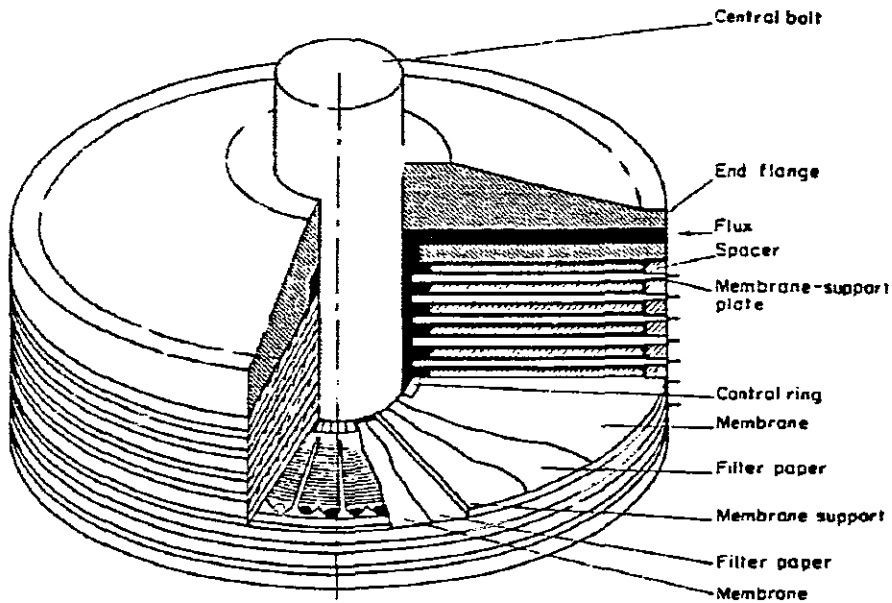
Figure 8.1: Flat sheet / Flat plate membrane module

- *Spiral wound*

    Flat sheets wound around a central tube, as shown in Figure 8.2. The membranes are glued along three sides to form "leaves" attached to a permeate channel (tube) along the unsealed edge of the leaf. The internal of the leaf contains a permeate spacer designed to support the membrane without collapsing under pressure. The permeate spacer is porous and conducts the permeate to the permeate tube. Several leaves are connected to the tube. A feed channel spacer (a net-like sheet) is placed between the leaves to define channel height and provide mass transfer benefits. The leaves are wound around the permeate tube and given an outer casing.
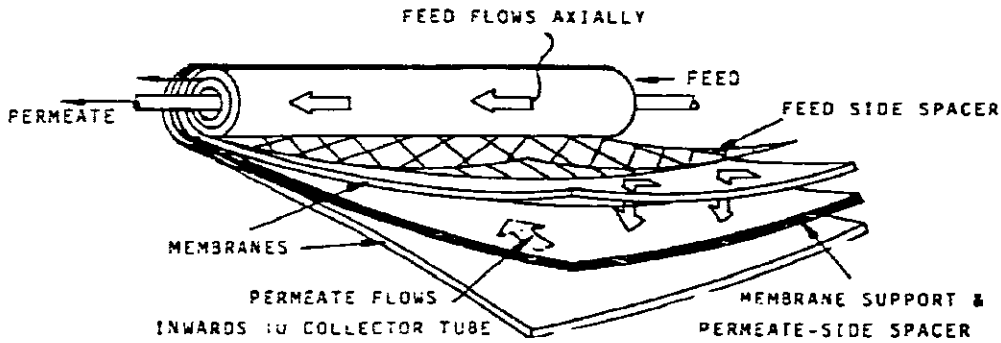
Figure 8.2: Spiral wound Module

- *Tubular*

    As seen from Figure 8.3, this module is similar to the shell and tube heat exchanger with tubes connected in series or parallel. Sometimes the membrane tubes are inserted into perforated metal support tubes, sometimes the tubes are self-supporting. Inorganic membranes can most easily be made in tubular format as single tubes or multi-canal monoliths.
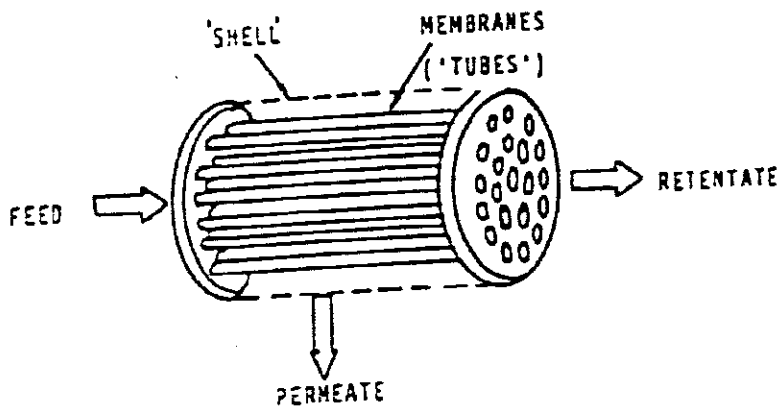
Figure 8.3: Tubular Module

For bioreactor systems the membranes are mostly arranged in parallel as this arrangement gives a lower velocity of the fluid in the membranes, which in turn will result in a lower pressure drop.

- *Hollow Fibre Modules (HFM)*

    These modules, as shown in Figure 8.4, use membranes that are 'self-supporting', i.e. walls are strong enough to avoid collapse or bursting. The outer diameter may be <0.5 to > 1.0 mm with an inner 'lumen' diameter of <0.3 to 0.8 mm. Hollow fibre modules contain thousands of fibres arranged in a 'bundle' and potted in epoxy to seal the element. This type of module is used for RO, UF and MF. Feed can be from the shell side or from the lumen side.
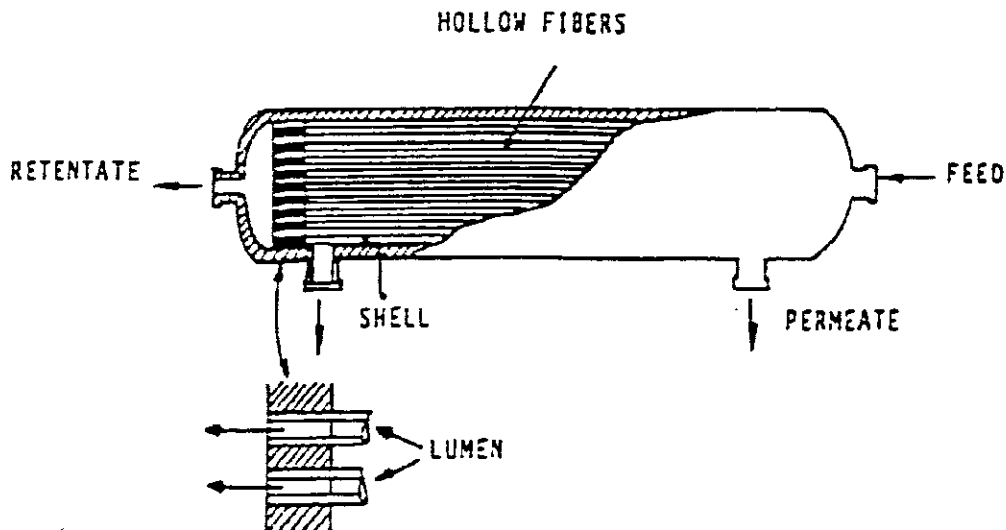
HOLLOW FIBERS

Figure 8.4: Hollow Fibre Module

According to Domröse *et.al* (1996), the membranes may be internally or externally skinned, but generally the membranes are embodied inside a shroud in a tube-in-shell configuration. The membrane ends are encapsulated in a resin to form a tube-sheet that is bonded and sealed to the inside of the shroud. All of these have different end-sealing caps or the like formed in the shroud of such modules.

The tubular flow reactor is chosen when it is desired to operate the reactor continuously but without back mixing of reactants and products. The reaction mixture passes through in a state of plug flow. It is assumed that not only the local mass flow rate but also the fluid properties, temperature, pressure and composition are uniform across any section normal to the fluid motion but changes from the inlet to the outlet of the reactor in the longitudinal direction. In an idealised tubular reactor all elements of fluid will take the same time to pass through the reactor and experience the same sequence of temperature, pressure and composition changes. The factors that must be taken into consideration are:

- whether plug flow can be attained
- heat transfer requirements
- pressure drop in the reactor
- ease and cheapness of construction.

8.4 Module Components

According to the invention by Domröse, *et.al.* (1996), a membrane module consist of the following components:

- a housing;
- a number of capillaries fitted into the housing;
- an inlet in the housing for charging a fluid into the capillaries;
- an outlet for discharging fluid out of the capillaries;
- a permeate outlet in the housing for discharging fluid after having passed through the walls of the capillaries and collecting around the capillaries;
- a number of apertures in the housing on at least one end of the housing
- a resin cast plug filling the appertures and the space between the capillaries in the region of the apertures, the resin cast plug forming a ring on the outside of the housing and simultaneously encapsulating the end of the housing.

According to Fane (2001), a membrane module consist of the following components
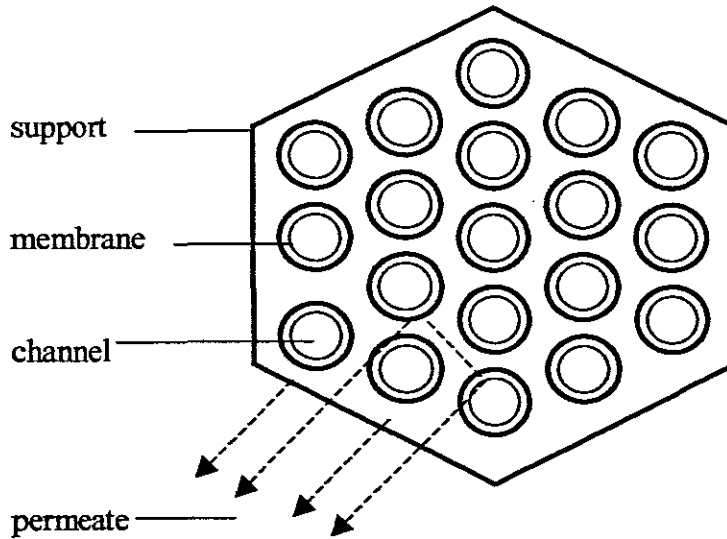
Figure 8.5: **Cross section showing membrane module components**

8.5 Module Operation

Fane (2001) also classified the design and operation into the following:

- Series vs parallel vs tappered cascade
- Continuous vs batch
- Cross flow vs Dead-end

In hollow fibre MF and UF it is common to operate at constant flux without crossflow, i.e. dead end. This means that biofilm resistance increases steadily as well as transmembrane pressure.

8.6   Module Design

Module design is crucial to the operation of the membrane process as this is a unit that must operate at a technical scale with a large membrane surface area to volume ratio and adequate air and liquid mass transfer. The method of potting the membrane, capillary spacing and the relative membrane size lead to a range of module design considerations. Due to the particular operating requirements of this particular and membrane type, information on the application thereof and the module design is very limited (Govender, 2000).

8.6.1   Design Concept

A simple design concept will be used to produce a module that can be easily machined, manufactured, repaired and serviced. Off the shelf standard components will be used to increase reliability and durability at a reasonable cost. The following design concept will apply, " *Design genius is simplicity*" (Domröse *et.al.*, 1998). This concept means that simplicity is not to be confused with inferior design or quality, but refers to a design which is functional and results in a reliable, long lasting, useful and user-friendly product.

8.6.2   Design requirements

To meet the multi-capillary membrane module requirements successfully, the design must meet minimum criteria, which can be summarised as follow:

- Consideration has to be given to the behaviour and properties of the biological materials employed. The mechanical inactivation of *LiP* and *MnP* is a well documented scale-up problem (Kirk *et.al.* 1986; Leisola *et.al.*, 1988; Linko, 1992). The reactor design will thus have to accommodate growth limitations of the WRF. This can be overcome by using the correct spacing between the membranes.

- The module must secure, position and protect membranes against damage.

- The module should allow for either heat or chemical sterilisation prior to the inoculation of the membranes. Depending on the capacity the module may too be heavy to sterilise in an autoclave. They may have to be constructed for in-situ sterilisation.

- The module construction must allow the operator to monitor biofilm growth and contamination inside the reactor at all times.

- The module must provide the connections for feed, permeate and concentrate flow. These channels must seal hermetically because any leakage is a possibility for contamination and renders a module useless.

- The operational design should be such that the least possible number of fittings, tubing and attachments required for the operation is used reducing the possibility of contamination entering the system.

8.6.3   Packing Density and Number of capillaries

Packing density will influence the system size and possibly the cost. The gap, or distance, between individual capillaries in a module is very important, as this will affect the growth of the microorganism. With increasing gap size, the number of capillaries that can be fitted into a module decrease, i.e. the packing density is reduced. A balance must be maintained between a high packing density and the process conditions.

8.6.4 Arrangement of capillaries

The membranes can be arranged in an equilateral triangular, square or rotated square pattern. The recommended membrane pitch, distance between the centres, is normally 1.25 times the membrane outside diameter and this will normally be used unless process requirements dictate otherwise. The recommended minimum clearance between the membranes is 6.4 mm (Coulson and Richardson, Vol 6, 1993).

The packing pattern can also be arranged around a centre capillary, around which the rest of the capillaries are grouped to form concentric circular layers, as shown in Figure 8.6. Other packing arrangements are also possible, with either two or three capillaries in the centre. Figure 8.6, is a schematic representation of the number of capillaries which can be packed into a module. This varies with the size of the gap between the individual capillaries.

$$N = 3n^2 + 3n + 1$$

N = number of capillaries

n = number of complete layers around the centre
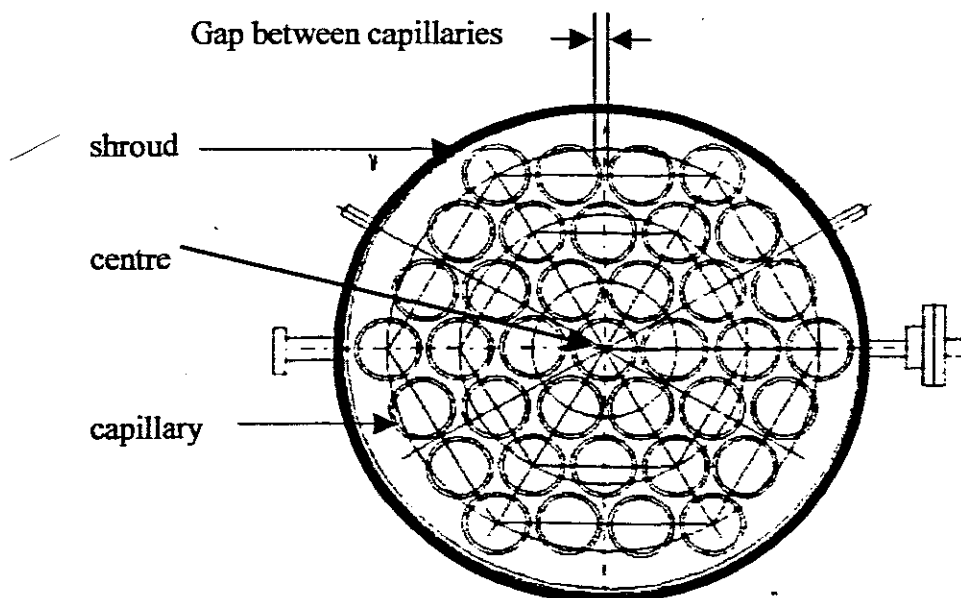
Figure 8.6 : Cross Section of a module capillary pattern (Modified from Domröse et.al.,1998)

8.6.5 Ease of manufacture and maintenance

When the membranes become completely blocked with the fungus or the fungus denatures, the membrane modules will have to be easily dismantled and cleaned. The membrane bundle also have to be replaced easily and quickly. The replacement of the membranes will influence the maintenance and labour costs.

8.6.6 Materials of construction

The housing can be made of metal or plastic or any other suitable material. The following materials of construction were considered:

Glass: The single fibre reactors are made of glass. This enables the operator to monitor the growth of the micro-organism and possible contamination. Problems encountered with glass are that it cannot be heat sterilised and breaks easily. If the reactors are designed for in-situ sterilisation they become, as a consequence, pressure vessels and the extensive use of glass becomes impractical. The preferred material of construction is a then Stainless Steel.

PVC has a working pressure of up to 600 kPa and can be used at operating temperatures of up to 45°C. PVC will enables the operator to monitor the growth of the micro-organism and check for any possible contamination.

Stainless Steel has an even thinner wall thickness and can operate at temperatures above 100°C.

Seals are typically made of silicone or other synthetic rubber or fluorinated plastics, with borosilicate glass being retained for sighting windows.

Some reactors would be constructed mainly of borosilicate glass with some parts, such as sensor ports and heating surfaces, in Stainless Steel. Machining, cutting, drilling, permeate outlet holes and chamfering and deburring are easier and faster in PVC than in Stainless Steel. Besides these advantages, the cost of PVC is much

PVC than in Stainless Steel. Besides these advantages, the cost of PVC is much lower than in Stainless Steel and with PVC the operator will be able to monitor biofilm growth and contamination on the inside of the reactor while in operation, that will not be possible with a Stainless Steel housing.

8.7 Summary

This chapter evaluated a possible scale-up procedure to a multi-capillary bioreactor system. The various module configurations that exist and that are in use were discussed. For the purposes of this work, the Hollow Fibre Module (HFM) seemed to be the most appropriate configuration, as the polysulphone internally skinned membranes that are used are self supporting. The membranes will be connected in parallel to give a lower velocity inside the membranes and consequently a lower pressure drop. The module will be operated in the dead-end filtration mode. Nutrient will be supplied from one inlet to the lumen and will be collected at one outlet on the shell side. The O_2 source will be supplied on the shell side and will also be collected at the permeate outlet.

The *"Design genius is simplicity"* concept will be applied, which means that simplicity should not be confused with inferior design and quality. The different module components and materials of construction were discuss and some parts of the module will be made of Stainless Steel and some parts of PVC. The most important design considerations are to allow enough space between the membranes for biofilm growth, to protect the membranes from damage, to prevent any leak and contamination and the materials of construction should be able to withstand sterilisation and should allow the operator to monitor the operation on the inside of the module. The module should be easy to clean and maintain.

CHAPTER 9

CONCLUSIONS AND RECOMMENDATIONS

9.1 Conclusions

It was clearly demonstrated that the single fibre membrane bioreactor is very suitable for biofilm growth. The reactor provided a suitable environment to continuously grow an immobilised biofilm of *P. chrysosporium* as a uniform thin film over the membrane. Biofilm thicknesses of up to 550 µm were obtained.

The gradostat concept was clearly and successfully illustrated within the reactor. Thicker biofilms were observed where higher nutrient conditions prevailed and thinner biofilms where lower nutrient conditions prevailed. Both radial and axial nutrient gradients were observed. Results also showed that all the ammonium that was supplied in the nutrient feed was used by the fungus, indicating nitrogen starvation. Glucose was also used by the fungus but was not completely depleted.

Enzymes were produced on a continuous basis, with peak activities of *MnP* observed on days 3 to 4 and *LiP* on days 9 to 11, depending on the conditions. From literature and the results in this work it was clear that nutrient feed flowrate, air flow rate, temperature, pH, O_2 concentration and nutrient concentration have an effect on biofilm growth and enzyme activity. This study evaluated the effect of these potentially important operating parameters on the feasibility and operational stability of the reactor and found that biofilm development and enzyme production is definitely affected by the set operating parameters. A sensitivity analysis was performed on temperature, by exposing the bioreactor to room temperature and a controlled temperature of 37°C, and O_2 concentration, by exposing the reactor to air (21% O_2) and pure O_2 (98%).

At room temperatures of less than 20°C biofilm growth was observed after 6 days as opposed to 3 days at 25°C and 2 days at 37°C. It was found that *P. chrysosporium* does grow and enzymes were produced at room temperature but that optimum

temperature for biofilm development and enzyme production is at 37°C. From the sensitivity analysis at different O_2 concentrations it appeared that biofilm development and enzyme production is higher at higher O_2 concentrations but because of limited experimental results no definite conclusion could be reached about the optimum O_2 concentration. However, it was established that biofilm development is adequate using air and that this method is also more economical than using pure O_2.

Three types of contamination were observed. Contamination was omni-present., which was overcome by using more stringent sterilisation techniques.

The effect of biofilm development on membrane pressure and permeability was monitored. It was found that bioflim development decreased membrane permeability and consequently increased pressure at the membrane inlet. A Modified Bruining model was successfully applied in the prediction of membrane pressure and permeability along the membrane with time.

A possible procedure to a multi-capillary system was evaluated. Taking all the design requirements and concepts into consideration, the hollow fibre membrane module (HFM) suited this application.

9.2 Recommendations

Once peak activities are observed, experiments should be performed to try and maintain the enzyme production at these levels by manipulating the nutrient feed concentrations and flow rates.

It was found that the optimum temperature for biofilm development and enzyme production is 37°C but the stability of the enzymes at this temperature should be determined.

To perform more experiments at different O_2 concentrations to determine the optimum concentration and economic feasibility of using higher concentrations.

Before these enzymes can be applied in the various different fields, they should be purified and isolated. It is recommended to evaluate the most effective and efficient purification and isolation techniques available.

A multi-capillary system should be build and evaluated for biofilm development and sustained enzyme production, in the presence of certain growth and environmental conditions, with the aim of comparing this membrane bioreactor system to conventional processes.

REFERENCES

Belfort G. 1989. *Membranes and bioreactors.* A technical challenge in biotechnology. Biotechnol. Bioeng. 33: 457-469

Bruining W.J. 1989. *A general description of flows and pressures in Hollow fibre membrane Modules.* Chemical Engineering Science. Vol. 44(6):1441 – 1447

Capdevila, C. Corrieu, G. and Asther M. 1989. *A feed harvest culturing method to improve lignin peroxidase production by P. chrysosporium INA-12 immobilised on polyurethane foam.* J. Ferm. Bioengng 68: 60-63.

Capdevila, C., Moukha S., Ghyczy M., Theilleux J., Gelie B., Delattre M., Corrieu G. and Asther M. 1990. *Characterization of peroxidase secretion and subcellular organisation of Phanerochaete chrysosporium INA-12 in the presence of various soybean phospholopid fractions.* Appl. Envrin. Microbiol. 56: 3811-3816

Chatterjee, S.G. and Belfort, G. 1986. *Fluid Flow in an idealised spiral wound membrane module.* J. Membrane Sci. 28, 191 –208.

Clark, J.M. and Switzer, R.L. 1976. *Experimental Biochemistry.* 2nd Ed. W.H. Freeman:New York.

Coulson, J.M. and Richardson, J.F. 1993. Chemical Engineering. Volume 6. 2nd Edition.

Domröse, S.E., Finch, D.A. and Sanderson, R.D. 1996. *Capillary Membrane Modules.* SA patent 96/1580

Domröse, S.E., Finch, D.A. and Sanderson, R.D. 1998. *Development of Transverse-Flow Capillary membrane modules of the modular and block types for liquid separation and bioreactors.* WRC Report No. 847/1/98.

Dosoretz, C. G., Chen, H.C and Grethlein, H.E. 1990. *Effect of environmental conditions on extracellular protease activity in ligninolytic cultures of P. chrysosporium.* Appl. Environ. Microbiol. 56 (2):395-400.

Dosoretz, C.G., Rotschild, N. and Hadar, Y. 1993. *Overproduction of lignin peroxidase by P. chrysosporium (BKMF 1767) under nonlimiting nutrient conditions.* Appl. Environ. Microbiol. 59(6):1919-1926.

Edwards, W.D. 1999. *Capillary membrane immobilised polyphenol oxidase and the bioremediation of inductrial phenolic effluent.* PhD Thesis. Rhodes University; Grahamstown.

Edwards, W. Bownes, R., Leukes, W.D., Jacobs, E.P., Sanderson, R., Rose, P.D. and Burton, S.G. 1999. *A capillary membrane bioreactor using immobilised polyphenol oxidase for the removal of phenols from industrial effluents.* Enzyme Microb. Tech. 24(3-4):209-217.

Faison B.D. and Kirk T.K. 1985. *Factors involved in the regulation of a ligninase activity in P. chrysosporium.* Appl. Envir. Microbiol. 49: 299-304.

Fane, T. 2001. Membrane, Science, Engineering and Art. 4th WISA-MTD Workshop. Stellenbosch: RSA

Feijoo, G., DosoretzC. and Lema, J.M. 1994. *Production of Lignin Peroxidase from Phanerochaete chrysosporium in a packed bed bioreactor with recycling.* Biotechnology Techniques 8(5): 363-368

Freeman, A. and Lilly, M.D. 1998. *Effect of processing parameter on the feasibility and operational stability of immobilized viable microbial cells.* Enzyme and Microbial Technology 23: 335 - 345

Glen, J.K. and Gold, M.H. 1988. *Manganese Peroxidase from Phanerochaete chrysosporium.* Methods in Enzymology 161:258-265.

Govender, S. 2000. *Optimisation studies on a membrane gradostat bioreactor for ligninase production using a white rot fungi*. M-Tech. ML Sultan Technikon: Durban.

Haemmerli, S.D.; Leisola, M. S.A. and Fiechter, A. 1986. *Polymerisation of lignins by ligninases from P. chrysosporium*. FEMS Microbiology Letters 35:33-36

Hamer, G. 1993. Bioremediation: *A response to gross environmental abuse*. Trends Biotechnol. 11(8):317-319.

Head, I.A. 1998. *Bioremediation towards a credible technology*. Microbiology. 144: 599-608.

Howell, J.A., Sanchez, V. and Field, R. W. 1993. *Membranes in bioprocessing: Theory and applications*. Chaplan and Hall, Cambridge.

Ishizaki, K.; Komarneni, S., and Nanko, M. 1998. *Porous Materials: Process Technology and applications*. Dordrecht: Kluwer Academic Publishers.]

Jacobs, E.P. and Leukes, W.D. 1996. *Formation of an externally unskinned polysulphone capillary membrane*. Journal of Membrane Science (121): 149-157

Jacobs, E. and Sanderson, R.D. 1997. *Capillary membrane production development*. Report to the WRC by the Institute for Polymer Science. WRC Report No 632/1/97.

Janshekar, H. and Fiechter, A. 1988. *Cultivation of Phanerochaete chrysosporium and production of lignin peroxidase in submerged stirred tank reactors*. J. Biotechnol. 8:97-112.

Kirk, T.K. Schultz,E., Connors, W.J., Lorenz, L.F. and Zeikus, J.G. 1978. *Influence of cultural parameters on lignin metabolism by Phanerochaete chrysosporium*. Arch. Microbiol. 117:277-285.

Kirk, T.K., Croan, S., Tien, M., Murtagh, K.E. and Farrel, R.L. 1986. *Production of mulltiple ligninases by P. chrysosporium: effect of selected growth conditions and use of a mutant strain.* Enzyme Microb. Technol. 8: 27-32

Kirk, T.K. and Farrel, R.L. 1987. *Enzymatic combustion: the microbial degradation of lignin.* Annual reviews of microbiology 41: 465-505.

Leisola, M.S.A. and Fiechter, A. 1985. *Ligninase production in agitated conditions by Phanerochaete chrysosporium.* FEMS Microbiol. Lett. 29:33-36.

Leisola, M.S. A., Hammaerli, S.D., Waldner, R., Schoemaker, H.E., Schmidt, H.W. H. and Fiechter, A. 1988. *Metabolism of a lignin model compound, 3,4 – dimethoxybenzyl alcohol by Phanerochaete chrysosporium.* Cellulose Chemistry and Technology 22:267-277.

Leukes, W. 1999. *Development and Characterisation of a Membrane Gradostat Bioreactor for the Bioremediation of Aromatic Pollutants using White Rot Fungi.* PhD Thesis, Rhodes University: Grahamstown.

Leukes, W.D., Jacobs, E.P., Rose, P.D., Sanderson, R.D. and Burton, S.G. 1996. *Secondary metabolite production.* RSA patent 95/7366. USA patent 08/705, 624 pending. EPO patent 963606333.4 pending.

Leukes, W. 2000. *Membrane Bioreactors: Appropriate Technology for Water Purification in South Africa.* WRC 20. WISA 2000 Biennial Conference and Exhibition: Sun City

Lewandowski, G., Armenante, P.M. and Part, D. 1990. *Reactor design for hazardous waste water treatment using a white rot fungi.* Water Res. 24(1):75-82

Linko, S. 1988(a). *Continuous Production of lignin peroxidase by immobilised P. chrysosporium in a pilot scale bioreactor.* J. Biotechnol. 8: 163-170

Linko, S. 1988(b). *Production and characterisation of extracellular lignin peroxidase from immobilised Phanerochaete chrysosporium in a 10-1 bioreactor.* Enzyme Microb. Tech.10:410-417.

Linko, S. 1992. *Production of P. chrysosporium lignin peroxidase..* Biotech. Adv. 10: 191-236.

Linton, E.S., Higton, G., Knowles, C.J. Bunch, A.W. 1989. *Monitoring microbiol growth in a hollow fibre reactor using an electric pressure sensor.* Enzyme Microb Technol. 11:283-288.

Lovitt, R.W. and Wimpenny, J.W.T. 1981. *Physiological Behaviour of Escherichia coli grown in opposing gradients of oxidant and reductant in the gradostat.* J. Gen. Microbiol. 127:269-276.

Martin, W. 2000. *Recovery of impregnated Gold from waste mine timber through biological degradation.* M-Tech., Cape Technikon: Cape Town.

Nicell, J.A., Bewtra, J.K., Taylor, K.E., Biswas, N. and St. Pierre, C. 1992. *Enzyme catalysed polymerisation and precipitation of aromatic compounds from waste water.* Water Sci. Technol. 25(3):157-164.

Quaile, J.P. and Levy, E.K. 1975. *Laminar Flow in a porous tube with suction.* Trans. ASME, J. Heat Transfer 2, 66.

Reddy, C.A. and D'Souza, T.M. 1994. *Physiology and molecular biology of the lignin peroxidase of Phanerochaete chrysosporium.* FEMS Microbiol. Rev. 13(2-3):137-152

Richardson, J.F and Peacock, D.G. 1994. *Chemical Engineering.* Volume 3 (Chemical and Biochemical Reactors and Process Control). 3rd Edition pp. 252-433

Siebel, M.A. 1992. *Attached growth reactors,* pp.139-162. (cited in Govender, 2000).

Tharakan, J.P. and Chau, P.C. 1986. *Operation and Pressure distribution of immobilised cell hollow fibre bioreactors.* Biotech. Bioengng. 28:1064-1071.

Tien, M. 1987. *Properties of ligninase from Phanerochaete chrysosporium and their possible applications.* CRC Crit. Rev. Microbiol. 15(2):141-16.

Tien, M and Kirk, T.K. 1983. *Lignin-degrading enzyme from the hymenomycete Phanerochaete chrysosporium Burds.* Science 221:661-663.

Tien, M and Kirk, T.K.1988. *Lignin Peroxidase* of *Phanerochaete chrysosporium.* Methods in enzymology (161): 238-249

Turton, R.; Bailie, R.C.; Whiting, W.B and Shaeiwitz, J.A. 1998. *Analysis, Sunthesis and Design of Chemical Processes.* Prentice Hall: New Jersey, pp 509 - 555

Venkatadri R. and Irvine, R.L. 1993. *Cultivation of Phanerochaete chrysosporium and production of Lignin Peroxidase in novel Biofilm reactor systems: Hollow fibre reactor and silicone membrane reactor.* Water Research 27(4): 591-596

Walsh, G. 1998. *Comparison of pollutant degrading capacities of Strains of P. chrysosporium in relation to phsiological differences.* Honors-Thesis, Rhodes University

Walsh, P.K. and Malone, D.M. 1995. *Cell growth patterns in immobilisation matrices.* Biotechnol. Adv. 13:13-43.

Willershausen H., Jager A and Graf H. 1987. *Ligninase production of P. chrysosporium by immobilzation in bioreactors.* J. Biotechnol. 6:239-243.

Wimpenny,J.W.T 1990. *Diffusion-limited growth.* pp. 65-84 (cited in Leukes, 1999)

APPENDIX A

GROWTH AND MAINTENANCE OF THE FUNGUS

A1: Preparation of the growth medium (Spore inducing medium)

The method for preparation of the growth medium was taken from Tien and Kirk (1988).

Add the following ingredients in order into a 1000 ml Schott bottle.

Glucose	10g	
Malt extract	10g	
Peptone	2g	
Yeast extract	2g	
Asparagine	1g	
KH_2PO_4	2g	
$MgSO_4.7H_2O$	1g	($MgSO_4$ = 2.05g)
Agar-agar	20g	
Thiamin-HCl	1mg	

Make up to 1000 ml mark with distilled water, close bottle with cap and shake to dissolve the powder. Cover with tinfoil to prevent contamination and put a piece of heat detecting tape (autoclave tape) on the foil to prepare for autoclavation. If no cap is available, cover the opening with non absorbent cotton wool and then wrap it with tinfoil. Label the bottle with the present date, your name and the description of the contents and place into autoclave for 20 minutes at 121°C to ensure sufficient sterilisation. The water level in the autoclave chamber must cover the bottom. After removing from the autoclave allow the content to cool down to a workable temperature before casting into the petri dishes.

A2: Casting of the Agar slants

Petri dishes

Working under a laminar flow hood and using the flaming technique (flame after opening and before closing the bottle). Fill each petri dish with the still hot agar (~60°C) by opening the lid only as far as necessary and pour agar evenly into it until the bottom of the dish is about 1 cm thick. Flame the agar flask outlet before and after the agar is poured into a petri dish to avoid any possible transferred contamination. Leave the lids slightly open for a while to prevent moisture forming (condensation) underneath the lids. After the agar has cooled down sufficiently, it will become stiff with a consistency of jelly. Now you can proceed with the inoculation of *Phanerochaete chrysosporium* spores.

Roux bottles

Working under an operating laminar flow hood and using the flaming technique, fill each Roux bottle with about 250 ml still hot agar. Cover the tops with non-absorbent cotton wool and leave bottles slightly elevated for air circulation. Allow the agar to cool down for a few hours; it will be stiff as jelly and ready for inoculation.

A3: Inoculation of *Phanerochaete chrysosporium* on the agar slants

Petri dishes

Work under an operating laminar flow hood and clean the surface thoroughly with 70% alcohol to avoid contamination. A platinum rod is used as the tool to transfer spores. Flame the tool under a bunsen burner (flaming technique) and cool it down by dipping it into the fresh agar located on the rim of the petri dish. Cut out a square piece (about 1 cm) of the inoculation culture and place in the middle of the fresh petri dish and cover the lid. Continue until all the petri dished are inoculated. Store the

petri dish upside down and incubate at 37 ^{0}C for approximately seven days until spores are ready. Label with your name and present date.

Roux bottles

Working under an operating laminar flow hood and using the flaming technique, cut out a square piece (about 1 cm) with a flamed object and place in the middle of the Roux bottle and cover with cotton wool. Store the Roux bottle lying on its side with the top slightly elevated and incubate at 37 ^{0}C for approximately seven days until spores are ready. Label with your name and present date.

A4:   Spore solution preparation

Autoclave the following equipment;
- 1000 ml distilled water in a schott bottle
- 20 ml syringe with glass wool
- 250 ml flask

Always work under a laminar flow hood and work as clean, considerate and careful as possible to avoid any form of contamination. Take all the above mentioned precautions to ensure maximum sterility.

Pour 5 ml cooled sterile distilled water into each petri dish containing spores and mycelium, under sterile conditions, close the lid and shake the water in rotational movements for one minute, to ensure that all spores are in solution. Transfer the washing solution from the petri dishes into a sterile 100 ml schott bottle, repeat this three to four times on one agar slant. Continue with this procedure until you have enough spore solution. The bottle now contains a spore / mycelium solution.

A5: Separation of spores from mycelium

Heat sterilise (autoclave) a sterile syringe with glass wool for 15 minutes. Filter the solution through a 0.22µm sterile filter using the sterile syringe with glass wool, into a 250 ml flask.

A6: Determination of spore purity and concentration

Spore purity

Under sterile conditions pipette a small drop of spore solution onto a slide, cover it with a cover slip and observe with a light microscope at * 100 magnification. You should see undamaged, uniform oval spores with a small size distribution and no or very few visible mycelium pieces.

Spore concentration

The spore solution concentration is determined by measuring absorbance at 650 nm with a Spectrophotometer . The spectrophotometer should be switched on at least 30 minutes before it is used in a fixed wavelength mode. The UV and visible lights should be switched on. Ordinary plastic cuvettes are used for the spore solution concentration. According to Tien and Kirk (1988) an absorbance of 1.0 cm^{-1} is approximately 5×10^6 spores/ml.

- Pour distilled water into a plastic cuvette and place into the spectrophotometer
- Blank the spectrophotometer by clicking on the word blank in the bottom left corner of the screen.
- Repeat two or three times until the absorbance reads close to 0.
- Replace the blank with a quartz cuvette filled with spore solution.
  (NB: Do not leaf the cover open for too long)
- Click on "Read Sample" at the top of the screen.

- Read off the absorbance and write it down.(e.g. 0.0741)

To obtain a million spores (example):

An absorbance of $\qquad$ 1 $\qquad$ = $\qquad$ 5×10^6 spores/ml

    i.e. $\qquad$ 0.0741 = $\qquad$ x

           x $\qquad$ = $\qquad$ $\dfrac{0.0741*(5 \times 10^6)}{1}$

                      = $\qquad$ 3.7×10^5 spores/ml

Therefore: 3.7×10^5 spores for every 1 ml

        i.e. 1×10^6 spores for every 2.7 ml (2700 µl)

Dissolve 2.7 ml of the spore solution into 250 ml sterilised distilled water. This solution will be used for inoculation of the reactor.

APPENDIX B

PREPARATION OF THE NUTRIENT
SOLUTION

B1.   Trace element stock solution

Dissolve 1.5 g Nitrilotriacetate in 800ml distilled water. After dissolving the nitrolotriacetate completely, adjust the pH to 6.5 with 1M KOH (28g/500ml). Add each component sequentially.

$MgSO_4$	3g	$(MgSO_4 * 7H_2O = 6.14g)$
$MnSO_4$	0.5g	$(MnSO_4 * H_2O = 0.56\,g)$
NaCl	1g	
$FeSO_4.7H_2O$	0.1g	
$CoCl_2$	0.1g	$(CoCl_2 .6\,H_2O = 0.187g)$
$ZnSO_4.7H_2O$	0.1g	
$CuSO_4$	0.1g	
$AlK(SO_4)_2.12H_2O$	10mg (0.01g)	
H_3BO_3	10mg (0.01g)	
$Na_2MoO_4.2H_2O$	10mg (0.01g)	

Make up to 1L with autoclaved distilled water. Filter sterilise the solution into an autoclaved bottle using a 0.22 μm filter. Autoclave for 20 minutes and store at 4°C. This solution should be light yellow.

B2.   Basal III Medium stock solution

KH_2PO_4	20g	
$MgSO_4$	5g	
$CaCl_2$	1g	$(CaCl_2 * 2\,H_2O = 1.32g)$
Trace element solution	100ml	(see B1 above)

Make up to 1L with autoclaved distilled water. Autoclave for 20 minutes and store at 4°C.

B3.   10% Glucose stock solution

Glucose   100g

Make up to 1L with autoclaved distilled water. Autoclave for 20 minutes and store at 4°C.

B4.   0.1M 2,2-dimethylsuccinate stock solution (pH 4.2)

2,2-dimethylsuccinate 13.045ml in 1L autoclaved distilled water.

Calculated as follow:

If powder:		
Mw	=	146 g/mol^{-1}
Moles	=	mass/Mw
0.1M	=	mass/146.1
mass	=	(0.1*146.1)
	=	14.61 g (put into 1L)
If liquid:		
If density	=	1.12 g/mol
	=	mass /volume
Volume	=	14.61/1.12
	=	13.045 ml (put into 1L)

Autoclave for 20 minutes and store at 4°C.

B5. Thiamin-HCl (Do not autoclave)

Thiamin-HCl   100mg/L stock

Filter sterilize through 0.22μm filter into sterile bottle and store at 4°C.

B6. Ammonium tartrate

Ammonium tartrate   8g

Make up to 1L with autoclaved distilled water. Autoclave for 20 minutes and store at 4°C.

B7. 0.02M Veratryl alcohol (light sensitive)

Veratryl alcohol   2.907ml in 1L

Calculated as follow:

If powder:		
Mw	=	168.19 g/mol^{-1}
Moles	=	mass/Mw
0.02	=	mass/168.19
therefore mass	=	3.3638 g/L
If liquid:		
If density	=	1.157 g/ml
	=	mass/vol
Therefore vol.	=	2.907 ml/L

Autoclave for 20 minutes.(store in dark place when not in use).

B8.   Nutrient medium composition

Basal III Medium	100ml
10% Glucose stock solution	100ml (carbon source)
0.1M 2,2-dimethylsuccinate	100ml (growth enhancer)
Thiamin	10ml (vitamin)
Ammonium tartrate	25ml (nitrogen source)
0.02M Veratryl alcohol (light sensitive)	100ml (growth enhancer)
Trace elements	60ml

Make up to 1L with distilled water. (Autoclave)

Points to remember:

- When dispensing culture media, always use sterile measuring cylinders and dispense into sterile containers.
- Always use autoclaved distilled water.
- All stock solutions should be sterilised before the time. It is therefore not necessary to autoclave the nutrient media again after it is made up.
- Nutrient medium must be kept at 4°C if not in use.

APPENDIX C

LIGNINOLYTIC ENZYME ASSAYS

C1: Lignin Peroxidase Assay

Lignin Peroxidase activity was determined spectrophotometrically at 25° using veratryl alcohol as the substrate (Tien and Kirk, 1988). The activity was measured by determining the rate of oxidation of veratryl alcohol to veratraldehyde. This was monitored at 310nm. The alcohol exhibits no absorbance at 310nm whereas the aldehyde absorbs strongly. The extinction coefficient used for veratraldehyde was $9300 \ M^{-1}cm^{-1}$. Use is made of this property in a continuous spectrophotometric assay. Activity is expressed in $U.L^{-1}$, where 1 Unit = 1 $\mu mol/min$.

Prepare the following stock solutions.

10 mM Veratryl Alcohol

- 1.454 ml into 1L distilled H_2O.
- Store at 4^0C in a dark place when not in use.

Calculated as follow:

If powder:		
Mw	=	168.19
Moles	=	mass/ Mw
0.01 mol/L	=	mass/ 168.19
therefore mass	=	1.6818 g/L
If liquid:		
If density	=	1.157 g/ml
Volume	=	1.454 ml/L

250mM Tartaric Acid

- Add 9.43 g to 80 ml dH$_2$O.

- Using 1M NaOH, adjust pH to 2.5 (i.e. add 40 g/l NaOH to distilled water to make 1M NaOH)

- Make up to 250 ml volume.

- Store at 4^{0}C.

Calculated as follow:

Mw	=	150 g/mol
0.25 M	=	0.250 mol/L
(150g/mol*0.25 mol/L)	=	37.725 g/L
Required	=	9.43 g/ 250 ml

5mM Hydrogen Peroxide (H$_2$O$_2$)

- Made up fresh daily

- Light sensitive, do not leave standing in direct sunlight for extended periods of time.

- 50 µl of 30% H$_2$O$_2$ in a 100 ml flask and make up to volume.

Assay material and method

	Blank	Sample
10 mM Veratryl Alcohol	200 µl	200 µl
250mM Tartaric acid	200 µl	200 µl
Distilled water	520 µl	220 µl
Enzyme solution		300 µl
** 5 mM H$_2$O$_2$	80 µl	80 µl
	TOTAL:	**1000 µl (1 ml)**

**Add everything into the eppindorf tube except the H$_2$O$_2$, which is added just before assaying.

Spectrophotometer settings:

- Kinetics Mode

- UV light switched on

- Read at 310 nm for 5 minutes at 10 seconds intervals.

- Factor: 1075.3

- Temperature: 25^0C

- Extinction coefficient: 9300 $M^{-1}C^{-1}$

Calculation of activity

- The object is to find a reading in Units per litre, where 1 Unit = 1 micro-mol substrate converted per minute (mM/minL).

- Take your absorbance readings and plot a graph showing absorbance vs. time.

- The initial slope (dA/dt) will give you the value for "initial rate of reaction".

- To convert this to "d conc./dt" use Lambert-Beer and divide by the extinction coefficient E which is 9300 $M^{-1}cm^{-1}$. This gives a value in mol/min L.

- Moles are now changed to micro-moles by multiplying by 10^6. This gives micro-moles/min L. Micro-moles/min = 1 unit. So your answer is now in Units per litre (U/L)

- Now you have to consider sample handling. First, you need to account for dilution in your assay. If you used 200 microlitres of enzyme sample solution in a 2ml reaction volume, this constitutes a dilution of 1 in 10. You therefore have to multiply your answer by 10.

- If you have concentrated your sample by using cut off tubes, you have to divide by your concentration factor. (If you fill your cut off tubes initially with 3ml and you have 0.5ml concentrate enzyme solution left, your factor would be 6).

  Dilution factor   =   1000/300   =   3

  (300µl of enzyme in 1 ml reaction mixture)

- As a guideline, if you have not concentrated your sample, then multiply your dA/dt readings (in minutes) by 1075.3

$$\text{Activity} = \left[\left(\frac{dA}{dt} * dilutionfactor \middle/ extinctioncoefficient\right)\right] * 60 * 1 \times 10^6$$

$$= \text{mM} / \text{minL}$$

$$= \text{U/L}$$

C2: Manganese Peroxidase Assay (Oxidation of ABTS)

The activity is based on the spectrophotometric determination of oxidation of ABTS by *MnP* in the presence of lactate, Mn^{2+} and H_2O_2 (Glenn & Gold, 1988).

Prepare the following Stock Solutions

1 M Na Lactate buffer

- 10.22 g lactic acids into 100 ml beaker
- add 80 ml distilled water.
- Adjust to pH 4.5 using 1 M NaOH and make up to volume. (If the volume is 100 ml and the pH is not at 4.5 yet, add NaOH until the pH is correct).
- Store at 4^0C.

1 M Na Succinate buffer

- 11.81 g succinic acid into a 100 ml beaker
- Add 80 ml distilled water.
- Adjust pH to 4.5 using 1 M NaOH and make up to volume with distilled water. (If the volume is 100 ml and the pH is not at 4.5 yet, add NaOH until the pH is correct).
- Store at 4°C

MnSO₄ solution

- Add 95 mg MnSO₄*H₂O to 100 ml distilled water.   (MnSO₄4H₂O = 125mg)

ABTS Solution (light green in color, and turns blue when oxidized)

- 50 mg ABTS into 25 ml volumetric flask and make up to volume with dH₂O.
- Store at 4⁰C.

*Reagent A

Add the ingredients in the following order into a 25 ml volumetric flask and mix with a magnetic stirrer.

- Egg albumin   150 mg
- 1M Na lactate buffer   2.5 ml

The stirring speed must be slow, as entire albumin must dissolve but without any physical damage that could cause denaturation of protein. After the protein has dissolved completely add the other reagents:

- 1M Na succinate buffer   2.5 ml
- MnSO₄ solution   1.0 ml
- ABTS solution   1.0ml

Make up with distilled water to 25ml. Centrifuge before use to give a clear supernatant.

**Reagent B
- 1 μl of 30% H₂O₂ in a 100ml volumetric flask.
- made up fresh and stored in a dark place.

Assay material and method

	Blank	**Sample**
Reagent A	350 µl	350 µl
Reagent B	350 µl	350 µl
Enzyme solution		300 µl
Distilled water	300 µl	

- Clear supernatant of Reagent A is used and is added together with Reagent B into an eppindorf tube.

- Add everything into the eppindorf tube except the enzyme solution, this is added just before assaying.

Spectrophotometer settings:

- Kinetics mode

- UV and visible light switched on

- Temperature 25°C

- Read at 420 nm for 3 minutes at 5 seconds interval.

- Factor: 277.77

- Extinction Coefficient: $3600 \text{ M}^{-1}\text{C}^{-1}$

Activity is calculated the same as explained before.

APPENDIX D

GLUCOSE AND AMMONIUM ASSAYS

D1:   Glucose Assay

Nelson's A Reagent

Na_2CO_3	(anhydrous)	12.5g
Potassium sodium tartrate		12.5g
NaHCO		10g
Na_2SO_4 (anhydrous)		100g

- Add these chemicals in order, shaking well after each addition.
- Make up to 500ml

Nelson's B Reagent

$CuSO_4.5H_2O$ 7.5g
- Add 1 drop concentrated H_2SO_4
- Add to 50ml dH_2O

Arsenomolybdate Reagent

Dissolve 25g ammonium heptamolybdate in 450ml dH_2O.
Add 21ml concentrated H_2SO_4

Dissolve 3g sodium arsenate in 25ml H_2O.
Add to the above acid.

- Store in a brown bottle for 24 hours at 37^OC.
- Reagent should be yellow with no green tint.

Preparation of Glucose standards:

Prepare 100ml nutrient media.

Prepare 100ml blank media (i.e. culture media with *NO GLUCOSE*).

Sample No	Blank media / [ml]	Nutrient media / [ml]	[Glucose standard] [%]
1	0	1.0	1.0
2	0.2	0.8	0.8
3	0.4	0.6	0.6
4	0.6	0.4	0.4
5	0.8	0.2	0.2
6	1.0	0	0

Assay method (Glucose standard samples for standard curve)

- Add 50µl of the glucose standard (made up as shown in the table) to 950µl dH$_2$O.
- Do this for samples 1 to 6 in duplicate, conc. 1% to 0 % respectively.
- Pipette 100µl of this mixture from each sample into a test tube.
- Just before using, mix Nelson's B:A 1ml:25ml.
  (This crystallizes on standing. If this happens, heat it a little.)
- Add 1ml of Nelson's mixture to each test tube.
- Heat vigorously in a boiling water bath for exactly 20 minutes.
- Place in cold water to cool.
- Add 1ml arsenomolybdate reagent. Allow to stand for 5 minutes and shake to dissolve precipitated copper oxide and reduce arsenomolybdate (vortex until 'fizz/bubbling' disappears).
- Add 8ml H$_2$O and shake.
- Read at 540nm using plastic cuvettes.

The glucose standard samples is used to obtain the standard curve, by reading the absorbance of the different samples and plotting it against glucose %

Assay method (Glucose samples from experiment)

The exact same methods as described previously is used, but instead of the glucose standard sample the sample from the experiment permeate is used.

The absorbance reading from the spectrophotometer is used on the standard curve to obtain the glucose % in the permeate.

D2: Ammonium Analysis

A Spectroquant Ammonium Test Kit (Merk [®]) was used to determine the amount of ammonium present in the permeate. The assay was carried out using manufacturer specifications.

Preparation of ammonium standards:

Prepare 100ml culture media (standard).

Prepare 100ml blank media (i.e. culture media with *NO AMMONIUM TARTRATE*).

Blank media / [ml]	Std media / [ml]	Ammonium [mg/L]
0	1.0	39
0.2	0.8	31
0.4	0.6	23
0.6	0.4	15
0.8	0.2	8
1.0	0	0

This is used to obtain the standard curve on the spectrophotometer, by reading the absorbance of the different samples and plotting it against ammonium concentration (mg/L).

Assay method

- Treat both the standards and samples the same.
- Take 50µl of samples and standards and add 950µl of dH_2O.
- (Dilute everything 1 in 10 before assaying so that the samples fall within the concentration range).
- Take 500µl of that and add to 4.5ml of dH_2O in a test tube.
- Add 600µl of 2A.
- Vortex and allow to stand for a bit at $30^{O}C$.
- Add 1 micro-spoon of reagent 2B to each sample.
- Vortex and allow to stand for 5 min at $30^{O}C$.
- Add 4 drops of reagent 2C to each sample.
- Vortex and allow to stand for 7 min at $30^{O}C$.
- Read at 690nm. Remember to read all samples and standards within 1 one of the assay.
- Use the quartz cuvettes.

APPENDIX E

PAPER SUBMITTED TO SEPARATIONS SCIENCE AND TECHNOLOGY FOR PUBLICATION

MONITORING THE EFFECT OF MICROBIAL GROWTH ON PRESSURE AND MEMBRANE PERMEABILITY IN A POLYSULPHONE MEMBRANE

M SOLOMON AND F W PETERSEN

Department of Chemical Engineering
Cape Technikon, P. O. Box 652, Cape Town, 8000
SOUTH AFRICA

ABSTRACT

This paper deals with monitoring the effect of microbial growth, *Phanerochaete chrysosporium*, on the axial pressure and permeability of a capillary membrane fixed into a bioreactor. The reactor was run in a dead-end filtration mode. A method was developed for the in-situ monitoring and prediction of membrane pressure and permeability. The viability of the membrane for the cultivation of *P. chrysosporium* was demonstrated. Growth within the relative confined macrovoids of the membrane contributed to loss of membrane permeability and an increase in pressure drop.

INTRODUCTION

The white rot fungus *Phanerachaete chrysosporium* and its extracellular enzymes *Lignin* and *Manganese Peroxidase* are known to catalyse the transformation and degradation of several recalcitrant aromatic pollutants. In terms of their ecological *niche*, white rot fungi (WRF) are those organisms that are able to degrade lignin, the structural polymer found in woody plants. Along with their ability to degrade these chemicals, WRF possess a number of advantages not associated with other bioremediation systems.

Few studies have reported the use of *P.chrysosporium* based reactor systems for wastewater treatment. Cultivation and immobilisation of micro-organisms within

hollow-fibres have some advantages over other methods, including the high densities to which cells may be grown, elimination of culture washout and simultaneous separation of product and biocatalyst. Other advantages include achievement of growth and immobilisation in a single step, the capacity for biocatalyst regeneration and amenability of the system to scale-up.

According to Linton, *et al.* [1], a major limitation to the use of hollow-fibre cell cultures is the difficulty of monitoring and controlling their growth and metabolism. Other limitations are the mass transfer rates encountered at high cell densities and the problems associated with excessive cell growth, leading to blinding and rupture of the internal ultrafiltration membrane. A number of factors are required if the fruits of biotechnology are to be optimally commercialised. Among these are the design and operation of novel bioreactors and the development of sensors and the necessary models for control algorithms enabling bioprocesses to be efficiently operated.

The application of this promising fungus in large scale waste water treatment and/or commercial production of ligninases has been hampered by the lack of bioreactor systems yielding consistent high levels of enzyme production under long term steady state conditions and controlled growth of the fungus.

The viability of a polysulphone externally unskinned membrane for the cultivation of *P. chysosporium* is demonstrated. A modification of the Bruining Model was used to develop a method for the in-situ monitoring and prediction of pressure and permeability along the membrane in the dead-end filtration mode with an incompressible Newtonian fluid in laminar flow inside the membrane. The effect of the microbial growth on the membrane pressure and permeability was monitored.

THEORY

The system used in this study is classified under fixed film bioreactors, operated in a mode in which the membrane acts as a support matrix for the biological catalyst. As shown in Figure 1, the membrane used in this study consists of a 1.2 mm inside diameter, internally skinned and externally unskinned, capillary membrane. The membrane acts as a filtration barrier to provide the biofilm with sterile, low-molecular mass nutrient sources.
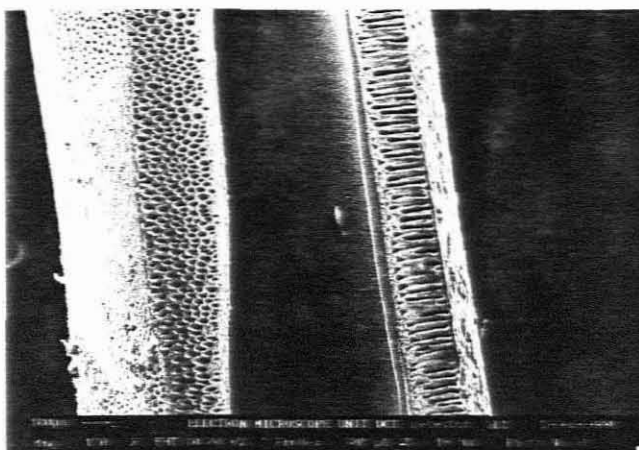
Figure 1: SEM photograph of the externally unskinned, internally skinned
polysulphone membrane used in this study.

A recent report by Bruining [2] gave a coherent description of flow phenomena
in hollow fibre membrane devices, which predict the pressures occurring under
various operating modes. The analysis had relevance to the more general case of
laminar and turbulent flow in porous ducts. The analysis was carried out for an
incompressible pure fluid with laminar flow inside the fibres. A constant pressure on
the module shell side was assumed.

Figure 2, taken and adjusted from [2], shows the flow configuration that was
used in this study. In this mode of operation F_2, which denotes the fraction retentate,
defined as the fibre side exit flow divided by the fibre side entrance flow, is equal to
zero.

Permeation Process	Situation	Retentate (F_2)
Dead-end filtration		$F_2 = \dfrac{Q_2}{Q_1} = 0$

Figure 2:   Mode of operation of membrane (Modified from Bruining [2])

Considering the module as shown in Figures 2 & 3, Q_1 will be the volumetric flow rate entering a single fibre at $z = 0$. The pressure at the entrance of the module was defined as P_1, the pressure at the exit of the fibre as P_2 and the pressure on the shell side as P_3. At a distance z from the entrance, the flow rate inside the fibre is Q and the pressure P.

According to Bruining [2], a mass balance over a section dz of the fibre gives

$$\frac{dQ}{dz} = -\prod d_i J \qquad \text{where} \qquad J = \frac{K(p - p_3)}{\mu d_w} \qquad (1)$$

$$\text{and} \qquad d_w = \frac{1}{2}d_i \ \text{in} \ \frac{d_o}{d_i}$$

where J is the local permeation flux in m/s, d_w is the average wall thickness in m, d_i is the inner fibre diameter in m, d_o is the outer fibre diameter in m and μ is the fluid viscosity in Pa.s. This indicates that the flux of the fluid through the membrane (contact angle $> 90°$ with the membrane material) is measured as a function of the pressure drop across the membrane. Because the biofilm on the membrane changes along the membrane and with time, the pressure drops along and across the membrane changes with time. K tends to change with biofilm growth on the membrane and is referred to as the fibre wall permeability coefficient measured in m^2.

For this set of equations the boundary conditions are:

$$\text{At} \qquad z = O \qquad Q = Q_1 \qquad \text{and} \qquad p = p_1 \qquad (2)$$

The following dimensionless groups was introduced by Bruining [2]:

$$x = z / L, \qquad [z = \text{the distance along the membrane (m)} \qquad (3)$$
$$L = \text{fibre length (m)}]$$

$$P_r \quad = \quad \frac{p - p_3}{p_1 - p_3} \qquad [\text{a dimensionless pressure}]$$

$$[\text{at} z = 0: \qquad p = p_1 \text{and} \ P_r = P_{r1} = 1 \text{ and} \qquad (4)$$
$$[\text{at} \ z = L: \qquad p = p_2 \text{ and} \ P_r = P_{r2}]$$

$$T_L \quad = \quad \frac{128 K l^2}{d_1^3 d_w} \qquad \text{[a dimensionless transport modulus]} \qquad (5)$$

T_L is a dimensionless (laminar flow) transport modulus representing the ratio of viscous flow resistance inside the fibre and the fibre wall permeation resistance.

After mathematical manipulation and by differentiation with respect to x and substitution the following homogeneous second-order differential equation was obtained:

$$\frac{d^2 P_r}{dx^2} \quad = \quad T_L P_r \qquad (6)$$

The solution of this equation is:

$$P_r = \cosh\left(x\sqrt{T_L}\right) - \frac{\psi_1}{\sqrt{T_L}} \sinh\left(x\sqrt{T_L}\right) \qquad (7)$$

By substitution of $\psi = \psi_2$ and $P_r = P_{r2}$ at x = 1 the following expression was obtained:

$$P_{r2} = \cosh\left(\sqrt{T_L}\right) - \frac{\psi_1}{\sqrt{T_L}} \sinh\left(\sqrt{T_L}\right) \qquad (8)$$

By defining the fraction of retentate at x = 1 as $\qquad F_2 = \frac{\psi}{\psi_2} = \frac{Q_2}{Q_1} \qquad (9)$

The following unique relation between F_2, T_L and ψ_1 is found:

$$\psi_1 = \frac{\sqrt{T_L}\ \sin\sqrt{T_L}}{\cosh\sqrt{T_L} - F2} \qquad \Psi_1 \quad = \quad \frac{\sqrt{T_L}}{\cosh\sqrt{T_L}} \frac{\sinh\sqrt{T_L}}{-\quad F_2} \qquad (10)$$

After mathematical manipulation the following equation was obtained:

$$\sqrt{T_L} = \left[\frac{1 + \left(1 - P_{r2}\right)^{1/2}}{P_{r2}} \right] \qquad (11)$$

This equation can be used to calculate the dimensionless transport modulus at $z = L$, by calculating P_{r2}, using the measured entrance pressure P_1 and outlet pressure P_2.

EXPERIMENTAL SET-UP AND PROCEDURE

The basic design of the bioreactor used in this study consisted of the membrane inserted into a glass manifold, onto which the fungus was immobilised. Air was filter sterilised and humidified before passing through the shell side of the reactor. Nutrient medium was pumped through the membrane lumen. A pressure gauge was used to measure the pressure at the inlet and outlet and a manometer to record the shell side pressure. The membrane was closed off after the pressure gauge at the outlet, to force the nutrient medium to permeate through the reactor. Permeate samples were collected and analysed for enzyme activity, temperature, relative redox potential, glucose and ammonium concentration on a daily basis.

The reactor was operated continuously for 2 weeks after which the reactor was dismantled and segments of the membrane were prepared for microscopic examination. Electron microscopy was used to measure cell densities and to assess the fungal morphology.
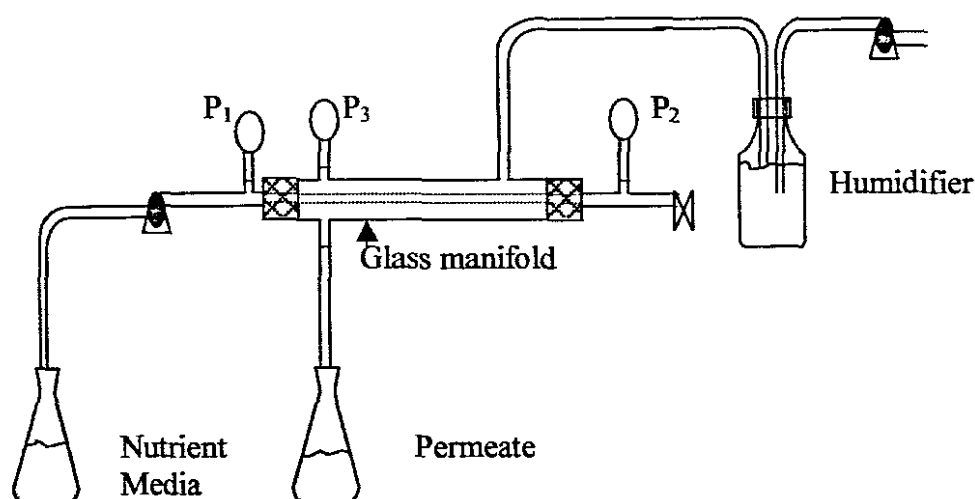
Air pump

Figure 3: Experimental set-up used in this study.

APPLICATION

It was assumed that there is no pressure drop on the shell side and that laminar flow is occurring inside the fibre. By measuring P_1, P_2 and P_3, the value of P_{r2} can be found using Equation 4 (where $p = p_2$) and the value of T_L (at $z = L$) can be calculated using Equation 11. Recalling the meaning of T_L(Equation 5) one can carry out experiments with different geometries (L, d_i, d_w) and find a value for the membrane permeability coefficient K at different values of z until $z = L$. In the case of a dead-end filtration experiment, without a shell side pressure drop, it is known that $F_2 = 0$. T_L is used to calculate the value of the dimensionless flow rate, Ψ_1, using Equation 10. T_L and Ψ_1 are used to calculate P_r at different values of z using Equation 7. Knowing P_r at different values of z, the pressure at this point can be calculated using Equation 4.

Using the correlations as described above, measurements were taken and calculations were done for a membrane without biofilm growth (referred to as the control), and a membrane with biofilm growth (referred to as an inoculated membrane).

RESULTS AND DISCUSSION

Pressure Measurements

For the control membrane inlet and outlet pressure readings stayed constant, at approximately 106325 Pa and 101675 Pa respectively, throughout the experiment. For an inoculated membrane, as shown in Figure 4, inlet pressure readings remained constant for the lag period until biofilm growth was visible on the membrane on day 3 and 4, after which it increased exponentially until it reached a stationary phase again. This could be an indication of the biofilm growth pattern on the membrane as this follows the same pattern as a typical growth curve. Outlet pressure was considerably lower that the inlet pressures, but followed more or less the same pattern.
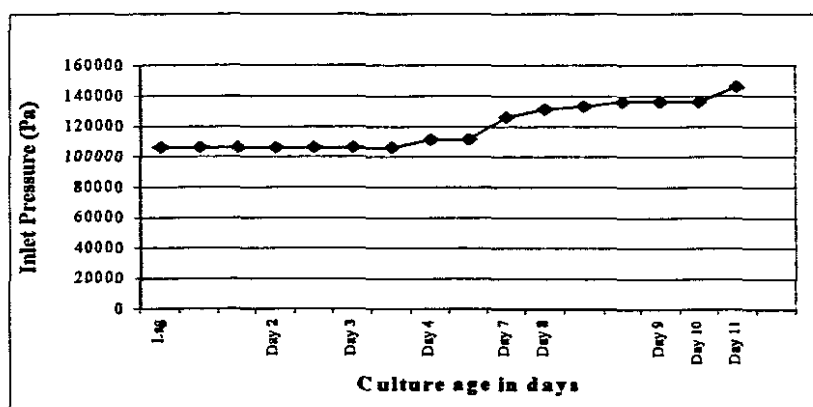

Figure 4: Inlet pressure for an inoculated membrane.

Pressure Prediction along the membrane

The manometer used to measure the pressure on the reactor side indicated a constant atmospheric pressure. Due to the difficulty of measuring the pressure along the membrane lumen, the model described previously was used to predict the pressure along the membrane. The outlet pressures that were calculated and predicted using the modified Browning model were compared to the measured outlet pressures. As shown in Figure 5, results indicate that the predicted outlet pressure is of the same

order of magnitude as the measured outlet pressure, P_2, and therefore proofs that this could be a reliable model for predicting the pressure along a hollow fibre membrane.
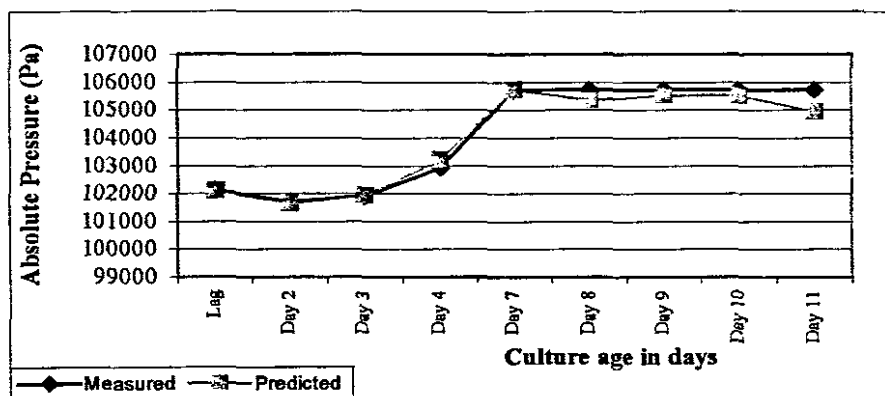

Figure 5: Outlet pressure for an inoculated membrane, Measured vs Predicted pressure

The system used is a dead-end filtration system and is run at a constant flux. The biofilm on the membrane increases with time, consequently the pressure drop along and across the membrane also increases with time. Figure 6 indicates that the pressure decrease from the inlet to the outlet. Inlet pressure increases exponentially after growth is visible on the membrane on day 4. This also shows that pressure can be used as an indication of the biofilm growth on the membrane. The axial pressure gradient observed appear to be greater that expected and vary with time. This could be explained by biofilm growth into the lumen. If this is typical behaviour it means that the membrane morphology needs to be adjusted, and action be taken to avoid pinholes which would provide the sites for growth through the membrane.
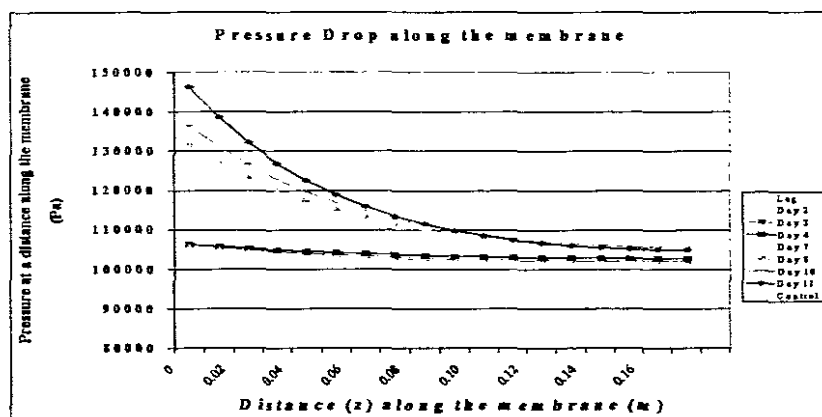
Figure 6: Predicted Pressure along a membrane with biofilm growth

Membrane Permeability (K in m²)

As shown in Figure 7, the permeability coefficient for the polysulphone hollow-fibre control membrane stayed constant throughout the experiment. Membrane permeability decreased from 2.67 E –11 m² at the beginning of the membrane to 1.28 E-12 m² at the end of the membrane. This curve remained constant throughout the experiment, indicating that the permeability for a membrane without biofilm growth is consistent.

Comparing this to a membrane with biofilm growth, as shown in the Figure 8, the permeability follows the same pattern from the beginning to the end of the membrane but decreases from day 1 to day 11. Permeability at the beginning of the membrane decreased from 2.67 E-11 m² on the control to a minimum of 2.00 E-11 m² during the experiment as shown in Figure 8. This is an indication that the biofilm thickness increased from day 1 to day 11 and that the macrovoid space decreased. Therefore, indicating that membrane permeability decreases as biofilm thickness increases.
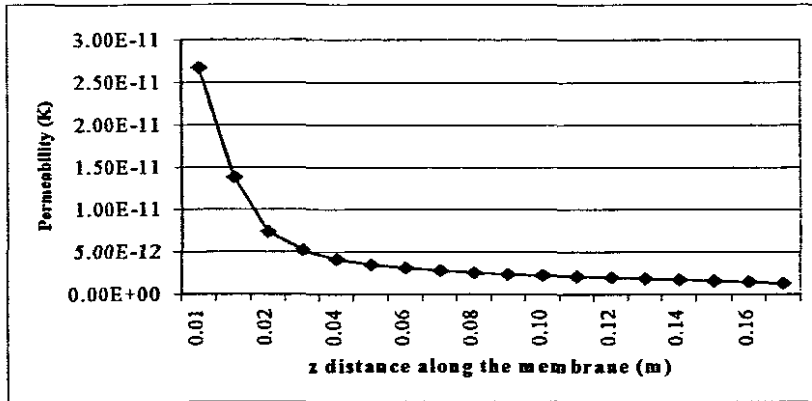
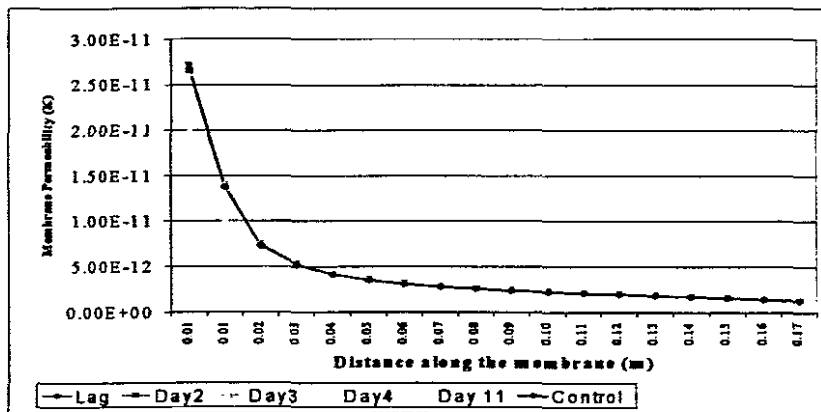Figure 7: Permeability for membrane without growth

Figure 8: Permeability for membrane with growth

Membrane Flux

This reactor is operated in a constant flux mode. The flux of the fluid through the membrane (contact angle > 90° with the membrane material) is measured as a function of the pressure drop across the membrane. The above graphs indicate that the applied pressure across the membrane is indeed the most significant factor affecting the permeability of this specific membrane.

CONCLUSIONS

For the control (membrane without growth) the inlet and outlet pressures remain constant throughout the experiment. Membrane permeability decreases exponentially from the inlet to the outlet but remains constant throughout the experiment.

For an inoculated membrane the axial and radial pressure drops increase as the biofilm thickness increases on the membrane. Growth within the relatively confined macrovoids of the membrane contributed to loss of permeability. The pressure and permeability can be used as a measure for biofilm growth on the membrane.

The outlet pressure measured corresponds to the predicted pressure using the modified Bruining model. This model can therefore be used for the prediction of pressure in a hollow fibre internally skinned, externally unskinned polysulphone membrane as was used in this study.

A coherent description of the pressure and permeability phenomena in hollow fibre devices has been given. The analysis also has relevance to the more general case of laminar flow in porous ducts. Finally, the analysis can be applied to determine fibre and module properties from simple experiments as demonstrated by an example.

REFERENCES

1.	Linton, E.A., Higton, G., Knowles, C.J. and B nch, A.W. *Monitoring microbiol growth in a hollow-fibre reactor using an electronic pressure sensor.* Enzyme Microbiology and Technology 1989, Vol. 11(May): 283-288.

2.	Bruining W.J. *A general description of flows and pressures in hollow fibre membrane modules.* Chemical Engineering Science 1989, Vol. 44(6): 1441 – 1447.

NOMENCLATURE

A	cross sectional area (m^2)
d	diameter (m)
d_i	membrane inside diameter (m)
d_o	membrane outside diameter (m)
d_p	pore diameter (m)
d_w	average wall thickness (m)
E	enzymes
F_2	Fraction of retentate (fibre side exit flow divided by fire side outlet flow)
J	local permeation flux (m/s)
K	fibre wall permeation coefficient (m^2)
K_p	proportional constant known as permeability coefficient (m^2)
L	membrane length (m)
n	number of complete layers around the centre
N	number of membranes per module
Q	liquid volumetric flow rate (m^3/s)
Q_1	liquid volumetric flow rate at membrane entrance (m^3/s)
Q_2	liquid volumetric flow rate at membrane outlet (m^3/s)
P	pressure (Pa)
P_r	dimensionless pressure
Pr_1	dimensionless pressure at membrane inlet
Pr_2	dimensionless pressure at membrane outlet
P_1	pressure at inlet of membrane (Pa)
P_2	pressure at outlet of membrane (Pa)
P_3	pressure on reactor shell side (Pa)
t	time (s)
T_L	dimensionless transport modulus
v	velocity (m/s)
x	dimensionless group equal to z divided by L
Ψ	dimensionless flow rate modulus
Ψ_1	dimensionless flow rate at membrane inlet
Ψ_2	dimensionless flow rate at membrane outlet

z   distance from membrane inlet (m)

π   pie

μ   fluid or solvent viscosity (Pa.s)

χ   membrane thickness or thickness of porous material (m)

ρ   fluid density (kg/m^3)

ABBREVIATIONS

LiP   *Lignin Peroxidase*

MnP   *Manganese Peroxidase*

MF   Microfiltration

UF   Ultrafiltration

HFM   Hollow Fibre Module

MMCO   Medium-molecular-mass cutt-off

MCMBR   Multi-capillary membrane bioreactor

SFMBR   Single fibre membrane bioreactor

SFCMBR   Single fibre capillary membrane bioreactor

SEM   Scanning Electron Microscopy

WRC   Water Research Commission

WRF   White Rot Fungus